

UDC 004

621.3

681.5

In print: ISSN 2545 – 4250

On line: ISSN 2545 – 4269

**JOURNAL
OF ELECTRICAL ENGINEERING
AND INFORMATION TECHNOLOGIES**

**СПИСАНИЕ
ЗА ЕЛЕКТРОТЕХНИКА
И ИНФОРМАЦИСКИ ТЕХНОЛОГИИ**

<i>J. Electr. Eng. Inf.. Technol.</i>	Vol.	No.	pp.	Skopje
	1	1–2	1–116	2016
<i>Спис. Електротехн. Инф. Технол.</i>	Год.	Број	стр.	Скопје

<i>J. Electr. Eng. Inf.. Technol.</i>	Vol.	No.	pp.	Skopje
	1	1–2	1–116	2016
<i>Спис. Електротехн. Инф. Технол.</i>	Год.	Број	стр.	Скопје

TABLE OF CONTENTS (СОДРЖИНА)

PREFACE (Предговор)	5–6
122. Kiril Demerdžiev, Živko Kokolanski, Vladimir Dimčev, Maja Celeska, Krste Najdenkoski, Vlatko Stoilkov WIND PARAMETERS ANALYSIS ON FIVE LOCATIONS IN MACEDONIA – THE SECOND MEASUREMENT CAMPAIGN (Анализа на параметрите на ветровите на пет локации во Македонија – Втора мерна кампања)	7–15
123. Gorjan Nadžinski, Mile Stankovski, Ivan Gočev DEALING WITH THE EFFECTS OF RANDOM TIME DELAY AND DATA DROPOUTS IN NETWORKED CONTROL SYSTEMS THROUGH ROBUST CONTROL (Справување со ефектите од случајни доцнења и губење податочни пакети во вмрежените контролни системи преку робусно управување)	17–23
124. Drilon Bunjaku, Jovan Stefanovski, Mile Stankovski DYNAMIC MODELLING AND ASYMPTOTIC POINT STABILIZATION CONTROL OF TWO DIFFERENTIAL WHEELED MOBILE ROBOT (Динамичко моделирање и контрола на приближувањето кон асимптотската стабилност на мобилен робот со две диференцијални тркала)	25–35
125. Samoil Samak, Igor Dimovski, Mirjana Trompeska, Vladimir Dukovski AVOIDING HEAVY COMPUTATIONS IN INVERSE CALIBRATION PROCEDURE FOR 7 DOF ROBOT MANIPULATOR (Процедура на инверзна калибрација за намалување на пресметковните операции кај робот управуван со 7 степени на слобода)	37–43
126. Elizabeta Lazarevska A NEURO-FUZZY MODEL FOR WIND SPEED PREDICTION BASED ON STATISTICAL LEARNING THEORY (Невро-фази модел за предвидување на брзината на ветерот базиран врз статистичка теорија на учење)	45–55
127. Hristina Čingoska, Zoran Hadži-Velkov, Ivana Nikoloska WIRELESS INFORMATION AND ENERGY TRANSFER: TRADEOFF FOR FAIR RESOURCE ALLOCATION (Безжичен пренос на информација и енергија со правична распределба на ресурси)	57–65

128. Liljana Gavrilovska, Pero Latkoski, Vladimir Atanasovski METHODS FOR RADIO SPECTRUM EVALUATION AND MONITORING (Методи за евалуација и мониторинг на радиоспектар).....	67–73
129 Marko Porjazoski, Pero Latkoski, Borislav Popovski SYSTEM FOR OTT SERVICES (Систем на наплата за OTT-сервиси)	75–81
130. Slavica Nasteska, Liljana Gavrilovska CONSUMERS “LOCK-IN” – A KEY ELEMENT OF THE SWITCHING COSTS IN MOBILE TELEPHONY IN THE REPUBLIC OF MACEDONIA („Заклучување“ од корисниците – клучен елемент во трошоците за промена на мобилен оператор во Република Македонија)	83–91
131. Vesna Andova, Sanja Atanasova, Elena Jovčevska, Viktorija Jordanova, Ilin Tolovski, Martin Rizov PROJECTING A HYDROGRAPHIC MAP OF THE REPUBLIC OF MACEDONIA (Моделирање на хидрографска мапа на Република Македонија)	93–100
INSTRUCTIONS FOR AUTHORS	101–102

Supplement:

132. Vladimir Dimčev, Blagoja Bogatinoski SURVEY OF THE ARTICLES PUBLISHED IN THE <i>PROCEEDINGS OF THE FACULTY OF ELECTRICAL ENGINEERING IN SKOPJE</i> Issues from Vol. 1. No. 1 (1977) to Vol. 22, No. 1–2 (2006) (Преглед на трудови објавените во <i>Зборникот на трудови на Електротехничкиот факултет во Скопје</i> од 1977 (год. 1, бр. 1) до 2006 (год. 22, бр. 1–2).....	103–116
---	---------

Dear readers and colleagues,

The Proceedings of Electrical Engineering Faculty in Skopje was published since 1977 and the last edition appeared in 2006. Since that year the publishing has been stopped.

This year the Faculty is renewing the publishing of Proceedings under the name Journal of Electrical Engineering and Information Technologies. The plan is to publish two numbers per year, as used to be done. The notable difference is that issues would be appeared in electronic format with open access to the manuscripts, beside the paper version. This change will enhance the Journal influence in scientific and experts community.

The Journal will publish original scientific and professional manuscripts from electrical engineering and information technologies fields. The manuscripts can be focused on theoretical analysis, experimental research or solutions of problems originating from practice. One of the leading motivations for publishing the Journal is continuous increase of the quality of scientific and practice work on the Faculty represented in the number of master and doctoral thesis. Also, our Faculty frequently organizes local and international conferences. It is our wish this Journal to serve as promoter for the best manuscripts from conferences, as well as for the best scientific and research results from master and doctoral thesis and other significant projects.

The Journal will offer opportunity for publishing manuscripts that have been published in renowned world journals, but because the page limit the manuscripts are usually presented in shortened versions. In our Journal the manuscripts could be presented with detailed analytical and numerical algorithms, without page limit. The most commonly this manuscripts are of substantial concern and have high citation rate.

Our long-term goal is to make this Journal recognized in the region and beyond and in short time to be evaluated with appropriate impact factor.



*sEditor in Chief
Academic Leonid Grčev*

Почитувани чииаители и колеги,

Зборникот на трудови на Електротехничкото факултет почнал да излеува во 1977 година, а последниот двоброј излеол во 2006 година кога неговоото излеување е прекинато.

Факултетот оваа година го обновува излеувањето на Зборникот, сега како Списание за електротехника и информациски технологии (Journal of Electrical Engineering and Information Technologies). Како и претходно, планирано е да излеуваат два броја годишно. Бидејќи промена е дека покрај печатената форма, Списанието ќе излеува и во електронска верзија со слободна достапност на трудовите за сите заинтересирани чииаители. Оваа промена може бидејќи да го зголеми влијанието на Списанието во научната и стручната јавност.

Во Списанието ќе се објавуваат оригинални научни и стручни трудови од областите на електротехниката и информациските технологии. Трудовите може да бидат фокусирани на теоретски анализи, експериментални испитувања, решенија на проблеми од праксата. Една мотивација за продолжување на издавањето на Списанието е континуираното зголемување на квалитетот на научната и стручната работа на Факултетот, што се огледа во бројот на магистерски и докторски дисертации. Од друга страна, Факултетот континуирано организира значајни национални и меѓународни конференции. Желба е Списанието да претставува медиум за промовирање на најквалитетните трудови од конференциите како и најквалитетните резултати од испитувањата во рамките на докторски и магистерски тези и други значајни проекти.

Во Списанието ќе можат да се публикуваат трудови кои веќе биле објавени во претходни светски списанија, но каде поради ограничување на бројот на страници најчесто биле презентирани во скратена верзија. Нашето Списание дава можност во трудовите детално да се претстават аналитичките и нумеричките остатоци, како и добиените резултати, а таквите трудови најчесто предизвикуваат висок интерес и цитирање.

Со сето тоа, нашата долгорочна цел е Списанието да биде препознатливо во регионот и пошироко и во додатоко време да биде вреднувано со соодветен коефициент на влијание (impact factor).

*Главен и одговорен уредник,
Академик Леонид Грчев*



WIND PARAMETERS ANALYSIS ON FIVE LOCATIONS IN MACEDONIA – THE SECOND MEASUREMENT CAMPAIGN –

**Kiril Demerdžiev, Živko Kokolanski, Vladimir Dimčev,
Maja Celeska, Krste Najdenkoski, Vlatko Stoilkov**

*Faculty of Electrical Engineering and Information Technologies,
"Ss. Cyril and Methodius" University in Skopje,
Rugjer Bošković bb, P.O. box 574, 1001 Skopje, Republic of Macedonia
kdemerdziej@feit.ukim.edu.mk*

Abstract: The world population growth and the technological development have increased the demands for electricity. Because of the limited deposits of fossil fuel and the negative impact its combustion causes to the environment, the electricity production technologies are orienting towards using the renewable energy sources. From all the renewable energy sources, the most studied one over the last decade is the wind. Wind parameters of interest in electrical study are its speed and direction; once they are measured it is easy to determine other characteristic parameters such as wind energy density on the specific location. In the manuscript, monthly and seasonal mean wind speeds are presented, alongside the wind energy density for five locations in the Republic of Macedonia, for almost four years of measurements.

Key words: monthly mean wind speeds; seasonal mean wind speed; scale parameter; shape parameter; wind energy density

АНАЛИЗА НА ПАРАМЕТРИТЕ НА ВЕТРОВИТЕ НА ПЕТ ЛОКАЦИИ ВО МАКЕДОНИЈА – ВТОРА МЕРНА КАМПАЊА –

Апстракт: Последицата од зголемувањето на популацијата на светско ниво и од големиот технолошки развој е сè поголемата побарувачка на електрична енергија. Имајќи ги предвид ограничените наоѓалишта на фосилни горива и негативното влијание на нивното согорување врз животната средина, производствените технологии сè повеќе се ориентираат кон искористување на обновливите извори на енергија. Од сите обновливи извори, најголема енергија е акумулирана во ветерот. Параметрите на ветерот кои се од интерес за негово проучување од електроенергетски аспект се, пред сè, неговата брзина и насока, а од нив се изведуваат и други карактеристични параметри како што е, на пример, густината на енергија на конкретна локација. Во овој труд се прикажани средните брзини на ветерот на месечно и сезонско ниво, како и густините на енергија кои ги поседува ветерот во одделни месеци, односно сезони, во текот на една година. Анализата е направена за пет локации на територијата на Република Македонија, за речиси петгодишен период на испитување.

Клучни зборови: средна сезонска брзина; средна месечна брзина; параметар на размер; параметар на форма; густина на ветерна енергија

INTRODUCTION

The first measurement campaign for establishing a wind database in the Republic of Macedonia was successfully completed with the construction of Wind Park Bogdanci, the second campaign was carried on in the period between July 2012 and

March 2016. In the second wind measurement campaign five locations were chosen according to several relevant factors [1, 2], such as:

- Wind atlas of Macedonia;
- Terrain configuration;
- Local infrastructure – proximity of electrical network and roads, etc.

The sites where the measurement campaign took place are: Staro Nagoričane, Sveti Nikole, Berovo, Mogila and Sopište. The measurement campaign started during the summer of 2012 and covered a continuous process of data acquisition except for some time intervals when certain malfunction in the equipment took place. In Table 1 the geographical coordinates of all five locations are presented, alongside with the altitude and the day when measurements began. Measured data from the measurement stations are sent to data center on a daily or half-day basis in a binary files with extension *rwd (Raw Wind Data) [1]. In order to have this files read and interpret, they have to be converted in text files using the software Symphony Data Retriever, NRG Systems. Once the data is converted in $t \times t$ format, it's easy to use it for wind energy estimation, by inserting it in some advanced software.

Table 1
Measurements sites

Site	Geographical coordinates	Altitude (m)	Measurement start
Sveti Nikole	N 041° 55.093' E 021° 56.792'	431	1. 7. 2012
Mogila	N 041° 11.303' E 021° 21.546'	702	20. 7. 2012
Staro Nagoričane	N 042° 18.070' E 021° 58.504'	1179	26. 8. 2012
Berovo	N 041° 44.042' E 022° 47.059'	608	21. 9. 2012
Sopište	N 041° 11.299' E 021° 21.562'	730	22. 9. 2012

WIND ENERGY PARAMETERS

The term wind energy actually means a kinetic energy which a floating wind mass possess when it moves on some distance above Earth's surface [3]. The power accumulated in the air mass with density ρ (kg/m³), moving at speed v (m/s) is given by:

$$P = \frac{1}{2} \rho A v^3, \quad (1)$$

where A (m²) is a blade sweep area.

As can be seen from (1), the power accumulated in wind depends on the air density and the cube of wind velocity. Further on, the air density depends on the air temperature and pressure, while the wind speed depends on the distance between the measuring point and the surface. The wind speed is also affected by roughness on Earth's surface such as: urban areas, rocky terrains, forests, etc.

In order, an initial assessment of the wind profile to be made, the mean wind speed is measured [4]:

$$v_m = \frac{1}{n} \sum_{i=1}^n v_i, \quad (2)$$

where n is the total number of measurements registered over given time period. It is not enough only the mean wind speed, but also one has to know the wind's distribution. The wind's distribution shows what values the wind speed may have on that particular location and the percentage of time when the wind blows with particular speed. Location with high energy potential is a location where the wind speed is high enough to cause nominal energy production from the turbine and all the wind speed deviate minimally from the mean value. In order to estimate the deviation from the mean value the standard deviation is used:

$$\sigma = \sqrt{\frac{\sum_{i=1}^n (v_i - v_m)^2}{n-1}}. \quad (3)$$

Wind speed variations can be calculated using some standard distribution function. Suitable distribution function for such a purpose is the Weibull distribution [5]. Using the Weibull distribution the probability function and cumulative probability functions can be calculated using:

$$f(v) = \frac{k}{c} \left(\frac{v}{c}\right)^{k-1} e^{-\left(\frac{v}{c}\right)^k}, \quad (4)$$

$$F(v) = \int_0^v f(v) dv = 1 - e^{-\left(\frac{v}{c}\right)^k}. \quad (5)$$

In both probability functions two parameters can be spotted: scale parameter c (in units of speed) and shape parameter k (dimensionless number). The scale parameter c value is related to the value of mean wind speed and the shape parameter k value is related to the standard deviation and the uniformity of the wind speed in a given site, the greater standard deviation the smaller shape parameter [6]. These two parameters vary on different sites and different observation periods. Their values are given with following equations:

$$k = \left(\frac{\sigma}{v_m}\right)^{-1.086}, \quad (6)$$

$$c = \frac{v_m}{\Gamma\left(1 + \frac{1}{k}\right)}, \quad (7)$$

where Γ is the gamma function. In general, these two parameters determine the wind speed range over which the wind turbine is likely to operate.

By using (1) and (4), the wind energy density can be calculated. Wind energy density is expressed in W/m^2 and is an indicator for the wind energy available on the location which can be further transformed into electricity [6, 7]. Because not only the mean speed, but the distribution as well is taken into account, power density is better indicator for wind energy potential than the mean speed. Wind energy power density can be calculated using:

$$\frac{P_w}{A} = \int_0^{\infty} \frac{1}{2} \rho v^3 f(v) dv = \frac{1}{2} \rho c^3 \Gamma\left(1 + \frac{3}{k}\right). \quad (8)$$

WIND SPEED DATA ANALYSIS

In this study, mean wind speed on monthly and seasonal basis is calculated for all five measurement sites, during the duration of measurement campaign. Scale and shape parameters alongside the wind energy density for every month/season are calculated as well. All the values are presented in separate tables. The monthly mean speed is calculated as average value per month from all daily mean speed values. The seasonal mean speed is calculated the same way, only the daily averages are regrouped in four year seasons as follows: spring March 21 to June 20, summer June 21 to September 22, autumn September 2 to December 20 and winter December 21 to March 20.

The calculation of monthly and seasonal wind mean speed is done using MS Excel software tool. The first step is to generate monthly reports for each measurement site using Symphony Data Retriever and save them to *.pdf format. The monthly PDFs are then converted to Excel files. When all the Excel files for one location are merged to one the calculation can be made. By using daily speed averages for every day in the year, standard deviation is calculated on monthly and seasonal basis. Shape parameter, scale parameter as well as wind energy densities are calculated from mean wind speed and standard deviation using equations (6), (7) and (8).

Sveti Nikole

In Table 2, the monthly mean wind speed is presented, alongside the values for shape and scale parameter and wind energy density for each month in the year, at Sveti Nikole measurement site.

The highest mean wind speed is 5.16 m/s and is calculated for June and July, while the lowest

value is calculated for November and it is 3.75 m/s. The standard deviation calculated for all months except for August is higher than 1 m/s which means that daily mean speeds differ significantly of the monthly mean value. This fact is verified with values in the fourth column of the table, where the shape parameter is presented. The shape parameter varies between 2.55 in December and 5.48 in August. Even though mean wind speed is equal for June and July, the wind energy density slightly differs in this two months, 100.35 W/m^2 in June and 96.8 W/m^2 in July.

Table 2

Calculated data on monthly basis at Sveti Nikole

Month	Mean wind speed (m/s)	Standard deviation (m/s)	Parameter		Wind energy density (W/m^2)
			Shape k	Scale c (m/s)	
1	4.28	1.63	2.85	4.81	69.61
2	4.93	1.91	2.79	5.53	107.23
3	4.82	1.73	3.04	5.40	95.72
4	5.09	1.67	3.35	5.67	107.35
5	4.06	1.59	2.76	4.57	60.63
6	5.16	1.31	4.41	5.66	100.35
7	5.16	1.17	5.02	5.61	96.80
8	4.08	0.85	5.48	4.42	47.16
9	4.17	1.13	4.14	4.59	54.09
10	4.04	1.13	3.99	4.46	50.05
11	3.75	1.16	3.57	4.16	41.67
12	4.02	1.70	2.55	4.53	61.91

For this measurement location it can be concluded that the wind energy density does not follow the value of mean wind speed, and so the highest wind energy density is calculated for February and April. The change in mean wind speed by month is presented on Figure 1.

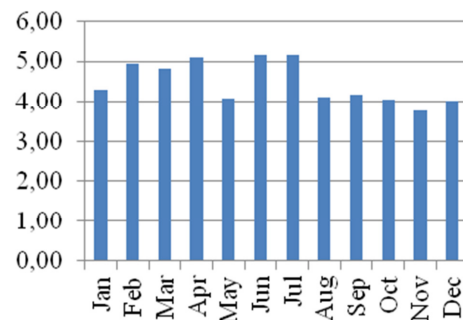


Fig. 1. Monthly mean wind speed at Sveti Nikole (m/s)

The same data, but averaged over time period of one season is presented in Table 3. The seasonal mean wind speed is the highest in summer and the lowest in winter, values are 4.64 m/s and 3.99 m/s respectively. High value for the mean speed is also calculated for spring period, 4.62 m/s. The change in mean wind speed on season basis is illustrated on Figure 2. The greatest variations around the mean value are noticed in winter period, which can be seen by standard deviation and shape parameter values 1.75 m/s and 2.84 respectively. The scale parameter value varies between 4.44 m/s in autumn and 5.14 in spring. Wind energy density is the highest in winter, 84.8 W/m², and the lowest in autumn, 50.74 W/m².

Table 3

Calculated data on seasonal basis at Sveti Nikole

Season	Mean wind speed (m/s)	Standard deviation (m/s)	Parameter Shape k	Scale c (m/s)	Wind energy density (W/m ²)
Spring	4.62	1.48	3.43	5.14	79.28
Summer	4.64	1.17	4.45	5.09	72.95
Autumn	3.99	1.26	3.50	4.44	50.74
Winter	4.57	1.75	2.84	5.13	84.80

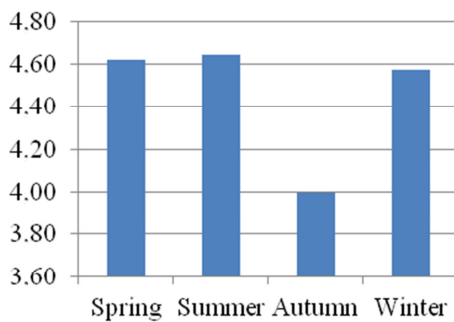


Fig. 2. Seasonal mean wind speed at Sveti Nikole (m/s)

Mogila

The mean wind speed, standard deviation, shape parameter, scale parameter and wind energy density calculated on monthly basis at this site are presented in Table 4. The two months where the highest mean speed is found are February and April, 4.51 m/s and 4.41 m/s respectively. The lowest monthly mean wind speed is 2.32 m/s and is calculated for December. Visually monthly mean wind speed change from month to month is illustrated on Figure 3.

Table 4

Calculated data on monthly basis at Mogila

Month	Mean wind speed (m/s)	Standard deviation (m/s)	Parameter Shape k	Scale c (m/s)	Wind energy density (W/m ²)
1	3.66	1.37	2.90	4.11	43.05
2	4.51	1.75	2.80	5.07	82.18
3	4.17	1.51	3.02	4.67	62.32
4	4.41	1.56	3.09	4.94	72.84
5	3.55	1.41	2.73	3.99	40.61
6	3.59	0.94	4.27	3.94	34.14
7	3.72	0.83	5.09	4.05	36.19
8	3.30	0.42	9.41	3.47	22.99
9	3.47	0.56	7.25	3.70	27.54
10	3.28	0.79	4.68	3.59	25.40
11	3.07	0.89	3.82	3.40	22.31
12	2.32	0.95	2.65	2.61	11.59

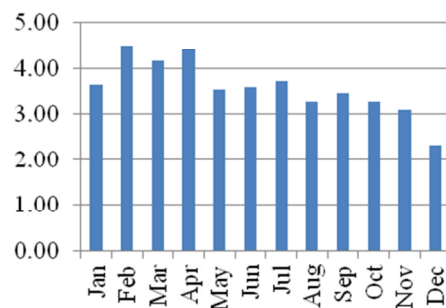


Fig. 3. Monthly mean wind speed at Mogila (m/s)

In the first five months standard deviation possess high values (higher than 1 m/s) which can also be noticed by observing the shape parameter, which varies from 2.80 to 3.10, for the period from January to May.

The deviation between the monthly mean speed and daily average speeds is the lowest in August, when the standard deviation is 0.42 m/s and the shape parameter is 9.41. Scale parameter follows the variation of mean wind speed from month to month and its value changes between 2.61 m/s in December and 5.07 m/s in February. Wind energy density also follows changes in mean speed and scale parameter, the lowest value is noticed in December, only 11.59 W/m², while the highest are found in February and April, 82.18 W/m² and 72.84 W/m² respectively.

In Table 5 the same data averaged over one year, with averaging time of one season is presented. The mean wind speed in all seasons varies be-

tween 3 m/s and 4 m/s, the highest spotted at winter, equals 3.92 m/s, the lowest spotted at autumn, its value is 3.01 m/s. The mean speed histogram is presented on Figure 4.

Table 5

Calculated data on seasonal basis at Mogila

Season	Mean wind speed (m/s)	Standard deviation (m/s)	Parameter		Wind energy density (W/m^2)
			Shape k	Scale c (m/s)	
Spring	3.87	1.34	3.16	4.32	48.45
Summer	3.52	0.67	6.10	3.79	29.50
Autumn	3.01	0.84	4.02	3.32	20.61
Winter	3.92	1.51	2.83	4.40	53.55

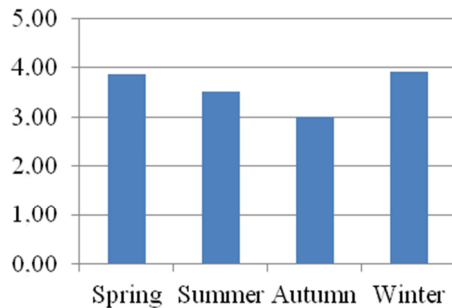


Fig. 4. Seasonal mean wind speed at Mogila (m/s)

During the summer and winter daily mean wind speed differs less from the average seasonal value. This conclusion is affirmed by the values of standard deviation and shape parameter during summer period. The variations round the mean value are the lowest in the winter. The shape parameter values for summer and winter are 6.10 and 2.83 respectively. Because of the small mean wind speed variation from season to season, the scale parameter changes between the values of 3.32 m/s at autumn and 4.40 m/s at winter. The wind energy density is the highest at winter, while the lowest at autumn.

Staro Nagoričane

In Table 6, mean wind speed is presented, as well as Weibull parameters of scale and shape, and wind energy density all averaged over one year time, with a period of averaging of one month. From the table it can be noticed that the highest monthly mean speeds are present in February, June and November, while the lowest value is found in August. The magnitudes of the mean wind speed in top three months are 7.22 m/s, 6.57 m/s and 6.70

m/s, respectively, while in August it is 5.29 m/s. The monthly mean speeds are presented on Figure 5. On this location, in January, huge variations between the mean speed and daily averages are presented.

Table 6

Calculated data on monthly basis at Staro Nagoričane

Month	Mean wind speed (m/s)	Standard deviation (m/s)	Parameter		Wind energy density (W/m^2)
			Shape k	Scale c (m/s)	
1	6.66	2.28	3.20	7.43	245.08
2	7.22	1.97	4.11	7.95	281.45
3	6.55	1.10	6.95	7.01	186.69
4	5.89	1.72	3.81	6.52	157.37
5	5.75	1.69	3.78	6.36	146.70
6	6.57	1.65	4.49	7.20	206.30
7	6.31	1.37	5.27	6.86	175.76
8	5.29	0.89	6.96	5.65	97.96
9	5.65	1.28	5.01	6.15	127.59
10	5.96	1.26	5.40	6.47	147.36
11	6.70	1.66	4.54	7.34	218.08
12	5.77	1.51	4.30	6.34	141.80

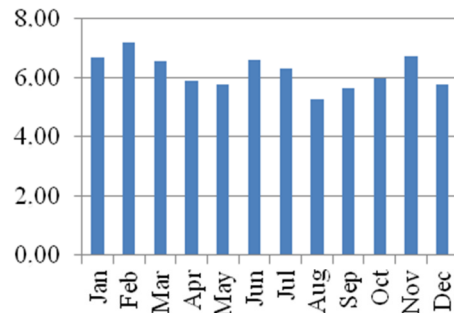


Fig. 5. Monthly mean wind speed at Staro Nagoričane (m/s)

The value of standard deviation is 2.28 m/s, while the shape parameter is 3.20. It is all the opposite in August, in this month the lowest from day to day variations are spotted, therefore the standard deviation is only 0.89 m/s and the k parameter is almost 7. Shape parameter in each month is approximately for 1 m/s higher than the mean wind speed in that particular month. From the changes in shape parameter the change in the wind energy density is calculated. The wind potential is the highest in February, while the lowest in August. The wind energy density changes from 97.96 W/m^2 to 281.45 W/m^2 .

The seasonal mean wind speed, alongside other Weibull parameters is presented in Table 7. As can be seen from Table 7, the wind blows at the highest speed during the winter, the mean value to be 6.68 m/s. During the summer period the lowest wind speed is present, together with the lowest variations between the seasonal and daily mean wind speeds. This fact can be noticed by observing the third and fourth column in Table 7. For the summer period the standard deviation is 1.27 m/s and the shape parameter is 5.29. The value of c parameter is higher than the mean speed and it varies from 6.38 m/s in summer to 7.38 m/s in winter. The wind energy density varies between 141.68 W/m² and 166.38 W/m² for the spring-autumn period, while at winter its value is much higher, 227.07 W/m². The change in mean wind speed on season basis is illustrated on Figure 6.

Table 7
Calculated data on seasonal basis
at Staro Nagoričane

Season	Mean wind speed (m/s)	Standard deviation (m/s)	Parameter Shape k	Parameter Scale c (m/s)	Wind energy density (W/m ²)
Spring	6.04	1.56	4.33	6.63	161.81
Summer	5.88	1.27	5.29	6.38	141.68
Autumn	6.16	1.43	4.90	6.72	166.38
Winter	6.68	1.89	3.93	7.38	227.07

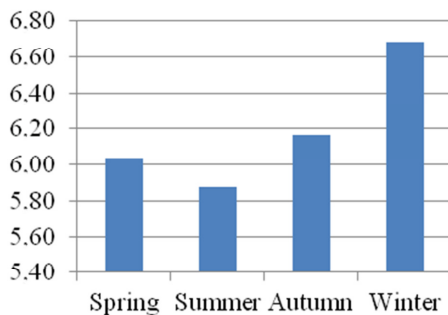


Fig. 6. Seasonal mean wind speed at Staro Nagoričane (m/s)

Berovo

The measured data, averaged on monthly basis, at Berovo site, is presented on Table 8 and Figure 7. From the table it can be noticed that the highest monthly mean wind speeds are present in February, March and April: 4.21 m/s, 4.18 m/s and 4.08 m/s respectively while the lowest amounts 3.03 m/s is present in August. At this site, it can be

noticed that the monthly mean speed in each month is lower than the mean speed at other sites and that there is also a lower variation between the daily averaged wind speed values and the monthly mean value. Except for January and February, the standard deviation is lower than 1 m/s and the shape parameter is higher than 5. In August the standard deviation is the lowest and its value is only 0.35 m/s.

Table 8
Calculated data on monthly basis at Berovo

Month	Mean wind speed (m/s)	Standard deviation (m/s)	Parameter		Wind energy density (W/m ²)
			Shape k	Scale c (m/s)	
1	3.88	1.25	3.42	4.32	47.04
2	4.21	1.21	3.88	4.66	57.25
3	4.18	0.94	5.07	4.55	51.48
4	4.08	0.86	5.42	4.42	46.96
5	3.54	0.65	6.35	3.81	29.96
6	3.83	0.80	5.47	4.15	39.00
7	3.68	0.79	5.30	3.99	34.62
8	3.03	0.35	10.45	3.18	17.73
9	3.27	0.49	7.83	3.48	22.94
10	3.27	0.58	6.54	3.51	23.46
11	3.33	0.85	4.42	3.65	26.96
12	3.24	0.83	4.38	3.55	24.89

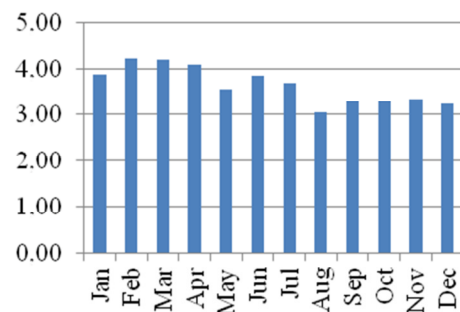


Fig. 7. Monthly mean wind speed at Berovo (m/s)

The scale parameter for every month is approximately 0.4 m/s higher than the mean wind speed. Because of the low mean wind speed and with low scale parameter, the wind energy potential is the lowest from all measurement sites. The wind energy density is the highest in February, 57.25 W/m², while the lowest in August, 17.73 W/m².

The seasonally averaged data are presented in Table 9. During the winter days the highest mean wind speed is 3.97 m/s, while the lowest 3.29 m/s are calculated for autumn. In the winter period the standard deviation is the highest, 1.12 m/s, which means the k parameter would be the lowest, 3.98. The scale parameter is higher than 4.2 m/s in spring and winter, while in summer and autumn it amounts 3.58 m/s and 3.57 m/s. The wind energy density is relatively low, it changes from value of 24.83 W/m² in autumn to 47.57 W/m² in winter. The mean speed histogram is presented on Figure 8.

Table 9

Calculated data on seasonal basis at Berovo

Season	Mean wind speed (m/s)	Standard deviation (m/s)	Parameter		Wind energy density (W/m ²)
			Shape k	Scale c (m/s)	
Spring	3.89	0.81	5.47	4.22	40.88
Summer	3.35	0.57	6.82	3.58	24.95
Autumn	3.29	0.72	5.22	3.57	24.83
Winter	3.97	1.12	3.98	4.39	47.57

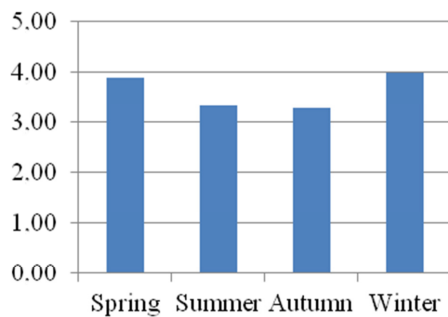


Fig. 8. Seasonal mean wind speed at Berovo (m/s)

Sopište

In Table 10 and Figure 9, the monthly averaged data for Sopište site are presented. At this site higher mean wind speed is present during the first half of the year. The highest value of 4,51 m/s is found in January, while the lowest are calculated in the last three months of the year, their values are 3.29 m/s, 3.24 m/s and 3.29 m/s respectively. As can be seen from the previous four sites, the highest standard deviation is usually present in the month when the highest wind speed is calculated. So the highest standard deviation is present in January, it amounts 1.86 m/s. The standard devia-

tion is high in February as well, while in other ten months it varies between 0.82 m/s in September and 1.15 m/s in April. August is the exception with less deviation around the mean value, standard deviation is only 0.63 m/s. Scale parameter follows the monthly mean wind speed, the parameter has the highest value in January, while the lowest in November. Because of, according to (8), cubic relation between the wind energy density and scale parameter, in January the value amounts 86.02 W/m², while in November it is only 25.58 W/m².

Table 10

Calculated data on monthly basis at Sopište

Month	Mean wind speed (m/s)	Standard deviation (m/s)	Parameter		Wind energy density (W/m ²)
			Shape k	Scale c (m/s)	
1	4.51	1.86	2.62	5.08	86.02
2	3.96	1.56	2.75	4.45	56.25
3	4.18	1.11	4.22	4.60	54.16
4	4.15	1.15	4.04	4.57	53.75
5	4.16	1.19	3.90	4.60	54.89
6	4.23	1.09	4.35	4.64	55.50
7	3.92	1.05	4.19	4.31	44.85
8	3.81	0.63	7.05	4.07	36.49
9	3.65	0.82	5.04	3.98	34.39
10	3.29	0.98	3.72	3.65	27.76
11	3.24	0.89	4.07	3.57	25.58
12	3.29	1.15	3.12	3.68	29.93

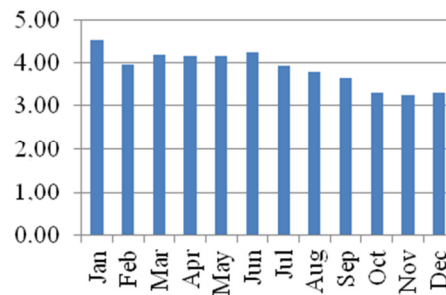


Fig. 9. Monthly mean wind speed at Sopište (m/s)

Seasonal average data is displayed in Table 11. The seasonal mean wind speed is the lowest during the autumn and it amounts 3.31 m/s, the highest being spotted in the winter months, 4.18 m/s. During the spring the mean speed value is a bit lower than the winter one. Standard deviation is

the lowest during the summer period, it amounts only 0.90 m/s, while in the winter it is 1.52 m/s. Shape parameter is related to the standard deviation, so it has the highest value in the summer, 4.85, and the lowest in the winter, 3.00. In all four seasons the scale parameter is approximately 0.4 m/s higher than the seasonal mean speed. Wind energy density is the lowest in autumn, it amounts 28.57 W/m², while in winter this value is approximately 2.5 times greater. The mean speed histogram is presented on Figure 10.

Table 11

Calculated data on sesonal basis at Sopište

Season	Mean wind speed (m/s)	Standard deviation (m/s)	Parameter		Wind energy density (W/m ²)
			Shape k	Scale c (m/s)	
Spring	4.10	1.08	4.28	4.51	51.07
Summer	3.86	0.90	4.85	4.21	40.87
Autumn	3.31	1.02	3.60	3.67	28.57
Winter	4.18	1.52	3.00	4.68	62.75

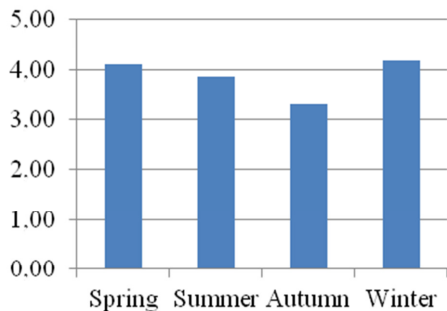


Fig. 10. Seasonal mean wind speed at Sopište (m/s)

SUMMARY AND CONCLUSION

In the manuscript, the overview of mean wind speed, Weibull parameters and wind energy density has been made, all of them averaged on one month or one year season basis. The analyses are made for five sites on the territory of the Republic of Macedonia, for almost four years of measurement data. For all five measurement sites, all data are presented in separate tables, the mean speed changes during a year time, on monthly or seasonal basis, are also illustrated in form of histograms.

From the tabular data, the similarities and differences at all five sites can be spotted. If one compares wind parameters at Staro Nagoričane with wind parameters at all other sites, the differ-

ence is evident in terms of higher mean wind speed and higher wind energy density. At this site the mean wind speed in almost every month/season is higher than 6 m/s, which is not the case with other sites, where the mean speed barely exceeds 4 m/s. In both the monthly and seasonal analyses, the wind energy density for each month/season is higher than 100 W/m² for Staro Nagoričane, while at other sites this parameter rarely exceeds 60 W/m². However, the higher wind speed generally gives the higher variation between the daily averages and the monthly or seasonal mean value. The standard deviation at Staro Nagoričane exceeds 1.5 m/s for most of the months/seasons, which is not case for other measurement sites. The measured data, as well as the area of the mountain terrain on this site, qualified Staro Nagoričane as possible location for construction of future wind park. The shortcomings of this location are bad roads and distance to the nearest transmission line.

From other four sites only Sveti Nikole site can be interesting regarding wind energy potential. At Sveti Nikole the mean wind speed reaches 5 m/s in certain months/seasons, and energy on surface unit reaches 100 W/m².

The one thing that is common for all five sites is the monthly and seasonal wind distribution. At all five sites the highest wind speed is present in winter and the lowest during the autumn. The exception is located only at Staro Nagoričane where the lowest energy potential can be spotted in the summer. On monthly basis, the strongest wind is found in February, while the poorest can be noticed in August.

This measurement campaign together with the first one show that the windiest regions in Macedonia are Ovče Pole and sites in proximity of Vardar valley, like Bogdanci and Gevgelija. Furthermore, in the near future more detailed analyses will be made for Staro Nagoričane location and possibility for building wind park.

Acknowledgements: The project presented herein has been supported by World Bank and Energy Agency of the Republic of Macedonia. The authors would like to express their appreciation for the opportunity to realize this complex project.

REFERENCES

- [1] Vladimir Dimčev, Vlatko Stoilkov, Krste Najdenkovski, Živko Kokolanski, Maja Celeska: *Establishing wind energy data base in the Republic of Macedonia*, Faculty of Electrical Engineering and IT, Skopje, September 2015.
- [2] Vladimir Dimčev, Vlatko Stoilkov, Krste Najdenkovski, Živko Kokolanski, Maja Celeska: *Summary report for*

- the second wind measurement campaign in the Republic of Macedonia*, Faculty of Electrical Engineering and IT, Skopje, April 2016.
- [3] Kiril Demerdžiev: *Wind energy potential measurement and data analysis*, bachelor thesis, Faculty of Electrical Engineering and IT, Skopje, October 2015.
- [4] I. Munteanu, A. I. Bratcu, N. A. Cutululis, E. Ceanga: *Optimal Control of Wind Energy Systems – Towards a Global Approach*, Springer-Verlag, London, 2008.
- [5] A. N. Celik: A statistical Analysis of Wind Power Density Based on the Weibull and Rayleigh Models at the Southern Region of Turkey, *Renewable Energy*, **29**, (2), 21–33 (2006).
- [6] Mahyoub H. Al-Buhairi, Ahmed Al-Haydari: Monthly and Seasonal Investigation of Wind Characteristics and Assessment of Wind Energy Potential in Al-Mokha, Yemen, *Energy and Power Engineering*, **4** (3), 125–131 (2012), doi: 10.4236/epe.2012.43017.
- [7] Sunday O. Oyedepo, Muyiwa S. Adaramola, Samuel S. Paul: Analysis of wind speed data and wind energy potential in three selected locations in south-east Nigeria, *International Journal of Energy and Environmental Engineering*, **3** (7), 1–11 (2012) (<http://www.journal-ijeee.com/content/3/1/7>).

DEALING WITH THE EFFECTS OF RANDOM TIME DELAY AND DATA DROPOUTS IN NETWORKED CONTROL SYSTEMS THROUGH ROBUST CONTROL

Gorjan Nadžinski, Mile Stankovski, Ivan Gočev

*Faculty of Electrical Engineering and Information Technologies,
"Ss. Cyril and Methodius" University in Skopje,
Rugjer Bošković bb, P.O. box 574, 1001 Skopje, Republic of Macedonia
milestk@feit.ukim.edu.mk*

A b s t r a c t: The concept of control over network is widely accepted and used in the world of automation, so the stability, safety, and robustness of the distributed and control systems are of key importance for their proper performance. Thus, it is essential to search for solutions of remote control problems like variable time-delay, data-loss, equipment malfunctions, and unauthorized network infiltrations. This paper gives an H_∞ robust control algorithm, which stabilizes a ZigBee networked control system in the presence of random delays, network overload, and data package loss.

Key words: networked control systems; robust control; H_∞ infinity control; data loss; random time delay; ZigBee

СПРАВУВАЊЕ СО ЕФЕКТИТЕ ОД СЛУЧАЈНИ ДОЦНЕЊА И ГУБЕЊЕ ПОДАТОЧНИ ПАКЕТИ ВО ВМРЕЖЕНИТЕ КОНТРОЛНИ СИСТЕМИ ПРЕКУ РОБУСНО УПРАВУВАЊЕ

А п с т р а к т: Концептот на управување преку мрежа е широко распространет и често употребуван во модерната автоматика, па затоа стабилноста, безбедноста и робусноста на дистрибуираните системи на управување се од клучно значење за нивно правилно функционирање. Затоа е неопходно да се бараат решенија на најчестите проблеми кај ваквите системи, како што се случајните временски доцнења, загубата на податоци, неисправноста на опремата и неавторизираните упади. Овој труд презентира робустен алгоритам за H_∞ управување, кој стабилизира вмрежен систем на автоматско управување преку мрежата ZigBee во присуство на случајни доцнења, преоптовареност на мрежата и загуба на податочни пакети.

Клучни зборови: вмрежени системи на автоматско управување; робусно управување; H_∞ управување; загуба на податоци; случајни временски доцнења; ZigBee

1. INTRODUCTION

A networked control system (NCS) is a term used to describe systems where sensors, actuators, and controllers are interconnected with a shared communication network [1]. The studying of these systems represents an interdisciplinary activity, as it encompasses both control theory and telecommunication. Therefore, in order to guarantee the stability and the quality performance of NCSs, analysis and design methods based both on the network and the control parameters are required [1, 2].

The situation where all the elements of a system share a common medium contributes for many advantages NCSs have in modern industry automation; especially the fact that systems are now far more efficient, flexible and easier to maintain. However, it also causes a wide range of drawbacks, some of the more serious being the conflicts of network access scheduling, and the subsequent data dropouts and time delays which these conflicts induce. This paper tests a control algorithm which is meant to robustly stabilize a given NCS by modeling the random time-delays and data package dropouts and uncertainties and perturba-

tions in the system, and by then setting the problem up as an H_∞ robust control problem and solving it. The system which will be used to test and simulate the algorithm on is a NCS where the communication network is based on the wireless ZigBee standard. ZigBee was chosen as it represents a standard with a growing popularity in industry and home automation.

The paper is organized as follows: firstly, a brief overview of NCS is given in Section 2, along with a survey on recent accomplishments in the field of control of NCS and dealing with delays, data dropouts, and scheduling conflicts; next, Section 3 will give a basic description of the ZigBee standard and a survey of its role in NCS; the design of the controller and the simulation results will be provided in Section 4, before Section 5 gives a conclusion and some ideas for future work.

2. NETWORKED CONTROL SYSTEMS

Networked control systems have long been an interesting research topic [1], [2], [3], [4]. Today they are widely used in industry and home automation, because NCSs provide flexibility and modularity, contributes for easier maintenance and adds redundancy to the entire control setup.

When all the components of a feedback control system are connected and communicating via a network which can be shared with other systems or entities, then this system can be classified as a networked control system (Fig. 1) [1]. In reality all connections between any two given system components, are established through some sort of network or medium. However, until recently modern control theory assumed that the exchange of signals, data, and information between the elements of a feedback control system, and the calculations inside the controller, take place instantaneously and without any delays or data losses. In reality, the emergence of large distributed systems and the growing complexity of control laws mean that the previous simplifications no longer hold. Networked control systems demand several previously unattended actions, such as modeling of the communication medium and its influence on the system, and taking into consideration the fact that signals travel in packages with a finite speed, and that sending, receiving, coding, and decoding of data takes time [3]. Therefore, occurrences such as random time delays, network access conflicts, and data dropouts have a significant impact on the NCS performance.

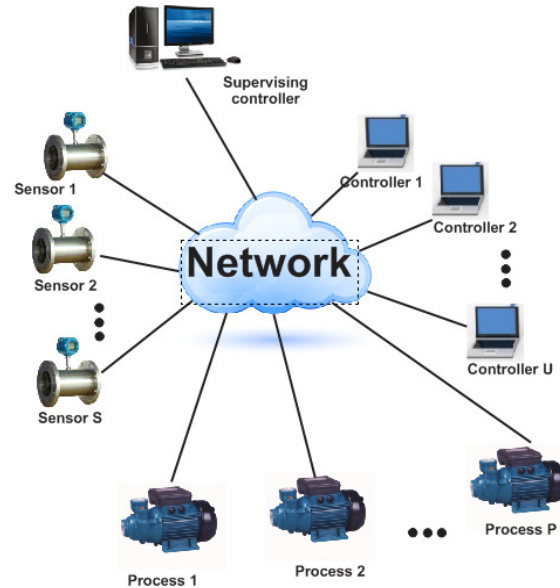


Fig. 1. Structure of a networked control system

The main efforts regarding NCS control are focused on dealing with the aforementioned problems. It has been generally agreed that the main issues which threaten the stability and the safety of NCS are network-induced delays, data loss, limited channel capacity, network security, and network access conflicts [1], [2]. There are three major approaches that are used for dealing with these issues [4]:

- the control-based approach explicitly takes into account the network characteristics and then considers the proper control methodologies for the given situation (i.e. the network is preexisting, and the controller is then derived);
- the network-based approach defines the control system independently from the network, and then states the network requirements accordingly (i.e. the system is preexisting, and suitable network parameters are then derived);
- the last approach represents a combination of the latter two, as it studies both the control and the network requirements in order to optimize the system.

The time delays in the networks occur due to the fact that the system shares the network with other elements and/or systems, so often the capacity of the network is overloaded. These network-induced delays can be modeled as constant delays (with the help of a buffer), or as variable and stochastic delays. The delays can be roughly lumped into two groups: the delays from the sensor to the

controller τ_{sc} (the time that passes from the moment the plant output is sampled, to the moment the controller starts calculating the next value of the control signal), and the delays from the controller to the actuator τ_{ca} (the time that passes from the moment the controller starts sending the data representing the control signal value, to the moment the actuator starts influencing the plant according to the sent signal). If we observe things on the physical level, we can expand to other types of delays, such as the waiting time delay τ_w (the time spent in waiting for the network to be available for sending data), the frame time delay τ_F (the time spent in framing the data packages on the transmitting side, and unpacking them at the receiving side), and the propagation delay τ_p (the time the data packages spend traveling to their destination). Of course, there exist many other network-induced delays, such as the ones caused by the network parameters and the communication protocol that is being used.

The choice of the network also has a significant influence on the time delays. If the NCS is connected with a cyclic service network (IEEE 802.4, IEEE 802.5, PROFIBUS), then the delays are deterministic and easy to incorporate into the system model; however, if the NCS is built on a random access network (Ethernet, CAN), then the delays are caused by the package collisions and are of a stochastic nature, which naturally makes them more difficult to model and to take into account.

Methods used to model the delays have ranged from conventional system identification tools [5], to using Markov chains [6], T-S fuzzy models [7], or ARMA models [8]. The compensation of the effects of this unwanted phenomenon has been done with many different approaches, such as: solving the problem as a LQG (Linear Quadratic Gaussian) problem [9]; modeling the delays as disturbances and posing the problem as a robust control problem, and thus trying to solve it with the respective existent tools [10]; introducing queues so as to represent the NCS as a time-invariant system [11]; using a state observer and a delay predictor and compensator, which relies on highly accurate modeling [12]; design of an event-based controller, which is therefore totally independent of the time delays [13].

Most recently, the framework for networked control systems has been extended to more approaches. These include but are not limited to [2]:

- quantization, which is motivated by the network capacity constraints;

- fault diagnosis, which is a process consisting of keeping track of system performance, and the detection, isolation, and identification of faults in the control loop;
- state estimation, which can be done by filtering (to estimate system states with noise), or by distributed data fusion (to improve the accuracy of the data by combining information from multiple network nodes);
- networked predictive control, which is based on general predictive control, but can refer to the system model or the network parameters (data package based predictive control, data-driven predictive control, etc.);
- cloud control, which merges the advantages of networked control system approaches and cloud computing.

Obviously, networked control systems play a significant role in automation and therefore the search for solutions of their most commonly occurring issues are of great interest.

3. THE ZigBee STANDARD IN NCS

The main reason for the growing popularity of wireless standards in industry automation is the increase in flexibility, effectiveness and range that is obtained when using a wireless network to implement a NCS. The ZigBee standard, developed by the IEEE workgroup 4 and the ZigBee Alliance at the beginning of the last decade, is a wireless communication standard specialized for low range, low cost, and long life Wireless Personal Area Networks. These characteristics make ZigBee and interesting candidate when considering a communication protocol for a NCS design [14].

The standard is based on the OSI model, but only contains the physical layer, the MAC sub layer, the network layer, and the application layer (user defined). The frequencies of operation are defined at 868 MHz in Europe, at 915 MHz in USA and Australia, and at 2.4 GHz worldwide, and the modulation methods used are DSSS (Direct-sequence spread spectrum) for the lower, and O-QPSK (offset quadrature phase-shift keying) for the higher frequencies. The standard defines three types of devices: coordinators (only one per network, represents the root of the network and coordinates all communication and network parameters), routers (responsible for data routing and network extension), and end-devices (representing the interface to the field devices, such as sensors and

actuators). The end-devices are active only for short intervals, enough to transfer data from the network to the process and/or vice-versa. This contributes to high efficiency and longer battery life of the communication modules. The most common network topologies are tree, star mesh network topology.

The ZigBee protocol supports two network access mechanisms: the non-beacon enabled mode, where a unslotted CSMA – CA (carrier sense multiple access with collision detection) is used, and the beacon enabled mode, where periodically emitted beacon signals coordinate the communication and the network access of the nodes. The latter method makes the communication more deterministic and also extends the battery life and lowers the duty cycle, as nodes are in sleep mode in between beacons.

As a wireless communication standard, lately ZigBee can often be found in many NCSs. Although its characteristics make it a somewhat preferable choice for a NCS standard, ZigBee NCSs still suffer from the same issues mentioned previously. A lot of research has gone into dealing with these problems specifically in ZigBee NCSs, more notably:

- Mouney, Juanole & Calmettes give the lowest acceptable sampling rate in these systems as 6.3 ms [15];
- Koubaa, Alves, Song & Nefzi [16] propose a slotted CSMA – CA mechanism in time sensitive applications;
- Rao & Marandin [17] give an improved back-off time calculation algorithm;
- Sobrino & Krishnakumar [18] define the black-burst network access mechanism;
- Umirov, Jeong & Park [19] propose the introduction of a play-back buffer which would introduce a fixed and deterministic delay in the network.

4. H_∞ CONTROLLER IMPLEMENTATION

The proposed H_∞ robust controller was designed by Yue, Han & Lam in [20]. It is used to stabilize an uncertain NCS, taking into account the effects of the network induced delays and the data dropout.

The authors represent the system with a continuous model with uncertainty, while at the same time modeling the delays and dropouts by introducing the sampling time and some discrete integer

values in the model. The total time delay in every iteration is a time-varying function of the quantity of data-loss in the network, and its value is given both an upper and a lower positive bound. The robust controller design theorem by Yue, Han & Lam states that a controller which stabilizes the system can be derived by solving a set of linear matrix inequalities given in [20]. The proof, which can also be found in [20], is based on the construction of a Lyapunov-Krasovskii functional and thus establishing the exponential stability criteria for the system, given by the said LMIs.

A controller as described above was designed for an unstable process (1) with further interference applied to the input (2), which was to be controlled and stabilized over a ZigBee network:

$$G(s) = \frac{0.1s^3 + 1.1s^2 + 0.975s + 0.225}{s^3 + s^2 - 0.25s - 0.25} \quad (1)$$

$$w(t) = \begin{cases} 0.3, & 2s \leq t \leq 4s \\ 0, & \text{otherwise} \end{cases} \quad (2)$$

The entire system was simulated in the special Matlab NCS extension TrueTime [21]. The network consisted of three different nodes (Fig. 2). The sensor/actuator node sampled data from the process in regular intervals and sent it to the controller, or acted on the process after receiving the control signal value from the controller. The controller node calculated the control signal upon receiving the measured values from the sensor, and then sent it to the actuator. The interference node applied a random uniform noise across the entire network. The controller also randomly executed an empty (dummy) task with higher priority than the control task, in order to simulate network overload. All the data propagation throughout the network was subjected to uniform random transport delays ranged between 0.1 s and 0.5 s (that is 2.5 times the sampling rate in the worst case).

Different scenarios were tested by using the opportunities provided by the TrueTime simulator. Simulations were run with different values for: the error and data loss probabilities, the physical positions of the nodes, the transmit power and receiver signal threshold, and the percentage of reduced network capacity. Other vital parameters were also established: the data rate was a standard 250 kbps, the sampling period was set at 200 ms, and the exponent of the path-loss function was set at 3.5, thus modeling air as the primary environment through which the radio waves travel. Also, the initial condition stated that in the beginning, the process output is $y = 1.7$.

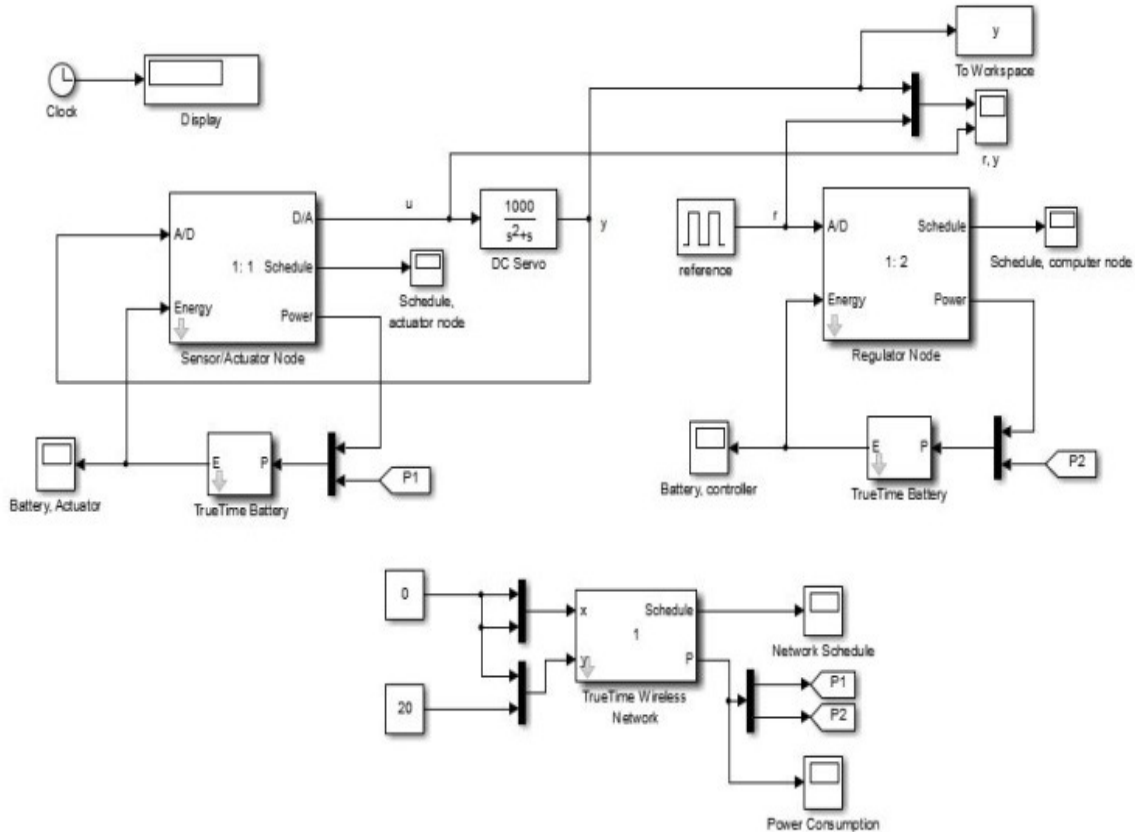


Fig. 2. Block structure of the NCS, as given in TrueTime

What follows are several graphs showing the system performance when the robust controller is implemented in different scenarios.

First and foremost, Fig. 3 shows the step response and the impulse response of the process, which makes clear the fact that we are dealing with an unstable system.

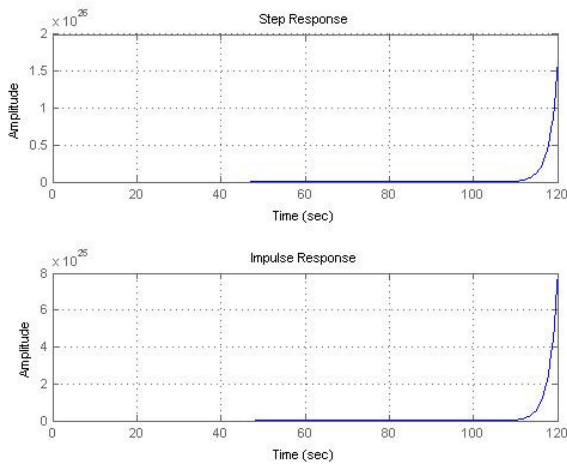


Fig. 3. Impulse and step response of the process

Next, in Fig. 4 we can see the system response when the controller is applied directly, when the network is not a part of the simulation. It is obvious that the controller has a stabilizing effect on the system, and a similar result can be seen in Fig. 5, where the system is being controlled over the ZigBee network, but in the absence of any negative effects.

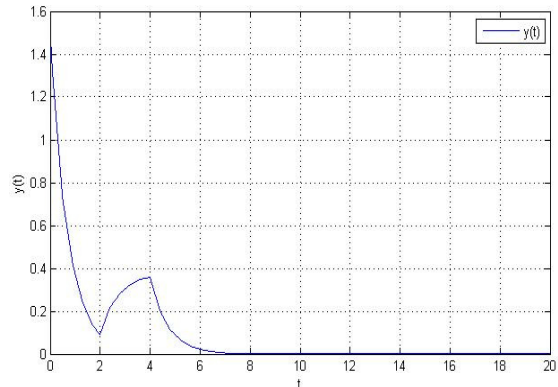


Fig. 4. Response of the controlled system without a network simulated

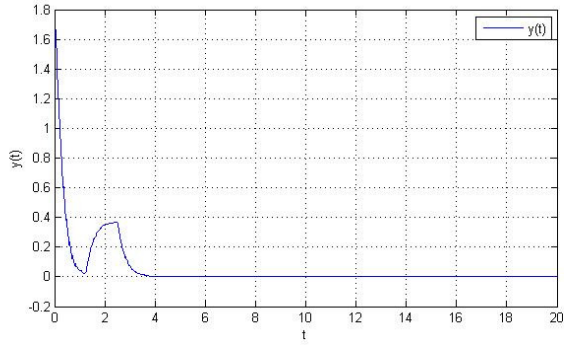


Fig. 5. Response of the NCS without any adverse effects simulated

Then, Fig. 6 shows simulation of the system performance in a situation with a probability of data loss of 25%. Also, there is no sending retry, as practice has shown that in most cases the data loss is not worth the extra delay induced by the retries. Fig. 7 shows the system performance when uniform interference is applied through the network, while Fig. 8 displays the response when the random transport delays are simulated.

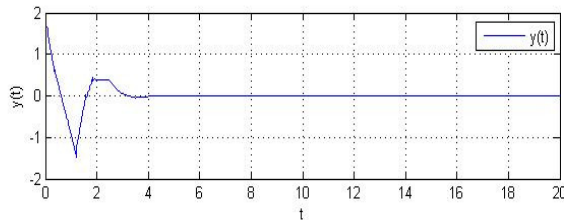


Fig. 6. Response of the NCS with 25% chance for data loss

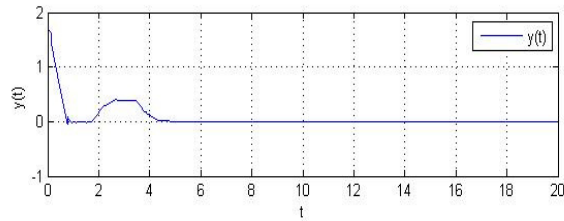


Fig. 7. Response of the NCS with uniform interference applied throughout the network

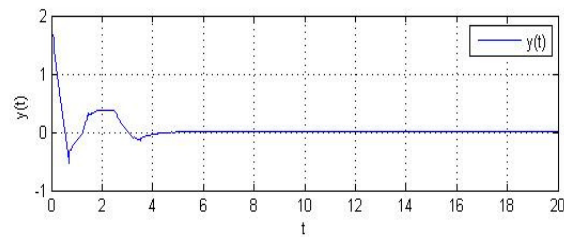


Fig. 8. Response of the NCS with random data propagation delays in the range [0.1s; 0.5s] simulated

It is obvious that the controller comfortably handles all the network obstructions, as the system responses conveniently converge to the stable state in all cases, only temporarily fluctuating around the 2s – 4s interval, when the external perturbation is applied to the system input.

Finally, Fig. 9 shows the system performance when all previously mentioned effects were being simulated at the same time: the propagation delay, the uniform disturbance, the 25% chance of data loss, and 70% network capacity. Yet again, the H_∞ controller successfully dealt with all these effects and stabilized the system in a relatively short time.

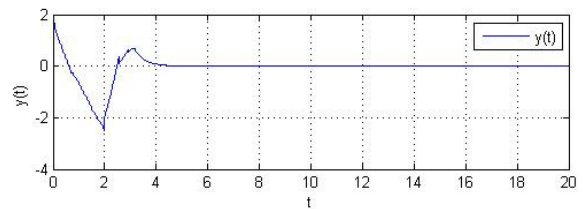


Fig. 9. Response of the NCS with 70% network capacity reduction and all other previous effects in action

Also, simulations of the system in the same conditions were made, but with different controllers applied. Fig. 10 shows the system performance under PID control (where the controller is tuned for the process without considering the network), and Fig. 11 displays the system performance with LQR control applied. Obviously, PID is unable to deal with the stochastic network occurrences, while LQR is not as effective as H_∞ , but it is still successful. This can be attributed to the fact that both LQR and H_∞ have the same core and are based on the same concepts of optimal control.

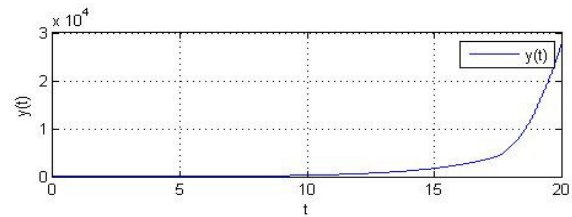


Fig. 10. NCS system response under PID control

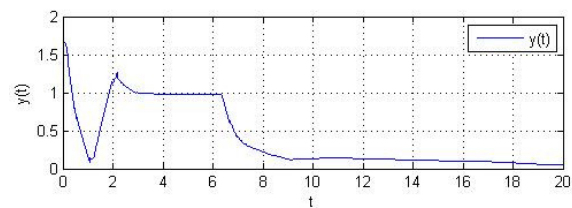


Fig. 11. NCS system response under LQR control

5. CONCLUSION

In this paper, a short overview of the issues of network induced delays and data loss in networked control systems was given. Then, ZigBee was proposed as a suitable choice for a communication protocol when implementing a wireless networked control system. An overview of important implementations of this standard in networked control systems was also elaborated. Finally, an existing H_∞ control algorithm for NCS was applied to an unstable and uncertain process through a ZigBee network, and the entire system was simulated in TrueTime in different scenarios in regard to the adverse network effects.

The analysis of the simulation results implied that the controller successfully handled the negative network occurrences, and thus it can be recommended to attempt a future practical implementation of this ZigBee robust controlled NCS, which would be found useful in many applications in industry, automation, smart sensor networks, and/or home automation.

REFERENCES

- [1] R. A. Gupta, M. Y. Chow: Networked Control Systems: Overview and research trends, *IEEE Transactions on Industrial Electronics*, pp. 2527–2535 (2010).
- [2] Y. Xia, Y. Gao, L. Yan, et al.: Recent Progress in Networked Control Systems – A Survey, *International Journal of Automation and Computing*, **12**, 4, 343–367 (2015).
- [3] L. Zhang, H. Gao, O. Kaynak: Network-Induced Constraints in Networked Control Systems – A Survey, *IEEE Transactions on Industrial Informatics*, **9**, 1, 403–416 (2013).
- [4] Z. Sun, H. Li, J. Wang: Recent advances in networked control systems, *International Conference on Control, Automation and Systems*, Seoul, Korea, 2007.
- [5] E. Kamrani, M. Mehraban: Modeling Internet delay dynamics using system identification, *Proceedings of ICIT*, 2006, pp. 716–721.
- [6] S. Shakkottai, A. Kumar, A. Karnik, A. Anvekar: TCP performance over end-to-end rate control and stochastic available capacity, *IEEE/ACM Transactions on Networking*, 2001, pp. 377–391.
- [7] H. Zhang, J. Yang, C. Su: T-S fuzzy-model-based robust H_∞ design for networked control systems with uncertainties, *IEEE Transactions on Indian Informatics*, 2007, pp. 289–301.
- [8] Q. Li., D. Mills: Jitter-based delay-boundary prediction of wide area networks, *IEEE/ACM Transactions on Networking*, 2001 pp. 578–590.
- [9] J. Nilsson, B. Bernhardsson, B. Wittenmark: Stochastic analysis and control of real-time systems with random delays, *Automatica*, **34**, 1, 57–64 (1998).
- [10] J. Hespanha, P. Haghshabrizi, Y. Xu: A survey of recent results in networked control systems, *Proceedings of IEEE*, 2007, pp. 138–162.
- [11] H. Chan, U. Ozguner: Closed-loop control of systems over a communication network with queues, *Int. J. Control*, **62**, 3, 493–510 (1995).
- [12] Y. Xia, G. Liu, D. Rees: H_∞ control for networked control systems in presence of random network delay and data dropout, *Proceedings of Chinese Control Conference*, 2006, pp. 2030–2034.
- [13] T. Tarn, N. Xi: Planning and control of internet-based teleoperation, *Proceedings of SPIE: Telemicrooperator and Telepresence Technologies*, 1998, pp. 189–193.
- [14] P. Baronti, P. Pillai, V. Chook, S. Chessa, A. Gotta, Y. F. Hu: Wireless Sensor Networks: A Survey on the State of the Art and the 802.15.4 and ZigBee Standards, *Journal of Computer Communications*, **30**, 7, 1655–1695 (2007).
- [15] G. Mouney, G. Juanole, C. Calmettes: On the implementation of one process control application type through a network considering three LANs: CAN, Wi-Fi, ZigBee, *17th OFAC World Congress*, 2008.
- [16] A. Koubaa, M. Alves, Y. Song, B. Nefzi: Improving the IEEE 802.15.4 slotted CSMA-CA for time-critical events in wireless sensor networks, *Workshop of Real-time Networks, Satellite workshop for ECRTS*, Dresden, Germany, 2006.
- [17] V. Rao, D. Marandin: Adaptive backoff exponent algorithm for ZigBee, *Next Generation Teletraffic and Wired/Wireless Advanced Networking*, 2006, pp. 501–516.
- [18] J. Sobrino, A. Krishnakumar: Quality of service in ad-hoc CSMA networks, *IEEE Journal on Selected Areas in Communications*, 1999, pp. 1535–1568.
- [19] U. Umirov, S. Jeong, J. Park: Applicability of ZigBee for real-time networked motor control systems, *International Conference on Control, Automation and Systems*, Seoul, Korea, 2008.
- [20] D. Yue, Q. Han, J. Lam: Robust H_∞ control and filtering of networked control systems, *Networked Control Systems: Theory and Applications*, London: Springer, 2008, pp. 121–151.
- [21] A. Cervin, M. Ohlin, D. Henriksson: Simulation of networked control systems using TrueTime, *Proceedings of the 3rd International Workshop on Networked Control Systems: Tolerant to Faults*, 2007.

DYNAMIC MODELLING AND ASYMPTOTIC POINT STABILIZATION CONTROL OF TWO DIFFERENTIAL WHEELED MOBILE ROBOT

Drilon Bunjaku¹, Jovan Stefanovski², Mile Stankovski³

¹*Informatics Engineering, FMCE at University of Mitrovica, Republic of Kosovo*

²*Control & Informatics Div., JP "Streževo", Bitola, Republic of Macedonia*

³*Faculty of Electrical Engineering and Information Technologies,*

"Ss. Cyril and Methodius" University in Skopje,

Rugjer Bošković bb, P.O. box 574, 1001 Skopje, Republic of Macedonia

drilon.bunjaku@uni-pr.edu

Abstract: In this paper, we present the dynamic modelling of two differential wheeled mobile robot, and also propose an easily implementable control strategy, for stabilizing the nonlinear and nonholonomic WMR system around the desired final posture. The asymptotic stability is approached by using two PI controllers. The dynamic model of WMR is used in the simulation environment of Matlab/Simulink, for testing the proposed stabilizing control strategy. The validity of control strategy is verified by the simulation results.

Key words: wheeled mobile robot; dynamic modelling; nonholonomic robots; stabilization control; linear controller

ДИНАМИЧКО МОДЕЛИРАЊЕ И КОНТРОЛА НА ПРИБЛИЖУВАЊЕТО КОН АСИМПТОТСКАТА СТАБИЛНОСТ НА МОБИЛЕН РОБОТ СО ДВЕ ДИФЕРЕНЦИЈАЛНИ ТРКАЛА

Апстракт: Во овој труд е претставено динамичко моделирање на мобилен робот со две диференцијални тркала и предложена е стратегија за контрола која може лесно да се имплементира за стабилизирање на нелинеарниот и нехолономичен систем на мобилен робот со тркала околу посакуваната крајна положба. Приближувањето кон асимптотската стабилност е изведено со два ПИ контролера. Динамичниот модел на мобилниот робот со тркала е искористен во симулацијата околина на Matlab/Simulink за тестирање на предложената стратегија за контрола на стабилизацијата. Валидноста на стратегијата е верификувана со резултатите од симулацијата.

Клучни зборови: мобилен робот со тркала; динамичко моделирање; нехолономични работи; контрола на стабилизација; линеарен контролер

1. INTRODUCTION

Nowadays, the complexity and hazardous of working process and working environment in many fields have been increased. Consequently, as a result, the interest of manipulation and mobile robots application have been exponentially increased last few years as well (for further details consult [1], [2]). We may find an application of mobile robot in fields like mining, military, medicine, aerospace, industry, under water, etc., which require high accuracy, responsibility, and reliability.

Therefore, wheeled mobile robots as a particular category of mobile robot are widely studied during the last decade, because of their simplicity and applicability. Wheeled mobile robots (WMR) are wheeled vehicles or platforms which are supposed to navigate from the initial point toward the desired or final point in an autonomous manner.

The mobile robot has visual, proximity, positioning and object detection capabilities [3].

The performance of the WMR depends on many factors, like types of sensors and actuators,

their sensitivities and limitations, but mainly it depends on the robustness of the designed controller. Controllers should be fast responsive and immune to the disturbances and parameter variations.

There are many research papers focused on designing the control of a wheeled mobile robot. Depending on the configuration of the robot, many of them have proposed a controller which track the desired trajectory in the most effective way in 2D space [4]–[6]. Mostly include the kinematic model of WMR, while very few include dynamic model due to the complexity of the model and high non-linearity degree.

However, because of the center-of-gravity (COG) shifts and load changes caused by large loads and the serious nonlinear friction at the high speed, the accuracy of the path-tracking decreases and the robots stray from the predefined path, which clearly increases the danger of hitting obstacles. Therefore, motion control is one of the most fundamental topics for mobile robots [7].

The navigation problem of mobile robots could be separated into four basic problems:

1. Obstacle avoidance,
2. Autonomous trajectory generation (path planning),
3. Trajectory tracking,
4. Point stabilization.

All the afore mentioned navigation problems ought to use localization sensors system. In [8] authors presented the impact of using the dead reckoning sensors on the improvement of positioning accuracy of GPS and DGPS in application of land vehicles. The road construction vehicles, farm vehicles and mining vehicles require accuracy of the order of a few centimetres. Hence, carrier phase differential GPS (CP-DGPS) technology provides such requirement. In [9] a nonlinear velocity independent control law has been designed for the farm tractor (relies upon the kinematic model) to perform both curved paths and straight lines following by using a CP-DGPS sensor. The GPS is limited for the indoor mobile robots application with high accuracy requirements. Therefore, the indoor GPS system with fix beacons could be used.

In the following text we group the cited papers by the separation, thus for the first and second navigation problem: in [10], authors elaborated a technique of constructing (generating) a feasible trajectory for WMR by assembling arcs of a simple curves, and extended the research by adding fuzzy logic control for obstacle avoidance.

In [11] authors analyzed the controllability of the nonholonomic multibody robots with inequality constrained, and proposed an algorithm for generating path planning based on a bitmap discretisation.

In [12] authors presented an algorithm for generating a trajectory by using simple arcs and straight lines. Furthermore, achieving obstacle avoidance through the composition of trajectories based on the set of configuration sub-goals that lead to collision-free motion.

This paper is confined to the trajectory tracking and the point-stabilization for WMRs moving/operating in the 2D real-world space, within the respective separation of navigation problem.

– Regarding the third navigation problem: In [13] a new kinematical control method, named Lyapunov-based Guidance Control (LGC), has been proposed for the trajectory tracking of non-holonomic WMRs. Through the application of back stepping methodology, in [14] is proposed a control scheme for trajectory tracking for the considered augmented model including kinematics and dynamics of the mobile robot.

In [6] authors proposed higher order sliding motion control based on the kinematic model for tracking the trajectory, the outcome results were satisfactory but it requires highly processing power compared to existing control methods. In [7] a digital acceleration control method is proposed for the path-tracking of a wheeled mobile robot to deal with COG shifts and load changes.

In [15] authors presented dynamic modelling of the WMR by using Lagrange formalism, and proposed two motion control laws for dynamic object tracking by using Lyapunov direct method and computed torque method.

– Regarding the fourth navigation problem: In [16] the Point Stabilization of Mobile Robots is achieved by using Nonlinear Model Predictive Control.

In [17] authors elaborated a method for posture stabilization of the wheeled mobile robot by using a hybrid automata-based controller.

In [18] authors extended the nonholonomic integrated model by double integrating it, because it fails to capture the cases where both kinematic and dynamic of WMR are taken into account. Then, logic-based hybrid controller was proposed that yields global stability and convergence of the closed-loop system to an arbitrarily small neighborhood of the origin.

Motivated by the scientific approaches which are used in aforementioned works, the problem of interest in this paper is to design a stabilizing control about a desired posture. In such a way, that it will bring WMR to navigate from initial posture to the predefined desired posture, and solve the problem of asymptomatic stability. Besides the existing methods, the novelty of this paper is the simplicity of understanding, and easily implementable in the practical real slow-speed operating WMR.

The organization of the paper is as follows. In Section 2 it is presented the kinematic modelling of the robot. Continuously, the elaboration of dynamic modelling of two differential wheeled mobile robot is given in Section 3. In Section 4 is presented the proposed control strategy for solving the problem of point stabilization, and it is followed by subsections of robot position control and robot orientation control. The simulation results for the proposed control system design are given in Section 5. The conclusion remarks are given in section 6.

Remarks on the notation. Matrices are denoted by upper-case letters, and vectors and scalars are denoted by lower-case letters.

2. KINEMATIC MODELLING

The number of possible wheeled mobile robots realizations is almost infinite, depending on the number, type, implementation, geometric characteristics, and motorization of the wheels [19].

The mobile robot in this paper is driven by two independent differential wheels, and one free-wheel or caster wheel for balancing the platform.

The robot posture in Cartesian space x, y, θ will be described by the global reference coordinate frame $\{0\}$.

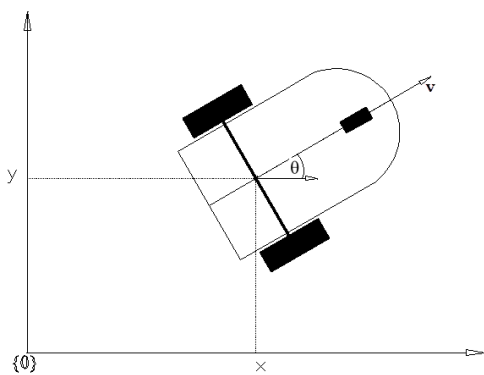


Fig. 1. WMR in 2D Cartesian space

Before proceeding with kinematic model some assumptions will be defined:

- 1) Both motors produce the same torque;
- 2) There is no friction on wheels or pure rolling without slipping;
- 3) The distribution of mass is uniform;
- 4) The robot will run on a flat surface, meaning the potential energy is zero;
- 5) There is no deformation on wheels or terrain.

The robot posture in Cartesian coordinate frame is specified by the generalized coordinate vectors $\mathbf{q}_B = [x_B, y_B, \theta]^T$ or $\mathbf{q}_G = [x_G, y_G, \theta]^T$. The point B is represented by x_B and y_B , which is the center of the wheel axis, while by x_G and y_G is represented the center of gravity of the platform. The distance between the center of the wheel axis B and the center of gravity G of the platform is denoted by l , while heading of point G with respect to point B defined the orientation angle θ of the platform.

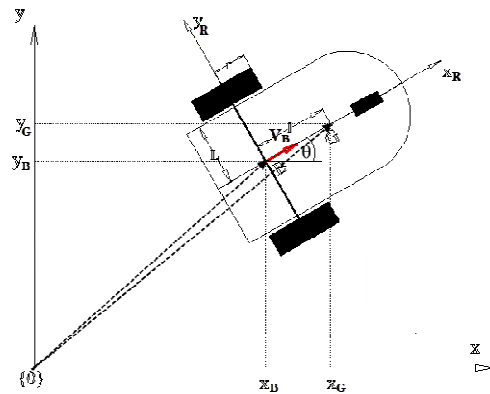


Fig. 2. Generalized coordinate vectors q_B, q_G in R^3

Linear velocity of the right respectively left wheel could be expressed as a function of it is angular velocity $v_r = r\dot{\theta}_r$ and $v_l = r\dot{\theta}_l$, where r is the radius of the driving wheel.

Based on the condition of assumption 2, the linear and angular velocity at point B could be expressed by the following

$$v = \frac{(v_r + v_l)}{2} = \frac{r\dot{\theta}_r + r\dot{\theta}_l}{2}, \quad (1)$$

$$\omega = \frac{(v_r - v_l)}{2L} = \frac{r\dot{\theta}_r - r\dot{\theta}_l}{2L}. \quad (2)$$

In matrix form:

$$\begin{bmatrix} v \\ \omega \end{bmatrix} = \begin{bmatrix} \frac{r}{2} & \frac{r}{2} \\ \frac{r}{2L} & -\frac{r}{2L} \end{bmatrix} \begin{bmatrix} \dot{\theta}_r \\ \dot{\theta}_l \end{bmatrix} = D \begin{bmatrix} \dot{\theta}_r \\ \dot{\theta}_l \end{bmatrix} \quad (3)$$

The position of center of gravity G could be described by the global reference frame $\{0\}$ in a vectorial form, in a complex plane:

$$\begin{aligned} x_g + \bar{j} y_g &= (x_b + \bar{j} y_b) + l(\cos \theta + \bar{j} \sin \theta) = \\ &= (x_b + \bar{j} y_b) + l e^{j\theta} \\ \overrightarrow{OG} &= \overrightarrow{OB} + \overrightarrow{BG} = \overrightarrow{OB} + l e^{j\theta}. \end{aligned} \quad (4)$$

If we differentiate the equation (4), the velocity relations could be found:

$$\overrightarrow{v_G} = \overrightarrow{v_B} + \bar{j} l \dot{\theta} e^{j\theta} \quad (5)$$

$$\overrightarrow{v_G} = \dot{x}_B + \dot{y}_G \quad (6)$$

$$\overrightarrow{v_B} = \dot{x}_B + \dot{y}_B = v e^{j\theta} \quad (7)$$

Through the substitution of (7) in (5), it is possible to express the velocity of point G in terms of the general linear v and angular $\dot{\theta}$ velocities:

$$\overrightarrow{v_G} = v e^{j\theta} + \bar{j} l \dot{\theta} e^{j\theta} = (v + \bar{j} l \dot{\theta}) e^{j\theta} \quad (8)$$

The velocity of point G could be expressed in term of the real and imaginary part, by approaching the substitution of (6) in (8):

$$\begin{aligned} \dot{x}_G &= v \cos \theta - l \omega \sin \theta \\ \dot{y}_G &= v \sin \theta + l \omega \cos \theta \end{aligned} \quad (9)$$

Wheeled mobile platforms are subject to non-integrable kinematic constraints, known as nonholonomic constraints (17). The nonholonomic constraint could be defined by eliminating the parameter v from equation (9):

$$\dot{y}_G \cos \theta - \dot{x}_G \sin \theta - l \omega = 0 \quad (10)$$

From equation (10) for $\theta = 0$ the velocity in y direction is zero, $\dot{y}_G = 0$, while for $\theta = \frac{\pi}{2}$ the velocity in x direction is also zero, $\dot{x}_G = 0$. This proves that as long as the assumption 2 holds, the nonholonomic WMR could only move in direction perpendicular to the wheels axis.

The definition of relationship between velocity of generalized coordinate vector \dot{q}_G as an output and controlled input of linear v and angular ω velocities is given by the following matrix:

$$\begin{bmatrix} \dot{x}_G \\ \dot{y}_G \\ \dot{\theta} \end{bmatrix} = \begin{bmatrix} \cos \theta & l \sin \theta \\ \sin \theta & l \cos \theta \\ 0 & 1 \end{bmatrix} \begin{bmatrix} v \\ \omega \end{bmatrix} = G(\theta) \begin{bmatrix} v \\ \omega \end{bmatrix}. \quad (11)$$

Through the application of equation (3) in (11), it is presented the relationship between the velocity of generalized coordinate vector \dot{q}_G and the controlled angular velocities of right respectively left wheel:

$$\dot{q}_G = G(\theta) \cdot D \begin{bmatrix} \dot{\theta}_r \\ \dot{\theta}_l \end{bmatrix}. \quad (12)$$

Now equation (12) represents the kinematic model of the WMR in implicit form. The explicit form of a kinematic model of WMR is given by the equation (13).

$$\begin{bmatrix} \dot{x}_G \\ \dot{y}_G \\ \dot{\theta} \end{bmatrix} = \begin{bmatrix} \frac{r}{2} \cos \theta - \frac{r}{2L} l \sin \theta & \frac{r}{2} \cos \theta + l \sin \theta \\ \frac{r}{2} \sin \theta + \frac{r}{2L} l \cos \theta & \frac{r}{2} \sin \theta - \frac{r}{2L} l \cos \theta \\ \frac{r}{2L} & \frac{r}{2L} \end{bmatrix} \begin{bmatrix} \dot{\theta}_r \\ \dot{\theta}_l \end{bmatrix} \quad (13)$$

Since at the output of the system the Degree of Freedom (DoF) which need to be controlled $[\dot{x}_G, \dot{y}_G, \dot{\theta}]$ is three, and at the input of the system the level of controllable DoF is two $[\dot{\theta}_r, \dot{\theta}_l]$, we confirm that the system (13) is nonholonomic. A system is nonholonomic when the controllable degree is less than the total degree which needs to be controlled, otherwise, the system is holonomic.

According to remarks (page 187) of [20], nonholonomic systems do not satisfy Brockett condition. Therefore, by using continuous control laws, it is impossible to arrive smooth asymptomatic stability at the desired point. However, approximated asymptotic stability region could be achieved, (see the last paragraphs of Section 4).

3. DYNAMIC MODELLING

Let's assume that both wheels will be rotated with the same angular velocity, but opposite direction of rotation, thus robot will rotate around its center of wheel axis (point B), as a result dynamic

torque would act, and the point G will pass a circle with radius l . Therefore, robot on the way to the final position and orientation, will create a trajectory by moving within this circle, see Figure 3. When the robot gets a curved road, at the center of gravity acts resultant acceleration, which could be expressed as:

$$\vec{a}_R = \vec{a}_d + \vec{a}_r + \vec{a}_{cor} \quad (14)$$

denoting by \vec{a}_d – the displacement acceleration, \vec{a}_r – the relative acceleration and \vec{a}_{cor} – Coriolis acceleration. The displacement and relative acceleration can be separated into their normal and tangential components.

$$\vec{a}_R = \vec{a}_{dn} + \vec{a}_{dt} + \vec{a}_{rn} + \vec{a}_{rt} + \vec{a}_{cor} \quad (15)$$

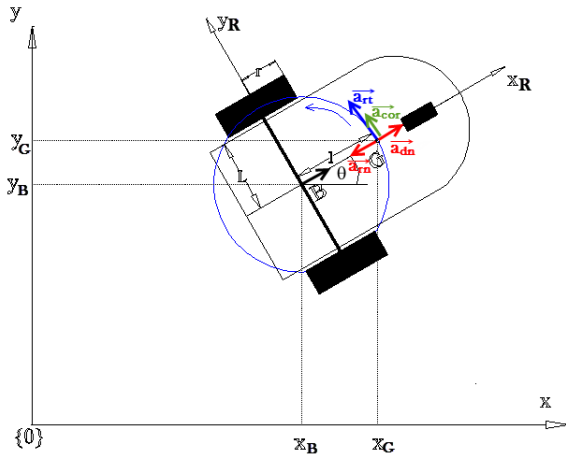


Fig. 3. Radial and tangential acceleration components

Since the WMR is nonholonomic it means that robot do not make displacement perpendicular to the wheel axis, hence $\vec{a}_{dt} = 0$. Considering that distance l doesn't change is constant, means that \vec{a}_{dn} is same for point B and point G .

The acceleration of the center of gravity G could be found by the derivation of equation (8)

$$a_G = (v - l\dot{\theta}^2)e^{j\theta} + j(l\ddot{\theta} + v\dot{\theta})e^{j\theta}. \quad (16)$$

The first component is the radial component, while the second component is the tangential component.

For the simplicity of understanding the equation (16), refer to the Figure 3. The correlation between (15) and (16) might be presented as:

$$a_G = (a_{dn} - a_{rn})e^{j\theta} + j(a_{rt} + a_{cor})e^{j\theta}. \quad (17)$$

The forward movement is produced by the dynamic force F_d and the rotational motion is produced by the dynamic torque τ_d . The magnitude of these forces are given by the following equation:

$$\begin{aligned} F_d &= m \cdot a_{rad} = m \cdot (v - l\dot{\theta}^2) \\ \tau_d &= (I_g + ml^2)\ddot{\theta} + mlv\dot{\theta} \end{aligned} \quad (18)$$

where: m is the total mass of the platform without wheels, I_g is the moment of inertia calculated for rotation around the center of mass. The dynamic force F_d and dynamic torque of the robot τ_d are generated by the dynamic driven torque of the right τ_{mr} and left τ_{ml} motors:

$$\begin{aligned} F_d &= \frac{(\tau_{mr} + \tau_{ml})}{r} \\ \tau_d &= L \frac{(\tau_{mr} - \tau_{ml})}{r} \end{aligned} \quad (19)$$

The dynamic model of WMR is represented in matrix form by merging the equations (18) and (19):

$$M\dot{v} + C(v) = B\tau \quad (20)$$

where:

$$\left. \begin{aligned} M &= \begin{bmatrix} m & 0 \\ 0 & I_g + ml^2 \end{bmatrix}, \\ C(v) &= \begin{bmatrix} -ml\dot{\theta}^2 \\ mlv\dot{\theta} \end{bmatrix}, \\ B &= \begin{bmatrix} \frac{1}{r} & \frac{1}{r} \\ \frac{L}{r} & -\frac{L}{r} \end{bmatrix}, \end{aligned} \right\} \quad (21)$$

The matrix M represents a positive definite inertial matrix, matrix C represents Coriolis and centrifugal matrix, B represents the input transformation matrix, $\tau = [\tau_{dr}, \tau_{dl}]^T$ and $\dot{v} = [\dot{v}, \dot{\omega}]^T$ represent vectors of controlled input dynamic torques and controlled output accelerations.

The dynamic model (20) is based on the coordinates of the WMR platform, for better modelling the physical system of WMR, the dynamic model should be extended including the dynamic models of actuating motors. The equation of motion could be written as:

$$\begin{aligned} I_{wm} \dot{\omega}_r + \tau_{dr} &= \tau_{mr} - \tau_{fr} \\ I_{wm} \dot{\omega}_l + \tau_{dl} &= \tau_{ml} - \tau_{fl} \end{aligned} \quad (22)$$

denoting by: I_{wm} – the inertia of each wheel plus the inertia of motor including the rotor inertia, τ_{mr} , τ_{ml} – the torque exerted from right, respectively left motor, and τ_{fr} , τ_{fl} – the friction torque from right respectively left motor.

The dynamic model of WMR including the dynamic of wheels plus motors could be defined through the substitution of equation (22) in (20) as:

$$M_{wm} \dot{v} + C(v) + B \tau_f = B \tau_m \quad (23)$$

where:

$$\left. \begin{aligned} M_{wm} &= \begin{bmatrix} m & \frac{2}{r^2} I_{wm} \\ 0 & I_g + ml^2 + \frac{2l^2}{r^2} I_{wm} \end{bmatrix}, \\ C(v) &= \begin{bmatrix} -ml\dot{\theta}^2 \\ mlv\dot{\theta} \end{bmatrix}, \\ B &= \begin{bmatrix} \frac{1}{r} & \frac{1}{r} \\ \frac{l}{r} & -\frac{l}{r} \end{bmatrix}, \\ \tau_m &= \begin{bmatrix} \tau_{mr} \\ \tau_{ml} \end{bmatrix}, \tau_f = \begin{bmatrix} \tau_{fr} \\ \tau_{fl} \end{bmatrix}, \end{aligned} \right\} \quad (24)$$

The matrix M_{wm} indicate the reduced form of positive definite Inertia matrix, while τ_m and τ_f represent vectors of generated motor torque and friction torque respectively. The dynamic modelling could be derived also by using Lagrange dynamic equation of motion. The dynamical modelling of two nonholonomic WMR using Lagrange formalism could be found in [21].

4. CONTROL STRATEGY

The control problem of robot stabilization could be separated in two individual control problems: robot positioning control and robot orientation control. The RPC must provide a control in such a way that robot will achieve the desired position (x_d, y_d) , regardless the orientation of the robot. The ROC besides achieving the desired position must assure achieving desired orientation of the robot (x_d, y_d, θ_d) .

The intention of control engineering is to find a feedback stabilizable controller, such that, the equilibrium point of the closed-loop system is asymptotically stable. Since the system is nonlinear

and non-holonomic, it means that there do not exist smooth time invariant state feedback controller, which renders the equilibrium point of a closed loop system being asymptotically stable.

A) Robot position control

The control problem is to find a solution to bring the WMR to the final position regardless the orientation. Since the Cartesian coordinates of the actual position of the robot are known from the GPS sensor, and coordinates of the final position are known to us from the task request (x_d, y_d) , then it is possible through simple equations to calculate the distance to a final position. The illustration of the problem is presented in Figure 4, denoted by Δr – the distance to the final position, α – the angle between the final position and Cartesian system, and θ – the heading angle of the robot.

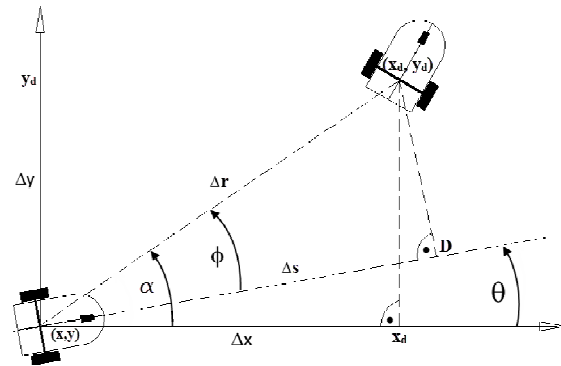


Fig. 4. Geometric solution of RPC

In order to solve the problem, assume a point D somewhere in the line of robot heading direction with distance Δs , such that, it will be the closest point from the final point. The angle to the final position from the heading orientation of the robot is defined as ϕ . In other words, it is the error between the assumed point D and the final point (desired position), defined as:

$$\cos \phi = \frac{\Delta s}{\Delta r} \quad (25)$$

The desired point (x_d, y_d) will be achieved if system control is designed, such that renders the $\Delta s \rightarrow 0$, $\phi \rightarrow 0$. Therefore, the positioning control problem will be solved by implementing such control strategy that provides such convergences.

The distance error respectively angular error are denoted by e_s , e_ϕ , and defined as:

$$\begin{aligned}
 e_s &= \Delta s = \Delta r \cdot \cos \phi = \\
 &= \sqrt{(x_d - x)^2 + (y_d - y)^2} \cdot \cos \phi = \quad (26) \\
 &= \sqrt{(\Delta x)^2 + (\Delta y)^2} \cdot \cos \phi
 \end{aligned}$$

$$\begin{aligned}
 e_\phi &= \phi = \alpha - \theta = \arctan\left(\frac{y_d - y}{x_d - x}\right) - \theta = \\
 &= \arctan\left(\frac{\Delta y}{\Delta x}\right) - \theta \quad (27)
 \end{aligned}$$

Through the implementation of above equations, in Figure 5, is presented the Block scheme of proposed control strategy for robot positioning.

The dynamic model is related with variable s and θ , by the following substitution

$$v = [v, \omega]^T = [\dot{s}, \dot{\theta}]^T.$$

The relation between the displacement of right and left wheel and the control signal s and θ , could be expressed by taking the inverse of equation (3), integrating it on both sides of expression and neglecting the integration constants.

$$\begin{bmatrix} \theta_r \\ \theta_l \end{bmatrix} = D^{-1} \begin{bmatrix} s \\ \theta \end{bmatrix} = D^{-1} \begin{bmatrix} u_s \\ u_\theta \end{bmatrix} = \begin{bmatrix} \frac{1}{r} & \frac{l}{r} \\ \frac{1}{r} & -\frac{l}{r} \end{bmatrix} \begin{bmatrix} u_s \\ u_\theta \end{bmatrix} \quad (28)$$

Equation (28) is used in the simulation environment to generate the reference inputs (outputs) on the wheels actuator control systems, when the vector $[s, \theta]^T$ is substituted by the control vector $[u_s, u_\theta]^T$.

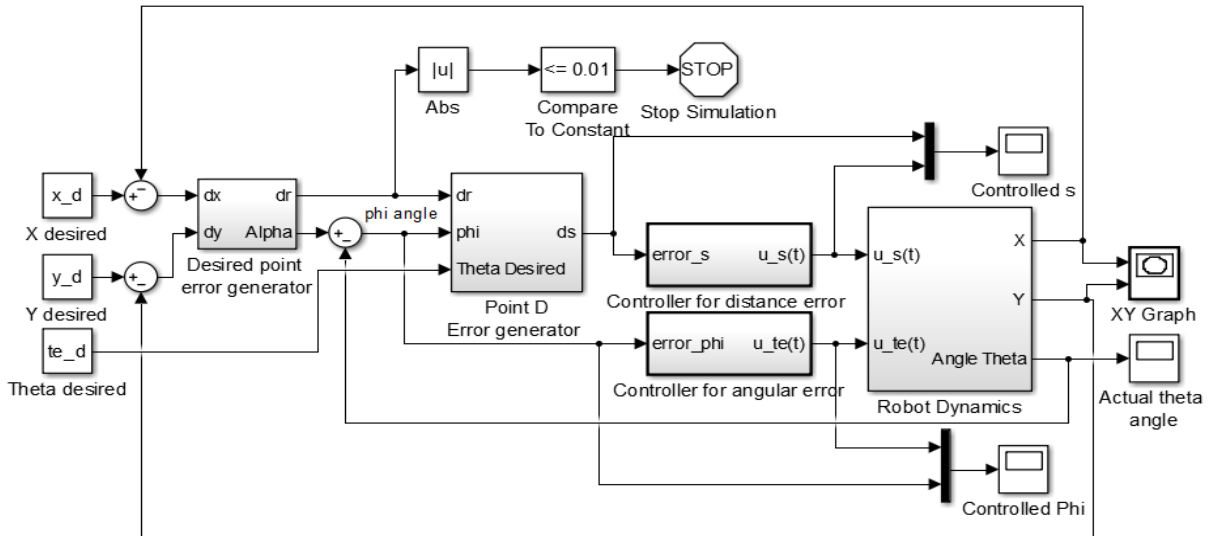


Fig. 5. Block schema of RPC Structure

B) Robot orientation control

The robot is not supposed to move straight to the final position, therefore, the control strategy design will take in consideration the orientation of the WMR at the final position.

The difference between the desired orientation angle θ_d and the angle to the final position α is defined by β , as $\beta = \theta_d - \alpha$. In order to solve the problem of the desired final orientation of the robot, assume a reference point R , as we would have rotated a final point for angle β in a clockwise direction, related to point B with radius Δr , see Figure 6.

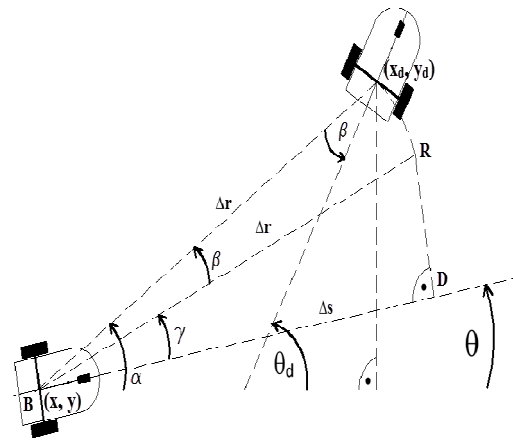


Fig. 6. Geometric solution of RPC and ROC

As the robot moves forward closer to the final posture, the desired orientation angle θ_d and final posture angle α will keep increasing, while β decreases. Continuously, as β decreases the reference point R will attempt to approach the final point with desired orientation.

Now, the angle between the heading direction of the robot and the reference point is denoted by γ , which could be expressed as

$$\gamma = e_\phi - \beta = 2\alpha - \theta_d - \theta.$$

The distance error respectively the angular error to the final orientation are denoted by e_s , e_θ as:

$$e_s = \Delta s = \Delta r \cdot \cos(\gamma) = \Delta r \cdot \cos(2\alpha - \theta_d - \theta)$$

$$e_\theta = \gamma$$

By applying the above formulas of this paper, in Figure 7 is presented the block scheme of proposed control strategy for position and orientation of WMR.

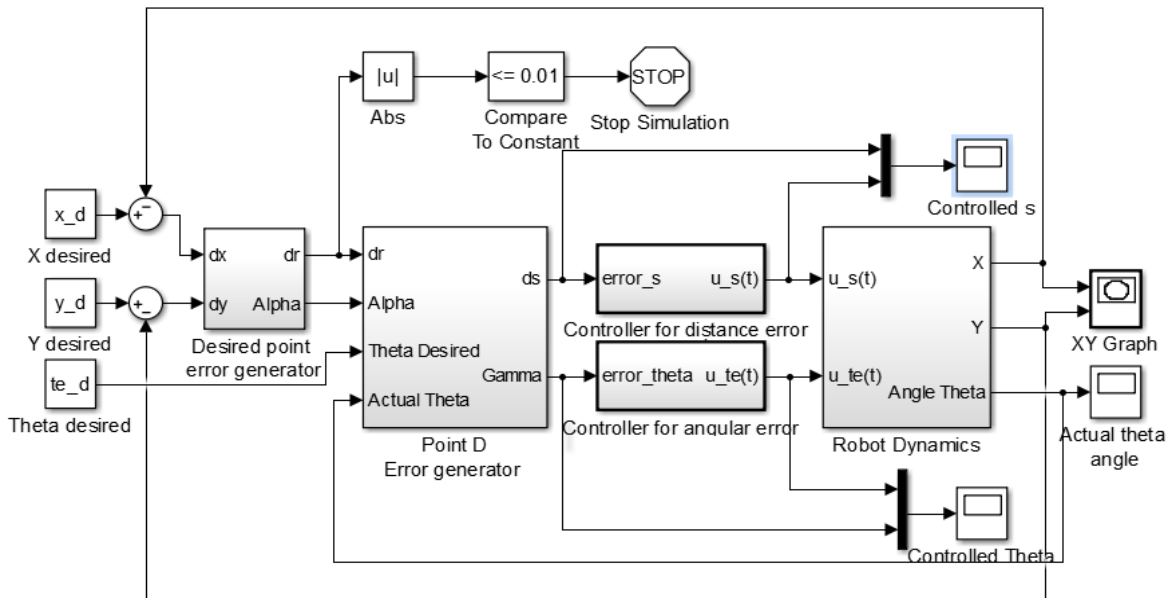


Fig. 7. Block scheme of RPC and ROC structures

In order to encapsulate the idea of robot stabilization about the desired posture, it could be summarized that: RPC attempts to move the robot toward point D , but simultaneously as $t \rightarrow \infty$, $\gamma \rightarrow 0$ point D approaches reference point R . While ROC as $t \rightarrow \infty$, $\beta \rightarrow 0$ will try to approach continuously reference point R toward final posture. The accuracy and sensitivity of sensor used for measuring the position of the platform, determines the circular region from the final point with a radius ε . When the mobile robot gets within this circular region $\Delta r \leq \varepsilon$, then it is approximated that both linear error e_s and angular error e_θ are zero. Therefore, at this point the approximated asymptotic stability problem is accomplished based on the geometric approach, wherein the proposed control strategy is subjected too.

Often in text books, approximated asymptotic stability region is referred as asymptotic stability, so we do in this paper.

5. SIMULATION RESULTS

The simulation results are obtained by using Matlab/SIMULINK. Since it is considered slow-speed operating two-wheeled mobile robot, any linear controller could be used for the proposed control strategy for stabilization of the robot about a desired posture. In this paper, two PI controllers are used, one for controlling the distance error e_s and the other for controlling the angular error e_θ .

$$\left. \begin{aligned} u_s(t) &= K_{ps} \cdot e_s(t) + K_{is} \cdot \int_0^t e_s(t) dt, \\ u_\theta(t) &= K_{p\theta} \cdot e_\theta(t) + K_{i\theta} \cdot \int_0^t e_\theta(t) dt, \end{aligned} \right\} \quad (29)$$

The performance of PI controllers could be adjust by tuning the gain parameters. Equation (23) is used to model Robot Dynamics block. The physical parameters taken to model the robot in the simulation are given: $m = 25$ kg, $r = 0.15$ m, $L = 0.3$ m, $l = 0.35$ m, $I_g = 0.25$ kg·m², $I_m = 0.01$ kg·m². The outer part and the heading shape of the virtual platform of a wheeled mobile robot is illustrated in Figure 8.

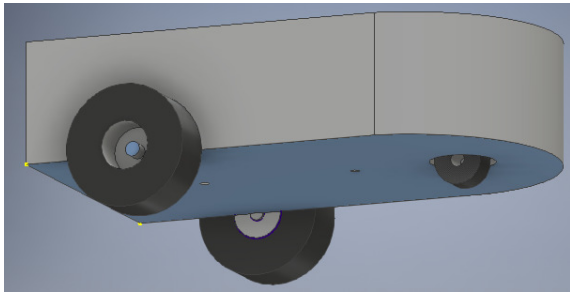


Fig. 8. Virtual platform of WMR

Various robot paths starting from the initial posture $[0, 0, 0^\circ]$ toward the final point $[20, 10]$ with different desired orientation angles θ_d are presented in Figure 9. Where paths with positive desired orientation angle $\theta_d > 0$ are presented with dash lines, while with solid lines are presented the negative ones. When the desired orientation angle is large, the robot needs to take a longer path.

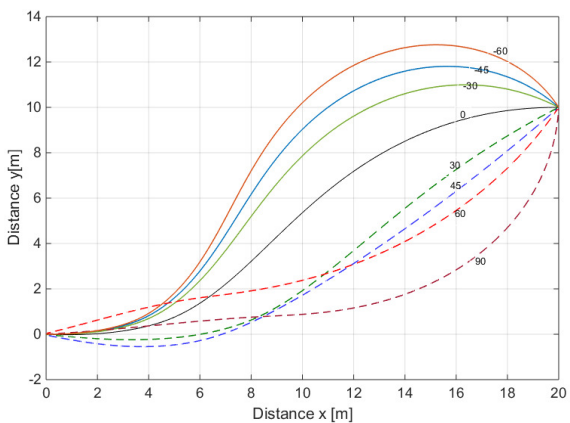


Fig. 9. Robot paths with various final desired orientation angle

In order to evaluate the efficiency of the proposed control strategy, in Figure 10 we have taken a scenario in such a way that robot starts in various initial points and goes to center point

$[0, 0]$. For initial points, $x \geq 0^+$ their final desired orientation angle is taken 180° , while for $x \leq 0^-$ the final desired orientation angle is taken 0° .

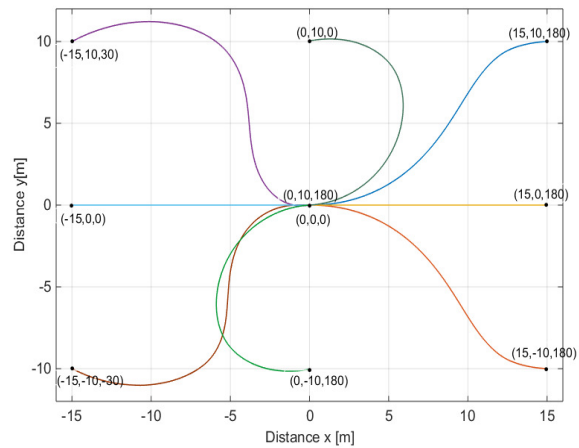


Fig. 10. Robot paths from various initial posture

In the following figures, according to a particular simulation of the robot path, starting from initial posture $[0, 0, 0^\circ]$ and going toward final posture $[20, 10, 0^\circ]$, are presented the convergences of angular and distance errors of RPC and ROC.

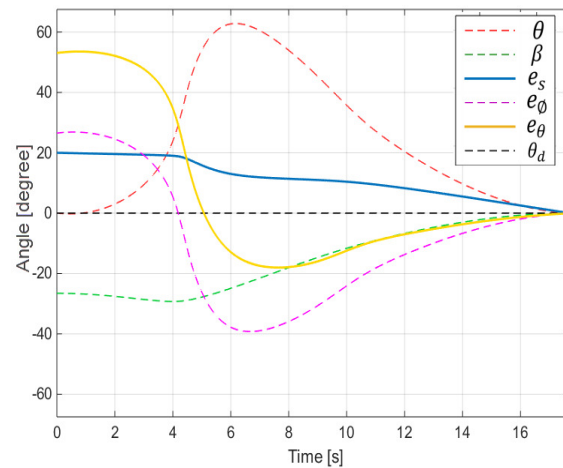


Fig. 11. Angular and distance errors of RPC and ROC for particular robot path

Furthermore, the angular velocity of a platform and the angular velocities of the left respectively right wheel are presented in Figure 12, but for the sake of a better illustration $\dot{\theta}_l$ and $\dot{\theta}_r$ are multiplied by a factor 0.1.

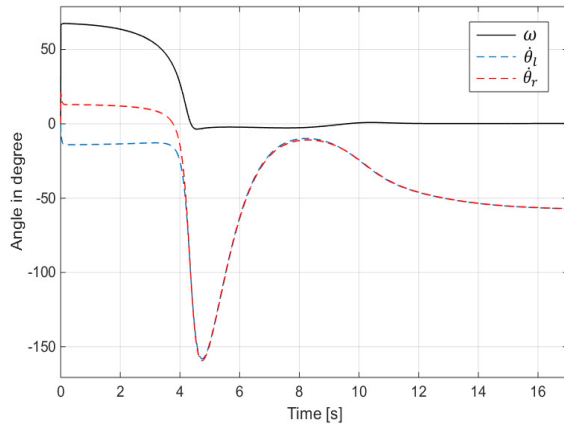


Fig. 12. Angular velocity and angular velocities of left and right wheel

The simulation results prove that an asymptotic stability could be achieved.

6. CONCLUSION

Even though, this WMR system is nonlinear and non-holonomic, the proposed control strategy assures asymptotic stability about the desired posture. The simulation has shown very satisfactory results and proved that as $t \rightarrow \infty$, an asymptotic stability could be achieved. Furthermore, a robot needs to take longer path when the desired final orientation angle is large, this is not an advantage but still it is admissible for different practical applications.

The proposed control strategy is implementable and only requires localization of the robot, the performance of the WMR could be adjusted by tuning the gain parameters of PI controllers. It is applicable only for the configuration of two differential wheeled mobile robot.

Future works will be focused on implementing the proposed control strategy in the real WMR, compare and evaluate the performance in the real situation.

REFERENCES

- [1] G. M. Dimirovski: "Vuk and Georgi: An Adventure into Active Systems via Mechatronics, Robotics and Manufacturing Engineering" (Plenary Lecture). In: *SISY2013. Proceedings of the IEEE 11th International Conference on Intelligent Systems and Informatics – Remembering Mimir K. Vukobratović*, (I. J. Rudas, B. Borovać, J. Fodor, General Chairs; I. Stajner-Papuga, technical Program Chair). The IEEE and Obuda University, Budapest, HU (ISBN 978-1-4799-0303-0; IEEE Catalog CEP1384C), September 2013, Subotica, RS. IEEE, 2013, pp. 11–19.
- [2] M. Vukobratović, G. Dimirovski: Modelling, simulation and control of robots and robotized FMS (flexible manufacturing systems), *Facta Universitatis, Series: Mechanics, Automatic Control and Robotics*, **1**, 3, 241–280 (1993).
- [3] A. Pajaziti, S. Buza, D. Bunjaku: Development and programming of the mobile platform with manipulation arm for rescue operations. In: *The 12th International Symposium "MINE ACTION 2015"*, 13th IARP WS. HCR-CTRO, 2015, pp. 157–160.
- [4] G. Lee, S. Jung: Line tracking control of a two-wheeled mobile robot using visual feedback, *International Journal of Advanced Robotic Systems*, **10**, 177 (2013), DOI: 10.5772/53729.
- [5] H. N. Pishkenari, S. Mahboobi, A. Alasty: Optimum synthesis of fuzzy logic controller for trajectory tracking by differential evolution, *Scientia Iranica*, **18**, 2, 261–267 (2011).
- [6] H. Aithal, S. Janardhanan: Trajectory tracking of two wheeled mobile robot using higher order sliding mode control. In *International Conference on Control Computing Communication & Materials*, 2013, pp. 1–4.
- [7] Y. Wang, S. Wang, R. Tan, Y. Jiang: Motion control of a wheeled mobile robot using digital acceleration control method, *Int J Innov Comput Inf Control (ICIC)*, **9** (1), 2013.
- [8] E. Abbott, D. Powell: Land-vehicle navigation using gps, *Proceedings of the IEEE*, **87**, 1, 145–162 (1999).
- [9] L. Cordesses, B. Thuilot, P. Martinet, C. Cariou: Curved path following of a farm tractor using a CP-DGPS. In: *Proceedings of the 6th Symposium on Robot Control*, 2000, pp. 489–494.
- [10] Z. M. Gacovski, G. M. Dimirovski: Mobile non-holonomic robots: Trajectory generation and obstacle avoidance, *Computational Intelligence for Modelling, Control & Automation: Evolutionary Computation & Fuzzy Logic for Intelligent Control, Knowledge Acquisition & Information Retrieval*, vol. 2, pp. 166–171 (1999).
- [11] J. Barraquand, J.-C. Latombe: Nonholonomic multibody mobile robots: Controllability and motion planning in the presence of obstacles, *Algorithmica*, **10**, 2–4, 121–155 (1993).
- [12] F. G. Pin, H. A. Vasseur: Autonomous trajectory generation for mobile robots with non-holonomic and steering angle constraints, *Intelligent Motion Control*, 1990, pp. 295–299.
- [13] M. Amoozgar, Y. Zhang: Trajectory tracking of wheeled mobile robots: A kinematical approach. In: *Mechatronics and Embedded Systems and Applications (MESA), 2012 IEEE/ASME International Conference*, IEEE, 2012, pp. 275–280.
- [14] I. Zohar, A. Ailon, R. Rabinovici: Mobile robot characterized by dynamic and kinematic equations and actuator dynamics: Trajectory tracking and related application, *Robotics and autonomous systems*, **59**, 6, 343–353 (2011).
- [15] Y.-T. Wang, Y.-C. Chen, M.-C. Lin: Dynamic object tracking control for a non-holonomic wheeled autonomous robot, *Tamkang Journal of Science and Engineering*, **12**, 3, 339–350 (2009).

- [16] F. Kuhne, W. F. Lages, J. M. G. da Silva Jr: Point stabilization of mobile robots with nonlinear model predictive control. In: *Mechatronics and Automation, 2005 IEEE International Conference*, vol. 3. IEEE, 2005, pp. 1163–1168.
- [17] P. Shi, Y. Zhao, Y. Cui: Modelling and control of wheeled mobile robot based on hybrid automata, In: *Control and Decision Conference (CCDC), 2010 Chinese*. IEEE, 2010, pp. 3375–3379.
- [18] Aguiar, A. P., Pascoal, A.: Stabilization of the extended nonholonomic double integrator via logic-based hybrid control. In: *Proc. of the 6th Int. IFAC Symposium on Robot Control*, vol. 1. The IFAC and Pergamon Press, Oxford, 2001, pp. 307–312.
- [19] G. Campion, W. Chung: Wheeled robots. In: *Springer Handbook of Robotics*. Springer, 2008, pp. 391–410.
- [20] R. W. Brockett et al.: Asymptotic stability and feedback stabilization, *Differential Geometric Control Theory*, 27, 1, 181–191 (1983).
- [21] E. Ivanjko, T. Petrinić, I. Petrović: Modelling of mobile robot dynamics. In: *7th EUROSIM Congress on Modeling and Simulation*, vol. 2, 2010.

AVOIDING HEAVY COMPUTATIONS IN INVERSE CALIBRATION PROCEDURE FOR 7 DOF ROBOT MANIPULATOR

Samoil Samak¹, Igor Dimovski¹, Mirjana Trompeska¹, Vladimir Dukovski²

¹*Institute for Advanced Composites and Robotics,
Prilep, Republic of Macedonia*

²*Faculty of Mechanical Engineering, "Ss. Cyril and Methodius" University in Skopje,
Rugjer Bošković bb, P.O. box 674, 1001 Skopje, Republic of Macedonia
igord@iacr.edu.mk*

Abstract: Procedure for determining commanded coordinates in machine space if desired coordinates are given is inverse calibration. A large amount of data is considered after measurement procedure and it is essential to locate desired point in the real space which is skewed due to measured geometric errors. The machine workspace is divided to cells using measurement points. It is depicted the importance of finding the proper cell in skewed 3D lattice, for calibration of translational axes of ATL machine with large workspace. To calibrate 7 DOF robot manipulator, this algorithm is extended. The problem of finding the proper cell in 7D skewed grid needs heavy computations and takes significant amount of computational time. Few ideas for avoiding these computations are described and the influence on the final precision of the calibration procedure is explored.

Key words: inverse calibration; geometric errors; robot manipulator

ПРОЦЕДУРА НА ИНВЕРЗНА КАЛИБРАЦИЈА ЗА НАМАЛУВАЊЕ НА ПРЕСМЕТКОВНИТЕ ОПЕРАЦИИ КАЈ РОБОТ УПРАВУВАН СО 7 СТЕПЕНИ НА СЛОБОДА

Апстракт: Процедурата за одредување координати кои можат да се контролираат во машинскиот простор со зададени координати се нарекува инверзна калибрација. Во текот на мерната постапка поради големата количина на податоци е особено важно да се одреди точната позиција на посакуваната точка во реалниот простор, која се преместува поради измерените геометриски грешки. Со користење на мерните точки машинскиот работен простор се дели на ќелии. За калибрација на транслаторните оски од ATL машина со голем работен простор е особено важно да се одреди соодветна ќелија во искривената 3D решетка. Алгоритмот е проширен за калибрација на робот со 7 степени на слобода (7 DOF) за маневар. Проблемот на наоѓање на соодветната ќелија во 7D искривената мрежа е комплексен и бара огромни пресметковни капацитети и време за нивно извршување. Во трудот се прикажани неколку начини за избегнување огромни пресметковни операции и објаснето е влијанието на калибрационата постапка врз крајната прецизност.

Клучни зборови: инверзна калибрација; геометриски грешки; робот за маневар

INTRODUCTION

In composite industry, Automated Fiber Placement (AFP) and Automated Tape Layup (ATL) technologies are used for producing large parts. Inaccuracy in position or orientation of the AFP/ATL head, as end-effector of robotized machine, may

cause some defects of the laminate and as well of the final product [1], [2].

To enhance accuracy of such robotized machines, comprehensive calibration procedure has been developed for linear axes of a 6 DOF ATL machine [3]. Due to the standards ISO 230-1:2012 [4] and ISO 230-2:2014 [5], as well to the ISO

technical report [6], 21 volumetric errors was taken in account.

Since all measurements were made on the machine with large workspace, large amount of data were obtained. Original algorithm for 3D volumetric calibration is implemented in Matlab and the results are verified using comparative analysis, comparing compensating predictions with the results of established calibration TRAC-CAL software. The algorithm is based on mathematical model for linear approximation of the total displacement error in the interior of the machine's workspace. That is nonparametric calibration, named black-box [7].

A comprehensive calibration algorithm has to cover both forward and inverse calibration. Forward calibration means to find actual coordinates if the nominal ones are given, both in machine space. If the desired coordinates are given and commanded coordinates should be found, it is the inverse calibration.

The measurement points for each axis divide the range of that axis to intervals. Crossing them, entire machine's workspace is divided to cells which dimension depends on the number of degrees of freedom (DOF) of the calibrated machine. In traditional approach, approximation of the total error is spanned over the workspace, taking into consideration the measured errors in the knots of the cells [7], [8], [9]. In our approach, we do linear approximation for every cell separately. Because of that, it is extremely important to determine the proper cell which contains the considered point.

Such idea is extended for calibration machines with more than 3 DOF. Virtual model for a 7 DOF robot manipulator is built. All kinematic calculations needed for calibration are done using screw theory [10]. Errors for all 7 axes are randomly generated, ensuring they are in expected range and distribution, similarly as in the case with 3 linear axes and their errors.

DETERMINE THE PROPER CELL IN 3D CASE

The most sensitive step in the inverse calibration procedure from aspect of computational time is determination of the grid proper cell for given desired coordinates in machine space.

After obtaining measurement results, all measurement points are stored for each axis separately. For 3 translational axes X , Y and Z , measurement was performed and the number of measurement points and their range are shown in Table 1.

Table 1

<i>Number of measurement points</i>			
	Number of points	Min (mm)	Max (mm)
X	322	940	8965
Y	142	520	4045
Z	50	-1200	25

This way, the machine's workspace is divided to 2,217,789 3D cells. Combining division point for each axis, nominal coordinates of the knot is obtained:

$$\mathbf{P}_{\text{nom}} = [x_{i,\text{nom}}, y_{j,\text{nom}}, z_{k,\text{nom}}]^T. \quad (1)$$

Using the kinematic model of the machine, actual coordinates are calculated and stored:

$$\mathbf{P}_{\text{act}} = [x_{i,\text{act}}, y_{j,\text{act}}, z_{k,\text{act}}]^T. \quad (2)$$

For storing all actual coordinates for all knots, large amount of memory is needed. That is impractical in higher dimension, so prior calculating and storing the actual knots is not done in the simulation of calibration model for 7 DOF machine.

Also, for each cell separately, coefficients of the error approximation polynomials are calculated and stored.

That way, forward calibration step is completed. Entire machine's workspace has two representations. Knots nominal coordinates determine the ideal workspace with ideal boxes as cells. Actual coordinates determines the real workspace, whose axes are skewed.

Figure 1 shows the way axes are skewed. The ideal workspace and its corresponding skewed workspace are visualized on Figure 2.

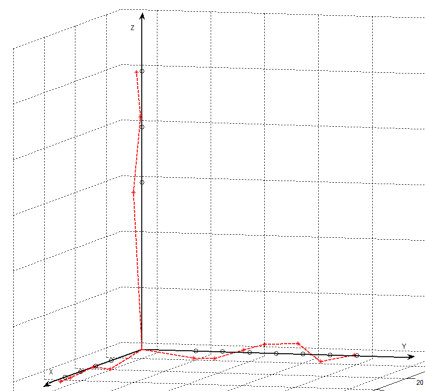


Fig. 1. The skewed coordinate axes

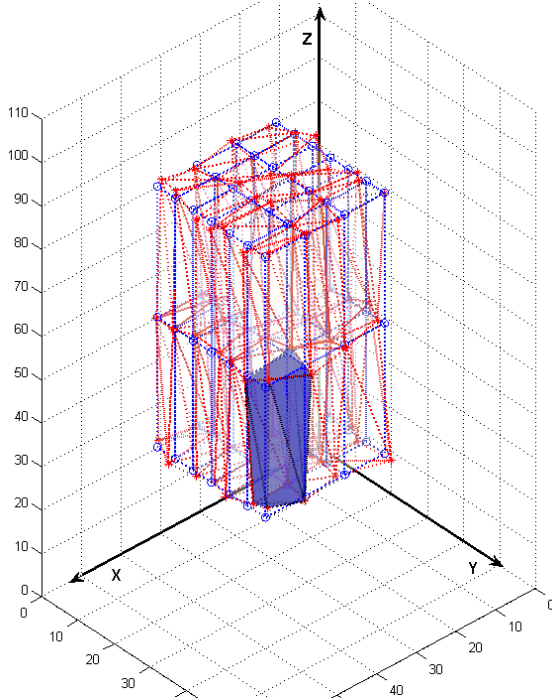


Fig. 2. The ideal and skewed grid of the workspace

Let

$$\mathbf{Q}_{des} = [x_{des}, y_{des}, z_{des}]^T \quad (3)$$

be the 3D point represent desired coordinates in machine space. Clearly, those coordinates are in the real, skewed space. One has to determine the proper real cell where the point \mathbf{Q}_{des} is located. This cell is polyhedron and is the convex hull of the set of 8 vertices, determined with their actual coordinates.

First, bisection method is applied to find the default cell. That means, the nominal values are used as partition for each axis, but appropriate actual knots are used to check whether the point \mathbf{Q}_{des} is inside the hull. If it does, the proper cell is found and it is the default one. If it doesn't, all neighbor cells, maximum 26 cells are tested to find the proper one.

The point on top left on Figure 3 shows the possibility point not to be in the default skewed cell.

An original algorithm is developed and implemented in Matlab, that determines whether the point \mathbf{Q}_{des} is inside the hull or not. This algorithm is based on linear algebra tools and determines whether the given point is on the same side from all the planes determined by triples of polyhedron vertices lying on the same face.

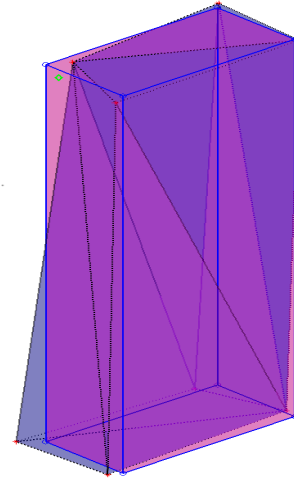


Fig. 3. Desired point outside the default cell

Similar approach is tested using built-in Matlab functions based on Delaunay triangulation and search function. In both cases, the same result as proper cell is obtained, and both procedures are time consuming.

After determining the proper cell, appropriate coefficient are loaded and inverse procedure is performed to find the commanded coordinates

$$\mathbf{Q}_{com} = [x_{com}, y_{com}, z_{com}]^T. \quad (4)$$

With obtaining the commanded coordinates \mathbf{Q}_{com} when desired ones \mathbf{Q}_{des} are given, the inverse calibration procedure is done.

Since determination of the proper cell spends most of entire computational time for the inverse calibration procedure, the question is how this determination is crucial for the accuracy after compensation and is it possible to avoid such computations.

Analysis of the data shown on Table 2, points out the importance of using right coefficients in inverse calibration procedure, since if default cell is taken instead of the proper one, ignoring the possibility of case shown on Figure 3, the precision after the calibration is much worse.

Taking the proper cell, deviation of the end-effector from the desired position is almost zero, since calculated deviations are in range close to the Matlab numerical accuracy. Calculated deviations in case of taking the default cell instead of the proper one are shown in the third column of the Table 2. One can conclude those deviations may be significant and finding the proper cell to use the proper coefficient for error approximation may be crucial.

Table 2

Proper cell vs. default cell in 3D

Point inside procedure	Number of callings	Default cell deviation (mm)	Ratio-computational time proper cell over default cell
Point 1	5	$51.9 \cdot 10^{-6}$	1.98
Point 2	19	$89.2 \cdot 10^{-6}$	2.74
Point 3	3	$11.4 \cdot 10^{-6}$	2.47
Point 4	4	$20.4 \cdot 10^{-6}$	2.11
Point 5	16	$21.6 \cdot 10^{-6}$	1.96
Point 6	4	$20.7 \cdot 10^{-6}$	1.80
Point 7	5	$11.2 \cdot 10^{-6}$	2.18

From aspect of computational time, in 3D case, finding the proper cell takes less than 3 times than the time needed for just taking the default cell. So, we decided always to search for the proper cell in the inverse calibration procedure in our calibration algorithm for 3 DOF machine.

CALIBRATION OF 7 DOF ROBOT MANIPULATOR

To test possibility of extension of this calibration procedure including rotational axes, virtual 7 DOF robotized machine is simulated. The kinematic chain contains 3 translational and 4 rotational axes. Due to the ISO standards [4], [5], [6], in total 61 geometric errors must be considered. All of them are included in the kinematic model. Forward and inverse kinematics procedures are implemented in similar manner as in [11] and [12], based on screw theory. Ideal forward kinematics and error forward kinematics procedures are implemented and the last one includes all 61 geometric errors. That makes possible to compare nominal and actual pose in pose space and determine the deviations for position, but for orientation as well.

There are 42 position dependent geometric errors, 6 errors for each axis. Therefore, measurement points must be considered for all 7 axes. Taking only 20 – 50 measurement points for the rotational axes, the number of combination for calculation of number of knots in the workspace in machine coordinates is extremely enlarged. That makes simple extension of the calibration procedure from 3 to 7 DOF impossible. It is not possible to calculate and to store actual machine coordinates for all the knots and error approximation polynomial coefficients for all the cells.

For given desired coordinates in machine space

$$\mathbf{Q}_{des} = [\theta_{1,des}, \theta_{2,des}, \theta_{3,des}, \theta_{4,des}, \theta_{5,des}, \theta_{6,des}, \theta_{7,des}]^T \quad (5)$$

real time calibration procedure is designed, including determination of the default cell based on bisection method, calculations of actual coordinates of all knots, generating error approximation polynomial coefficients for the default cell and algorithm to determine the proper cell in skewed 7D space. The last one is critical, since it is time most consuming. The goal is to obtain the appropriate commanded coordinates in machine space

$$\mathbf{Q}_{com} = [\theta_{1,com}, \theta_{2,com}, \theta_{3,com}, \theta_{4,com}, \theta_{5,com}, \theta_{6,com}, \theta_{7,com}]^T \quad (6)$$

in real time.

Large data set for 42 position dependent geometric errors is generated randomly. These errors are in the similar range and distribution as the data obtained for calibrating 3 DOF machine. Remaining 19 position independent geometric errors are randomly generated in the same manner. All 61 geometric errors are included in the calibration procedures.

The simulation for calibration of a 7 DOF robot manipulator is implemented in Matlab as well.

Forward calibration procedure is performed in reasonable computational time. That means if the nominal coordinates in machine space are given, the actual coordinates could be calculated in real time.

For inverse calibration procedure, searching for proper cell in a 7D skewed space is too much time consuming and makes idea impossible to realize in real time.

AVOIDING HEAVY COMPUTATIONS IN 7D

A heavy computations are needed to determine whether some 7D point in inside the convex hull of a set of 7D points.

Mathematical foundation of the problem is in combinatorial topology [13]. There are 128 vertices in 7D case and the cell in ideal space is simplicial complex. Its underlying space is linear polyhedron in dimension 7. When actual coordinates are calculated, the set of 128 points are obtained, and one needs to find the convex hull of such set of 7D points. Partition of that hull to 7-simplices is needed and test if the given point is inside any 7-simplex.

The fastest way to make such partition is extension of Delaunay triangulation method [14] in higher dimension [15], [16].

Since entire procedure is implemented in Matlab, its built-in functions Delaunayn and tsearchn are used. Correctness is visually verified in 2D and 3D and few tests are performed to ensure the same answer is obtained with using these functions and using topological test over all combinations of 7-simplexes.

For most points given with desired coordinates in machine space, only one call of these two functions is sufficient, since most of that points would lie in the default cell and searching for that cell is easy and fast, due to bisection method. But, even one calling of these functions is time consuming and makes entire calibration procedure impracticable for real time computing. For such “good” point, approximately 94% of computational time takes the check it is inside the default cell. The function Delaunayn spends approximately 6.8 seconds and the function tsearchn spends around 3 seconds. It is clear, that these heavy computations should be avoided.

Naive idea to assume the point is “good” and it lies in the default cell, could lead to undesired deviations as 3D case showed.

If any coordinate of desired point (5) is near the measurement point in some predefined tolerance, there is chance desired point not to be “good” one. Ideally, in that case, the neighbor cells should be checked, but it is totally impractical, since the number of neighbors is large, and computational time for one check is large as well. But, taking the neighbor cells into account, without insisting to determine which one is the proper, is the right idea for avoiding heavy computations.

That means, for such potentially “bad” point with desired coordinates in machine space, to extend the neighborhood and instead of taking only one linear polyhedron in dimension 7 as proper cell, to take few of them, at most $128 = 2^7$ such cells. Calculating the actual coordinates and approximation coefficient for all neighbour cells is much cheaper than performing Delaunay 7D test.

Taking the average of appropriate coefficients of all such neighbour cells, for each dimension separately, the new approximation polynomial is obtained. The inverse calibration procedure is performed and the commanded coordinates are obtained, without calling the heavy computation functions.

One may expect to have losing of accuracy, so obtained commanded coordinates in machine space should be transformed in pose space and the deviations of position and orientations from the ideal ones should be calculated, and they should be compared against the appropriate deviations if the proper cell was taken in inverse calibration procedure.

RESULTS

Nine 7D points were sampled, all with desired coordinates (5), and simulation is done for all of them. Three of sampled points were “good” – they are inside the default cell, and 6 of them were critical under the predefined tolerance, determining different numbers of neighbour cells that must be taken into account in polynomial coefficient calculations.

For the desired coordinates (5), ideal pose coordinates are calculated, in pose space, calling the ideal forward kinematics procedure. In that procedure, it is assumed ideally, no geometric errors exist. The position of the end-effector is represented with 3D vector \mathbf{R}_p , whose coordinates are expressed in millimeters. The orientation is represented with 2 unit 3D vectors \mathbf{R}_{o1} and \mathbf{R}_{o2} , so their coordinates are dimensionless numbers.

$$\text{Pose}_{\text{ideal}} = [\mathbf{R}_p \ \mathbf{R}_{o1} \ \mathbf{R}_{o2}] \quad (7)$$

To analyze how the choice of the cell in skewed 7D space influences to the accuracy, 3 different strategies are applied:

- Strategy 1: Looking for the proper cell, no matter how long it lasts.
- Strategy 2: Taking the default cell, no matter whether the point is critical or not.
- Strategy 3: Taking neighbor cells into account if appropriate coordinate is near measurement point under predefined tolerance and calculating the error approximation polynomial coefficients as average of the appropriate coefficient for all that cells.

For every strategy applied, different commanded coordinates are obtained. Calling the error forward kinematics procedure, for commanded coordinates obtained by i -th strategy ($i = 1, 2, 3$), the real pose is calculated:

$$\text{Pose}_{\text{real},i} = [S_{p,i} \ S_{o1,i} \ S_{o2,i}]. \quad (8)$$

Accuracy estimation is made calculating the deviations from real pose to ideal pose.

Position deviation for i -th strategy ($i = 1, 2, 3$) is 3D vector with coordinates expressed in millimeters:

$$\Delta_i = R_p - S_{p,i} \quad (9)$$

In the Table 3, norm of Delta deviation vector is given for each strategy.

Table 3

Position deviations

	Number of callings Delaunayn and tsearchn	Position deviation (mm)		
		Strategy 1	Strategy 2	Strategy 3
Pt. 1	1	$269.6 \cdot 10^{-6}$	$269.6 \cdot 10^{-6}$	$190.3 \cdot 10^{-6}$
Pt. 2	1	$685.2 \cdot 10^{-6}$	$685.2 \cdot 10^{-6}$	$584.1 \cdot 10^{-6}$
Pt. 3	1	$365.7 \cdot 10^{-6}$	$365.7 \cdot 10^{-6}$	$490.9 \cdot 10^{-6}$
Pt. 4	16	$447.4 \cdot 10^{-6}$	$684.5 \cdot 10^{-6}$	$177.9 \cdot 10^{-6}$
Pt. 5	19	$211.3 \cdot 10^{-6}$	$264.5 \cdot 10^{-6}$	$270.6 \cdot 10^{-6}$
Pt. 6	28	$993.8 \cdot 10^{-6}$	$1108 \cdot 10^{-6}$	$43.2 \cdot 10^{-6}$
Pt. 7	28	$557.9 \cdot 10^{-6}$	$716.2 \cdot 10^{-6}$	$708.2 \cdot 10^{-6}$
Pt. 8	275	$556.7 \cdot 10^{-6}$	$811.6 \cdot 10^{-6}$	$339.6 \cdot 10^{-6}$
Pt. 9	343	$203.6 \cdot 10^{-6}$	$242.4 \cdot 10^{-6}$	$44.6 \cdot 10^{-6}$

In the Table 4 accuracy estimation for orientation of the end-effector is made taking the average of the norms of 2 Epsilon deviations:

$$\begin{aligned} \text{Epsilon1}_i &= R_{o1} - S_{o1,i} \\ \text{Epsilon2}_i &= R_{o2} - S_{o2,i} \end{aligned} \quad (10)$$

Table 4

Orientation deviations

	Number of callings Delaunayn and tsearchn	Orientation deviation		
		Strategy 1	Strategy 2	Strategy 3
Pt. 1	1	$0.35 \cdot 10^{-6}$	$0.35 \cdot 10^{-6}$	$0.82 \cdot 10^{-6}$
Pt. 2	1	$0.82 \cdot 10^{-6}$	$0.82 \cdot 10^{-6}$	$0.93 \cdot 10^{-6}$
Pt. 3	1	$0.55 \cdot 10^{-6}$	$0.55 \cdot 10^{-6}$	$0.79 \cdot 10^{-6}$
Pt. 4	16	$0.59 \cdot 10^{-6}$	$0.72 \cdot 10^{-6}$	$0.15 \cdot 10^{-6}$
Pt. 5	19	$0.18 \cdot 10^{-6}$	$0.26 \cdot 10^{-6}$	$0.22 \cdot 10^{-6}$
Pt. 6	28	$1.25 \cdot 10^{-6}$	$1.32 \cdot 10^{-6}$	$0.05 \cdot 10^{-6}$
Pt. 7	28	$0.47 \cdot 10^{-6}$	$0.71 \cdot 10^{-6}$	$0.95 \cdot 10^{-6}$
Pt. 8	275	$0.88 \cdot 10^{-6}$	$0.51 \cdot 10^{-6}$	$0.42 \cdot 10^{-6}$
Pt. 9	343	$0.23 \cdot 10^{-6}$	$0.35 \cdot 10^{-6}$	$0.02 \cdot 10^{-6}$

Strategy 1 is expected to be dominant in accuracy reaching, since heavy computations are made to find the proper 7D cell. In strategy 3, extension of the local space is made and more knots in skewed space are taking into account to have influence on error approximation in such point. It allows avoiding the heavy computations as Delaunay procedure is. It was expected accuracy to be worse and hopefully near to the accuracy of strategy 1. Surprisingly, strategy 3 gives the best results for 6 of sampled points, reaching the smallest position deviations and the best results for 4 of the sampled points, reaching the smallest orientation deviations.

Strategy 2 has the best computational time in all cases, since no Delaunay procedure is taken and the smallest number of knots needed to be taken into account. In the Table 5 ratios between computational times of strategy 1 and strategy 3 over strategy 2 are given. For “good” points, strategy 1 spends 8.7–11.4 times more computational time than strategy 2. For “bad” points, this ratio is between 182.9 and 3825.0. That shows that searching for proper cell is practically impossible in 7D.

Strategy 3 spends 2.3–106.2 times more computational time than strategy 2 and it depends on the number of neighbor cells taken into account. Most of computational time is spend to calculate the actual coordinates of the knots, so it could be reduced using strategy for caching the actual coordinates of the knots.

Table 5

Computational time

	Number of callings Delaunayn and tsearchn	Ratio-computational time		Number of neighbor cells taken in Strategy 3
		Strategy 1 over Strategy 2	Strategy 3 over Strategy 2	
Pt. 1	1	11.4	2.3	2
Pt. 2	1	11.4	5.3	4
Pt. 3	1	8.7	13.7	16
Pt. 4	16	182.9	24.7	32
Pt. 5	19	196.9	7.2	8
Pt. 6	28	352.1	113.0	128
Pt. 7	28	411.2	27.5	32
Pt. 8	275	3317.6	51.0	64
Pt. 9	343	3825.0	106.2	128

CONCLUSION

The comprehensive calibration procedure for 3 DOF robotized machine is implemented and its results are verified. To extend this concept to calibration model for 7 DOF robotized machine, the most computational time consuming step is identified and ideas for avoiding it in 3D are explored, from aspect of level of losing the needed accuracy.

Calibration procedure is extended for 7 DOF machine and all functions are created, including the new kinematic model. All 61 geometric errors are taken into account. Simulation is done and 9 sample points are tested.

Finding the proper cell in skewed 7D space is extremely time consuming and should be avoided. For given 7D point with desired coordinates in machine space and predefined tolerance, default cell is found using bisection method and all neighbor cells are determined if the point is critical (strategy 3).

This way, for critical points, wider local space is used to calculate error approximation polynomial coefficients. That lead to better approximation of such coefficients and results with smaller position and orientation deviations even in comparison with the deviations obtained in strategy 1, where always proper cell is found and only the knots of that cell influence on the interior point error estimation.

This strategy allows avoiding the heavy computations to find the proper cell, without significant lose in accuracy, if any.

Its computational time is predictable and in worst case is 128 times computational time of strategy 2. It could be additionally reduced if actual coordinates of the knots are cached, which makes this strategy conducive for real time implementation of calibration procedure for a 7 DOF robot manipulator.

REFERENCES

- [1] S. Zhu: *An automated fabric layup machine for the manufacturing of fiber reinforced polymer composite*, Graduate Theses and Dissertation – Paper 13170, Iowa State University, 2013.
- [2] A. Jordaens, T. Steensels: *Formation of defects in flat laminates during automatic tape laying* (framework of a master's thesis), Faculty of Engineering Technology, Leuven, Belgium, 2015.
- [3] S. Samak, I. Dimovski, V. Dukovski, M. Trompeska: Volumetric calibration for improving accuracy of AFP/ATL machines, *7th International Scientific Conference of Defensive Technologies, OTEH 2016*, unpublished.
- [4] ISO 230-1:2012: *Test code for machine tools – Part 1: Geometric accuracy of machines operating under no-load or quasi-static conditions*. An International Standard, by International Standards Organization, 2012.
- [5] ISO 230-2:2014: *Test code for machine tools – Part 2: Determination of accuracy and repeatability of positioning of numerically controlled axes*. An International Standard, by International Standards Organization, 2014.
- [6] Technical report: *Machine tools – numerical compensation of geometric errors*, ISO/TR 16907:2015, ISO, 2015.
- [7] B. W. Mooring, Z. S. Roth, M. R. Driels: *Fundamentals of Manipulator Calibration*, John Wiley & Sons Inc., 1991.
- [8] J. S. Shamma, D. E. Whitney: A Method for Inverse Robot Calibration. *Journal of Dynamic Systems, Measurement, and Control* **109**, 1, 36–43 (1987).
- [9] D. C. Lu, M. J. D. Hayes: Robot Calibration Using Relative Measurements, *The 14th IFToMM World Congress*, Taipei, Taiwan, October 25–30, 2015.
- [10] R. M. Murray, Z. Li, S. S. Sastry: *A Mathematical Introduction to Robotic Manipulation*. CRC Press; 1994.
- [11] S. Xiang, Y. Altintas: Modeling and compensation of volumetric errors for five-axis machine tools. *International Journal of Machine Tools and Manufacture*, **101**, 65–78 (2016).
- [12] J. Yang, Y. Altintas: Generalized kinematics of five-axis serial machines with non-singular tool path generation. *International Journal of Machine Tools and Manufacture* **75**, 119–132 (2013).
- [13] M. K. Agoston: *Computer Graphics and Geometric Modeling – Mathematics*, Springer, 2005.
- [14] M. K. Agoston: *Computer Graphics and Geometric Modeling – Implementation and Algorithms*, Springer, 2005.
- [15] R. A. Dwyer: Higher-dimensional Voronoi diagrams in linear expected time. *Discrete & Computational Geometry* **6**, 3, 343–367 (1991).
- [16] C. B. Barber, D. P. Dobkin, H. Huhdanpaa: The quickhull algorithm for convex hulls. *ACM Transactions on Mathematical Software (TOMS)* **22**, 4, 469–483 (1996).

A NEURO-FUZZY MODEL FOR WIND SPEED PREDICTION BASED ON STATISTICAL LEARNING THEORY

Elizabeta Lazarevska

*Faculty of Electrical Engineering and Information Technologies,
"Ss. Cyril and Methodius" University in Skopje,
Rugjer Boshkovik bb, P.O. box 574, 1001 Skopje, Republic of Macedonia
elizabeta.lazarevska@feit.ukim.edu.mk*

Abstract: Wind is free, clean, and renewable source of energy and is fast becoming a desired alternative to conventional energy resources such as fossil fuels. That is why more and more countries are intensifying their efforts in wind energy research and harnessing. Among other wind characteristics, wind speed is crucial for planning, designing and operating wind energy systems. This is the reason for much research in the field of wind speed modelling and prediction. There are many research papers dealing with the problem of forecasting the wind speed, which requires special attention because of time-varying, stochastic and intermittent nature of wind. It has been shown in literature that among the many proposed models for wind speed prediction, the models based on soft computing techniques such as artificial neural networks, neuro-fuzzy inference systems and machine learning are superior in terms of approximation accuracy. While there are many neural models for wind speed prediction that deploy different learning methods, and there are many hybrid models based on fuzzy logic, neural networks and genetic algorithms etc., the research conducted in this work has shown that practically there are no neural models based on relevance vector machine and no neuro-fuzzy models that apply RVM learning mechanism, which is state of the art technique. This paper presents possibly for the first time in literature a neuro-fuzzy model for wind speed prediction based on Vapnik's statistical learning theory, Tipping's relevance vector machine and Kim's fuzzy inference system. The model is a fuzzy inference system of a Takagi-Sugeno type that relies on extended relevance vector machine for learning its parameters and fuzzy rules. The wind speed is modeled by means of available meteorological data such as total solar radiation, ambient temperature, humidity, atmospheric pressure, etc. The performance of the model is validated through its performance index and compared to other fuzzy and neural models for wind speed prediction. The simulation results show clearly that the model possesses excellent features and the best performance in terms of accuracy.

Key words: wind speed prediction; neuro-fuzzy modelling; extended relevance vector machine; kernel function; relevance vectors

НЕВРО-ФАЗИ МОДЕЛ ЗА ПРЕДВИДУВАЊЕ НА БРЗИНАТА НА ВЕТЕРОТ БАЗИРАН ВРЗ СТАТИСТИЧКА ТЕОРИЈА НА УЧЕЊЕ

Abstract: Ветерот е бесплатен, чист и обновлив извор на енергија и брзо прераснува во посакувана алтернатива на конвенционалните извори на енергија како што се фосилните горива. Затоа сè повеќе земји ги интензивираат напорите во насока на истражување и искористување на енергијата на ветерот. Меѓу другите карактеристики на ветерот, неговата брзина е клучна при планирањето, дизајнирањето и искористувањето на ветроенергетските системи. Ова е причината за многубројните истражувања во областа на моделирање и предвидување на брзината на ветерот. Голем број научни трудови се занимаваат со проблематиката на предвидување на брзината на ветерот, која бара огромно внимание поради временски променливата, стохастичка и интермитентна природа на ветерот. Во литературата е покажано дека меѓу многуте предложени модели за предвидување на брзината на ветерот, моделите базирани врз меките компјутерски техники, како што се вештачките невронски мрежи, невро-фази-инферентните системи и машинското учење, се супериорни од аспект на точноста на предвидувањата. Иако постојат многу невронски модели за предвидување на брзината на ветерот кои применуваат различни методи на учење и многу хибридни модели базирани врз фази логика, невронски мрежи, генетски алгоритми итн., спроведеното истражување во овој труд покажува дека практично не постојат невронски модели базирани врз релевантноста на механизмот на векторите и невро-фази-моделите кои применуваат МВР механизми на учење, кои се сметаат за најсовремени техники. Во овој труд, можеби за првпат во литературата, е претставен невро-фази модел за предвидување на брзината на ветерот базиран врз статистичката теорија на учење на Вапник, механизмот на вектори на релевантност на

Типинг и фази-логичкиот систем на Ким. Моделот е фази-логички систем од типот Такаки-Сугено кој се потпира на проширен механизам на вектори на релевантност за учење на параметрите и фази-правилата. Брзината на ветерот е моделирана според достапните метеоролошки податоци: вкупно сончево зрачење, амбиентална температура, влажност, атмосферски притисок итн. Перформансите на моделот се валидирани преку неговиот индекс на перформанси и се споредени со други фази и невронски модели за предвидување на брзина на ветерот. Резултатите од симулацијата јасно покажуваат дека моделот се одликува со одлични карактеристики и нуди најдобри перформанси од аспект на точноста.

Клучни зборови: предвидување на брзина на ветерот; фази-невронско моделирање; проширен механизам на вектори на релевантност; кернел функција; вектори на релевантност

INTRODUCTION

The negative environmental impact of excessive exploitation of fossil fuels and their depletion have led to increased interest in renewable and clean energy sources [1]. Wind is one such source due to the fact that wind energy is free, environmental friendly, and inexhaustible [2]. In order to meet the highly increased energy demands caused by modern ways of living and reduce negative environmental issues such as the global warming, more and more countries are assigning a high priority to wind energy harnessing [3]. As a matter of fact, wind energy is now considered as the fastest growing source and this trend is expected to continue [4].

The bottleneck of wind energy utilization is the time-varying, stochastic, intermittent, and complex nature of wind speed. It is well-known that there is a non-linear cubic relationship between wind speed and the power output of wind turbines [5], which means that only a small deviation in wind speed will result in a large deviation in wind power output of the wind turbines. Therefore, it is of utmost importance for wind energy systems to accurately measure and estimate wind speed at a given site [6–8]. Normally, engineers deploy anemometers for measuring wind speed. However, measurement of wind speed is considered the most difficult among various climatological variables. For one, in a wind farm multiple anemometers must be used since the wind speed varies from one wind turbine to another and for other, the masts for mounting cup anemometers, which are the accepted standard for resource assessment, inevitably become much taller as wind turbines grow in size, thus making the application of wind anemometers much more expensive. The high cost of wind anemometers discourages their widespread application, which is why engineers replace wind anemometers with digital wind speed estimators for broad applications, such as in wind farms [9–10].

Many wind speed estimation methods are presented in the literature as of the present moment [11–17]. They can be classified according different

criteria. One such classification is according to the adopted prediction period. Different time scale horizons have been applied for wind speed prediction ranging from several minutes to several days, but all of them can be classified according to Table 1 [18].

Table 1

Different wind speed prediction horizons

Class	Time scale	Main application
Very short range forecasting	A few seconds to 30 min	Turbine active control
Short range forecasting	30 min to 6 hours	Power system management, energy trading
Medium range forecasting	6 hours to 1 day	Wind generator on/off decision, operational security, electric market purposes
Long range forecasting	1 day to 1 week	Unit commitment decision, maintenance scheduling

Another classification of wind speed prediction models can be performed based on the applied method, as is shown in Table 2.

The persistence is the simplest method for wind speed prediction that is based on the assumption of a strong correlation between present and future values of wind speed. In other words, it assumes that the future values of wind speed equal the present value. Despite its simplicity, the model is as good as any for short term predictions. Its accuracy decreases rapidly with increasing prediction time scale.

The numerical weather prediction (NWP) models use mathematical models of the atmosphere and oceans to predict the weather based on current weather conditions. The complex mathematical calculations involved in modern weather prediction require super powerful computers, and yet, the forecasting ability of NWP does not extend past several days, due to the errors caused by the chaotic nature of the partial differential equations governing the atmosphere.

Table 2
Classification of Wind Speed Prediction Models

Prediction wind speed	Persistence		
	Numerical weather prediction		
	Regression analysis	Linear regression	
		Least squares (LS)	
	Statistical	Nonlinear regression	
		Algebraic curve fitting	
		Autoregressive moving average (ARMA)	
		Time-series	Autoregressive integrated moving average (ARIMA)
			Bayesian model averaging (BMA)
			Grey predictor (GP)
Soft computing	Artificial neural networks (ANN)		
	Support vector machines (SVM)		
Hybrid soft computing techniques			

Present understanding is that this chaotic behavior limits accurate forecasts to about 14 days regardless how accurate the input data are and how precise the model is.

Statistical prediction methods include regression, and time-series models. Regression analysis is frequently used for prediction and forecasting, in which domain its application substantially overlaps with the field of machine learning. Some of the most familiar methods are linear regression and ordinary least squares regression, which are considered parametric, in that the regression function is defined in terms of a finite number of unknown parameters that are estimated from the data. The regression models define the relation between past values of wind speed, as well as past and forecast values of meteorological variables, and wind speed measurements.

Along with the traditional forecasting methods, soft computing methods can also be used for wind speed prediction. Recent research works have focused on artificial neural networks (ANN), and support vector machines (SVM), which generally produce superior approximation performance compared to other forecasting techniques. The wind

speed models based on artificial intelligence techniques, such as NN and SVM, belong to the class of black-box models.

Hybrid models for short-term wind speed prediction unite different modelling techniques and approaches, such as NN and genetic algorithms (GA), or NN and fuzzy inference systems (FIS). Much more insight into different techniques for wind speed prediction can be found in [19–21].

This paper presents a new approach to wind speed forecasting based on fuzzy logic and neural network techniques. The proposed neuro-fuzzy model for prediction of wind speed is a fuzzy inference system (FIS) with a learning mechanism based on statistical learning theory and extended relevance vector machines (RVM). The conducted research has shown that there are less than few papers presenting wind speed forecasting using RVM [22, 23], and none presenting a neuro-fuzzy model of wind speed based on extended RVM. Reference [22] proposes a neural model for a day ahead wind speed prediction that utilizes relevance vector learning machine. The algorithm combines Gaussian kernel functions and polynomial kernel functions in order to obtain mixed kernel functions for RVM. The obtained model is compared to other neural models based on back propagation learning algorithm (BP) and SVM and [22] claims that the simulation results have shown that the RVM model is more effective and robust and has better performance in terms of approximation accuracy, simulation and processing time, and model complexity than the applied BP and SVM models. Reference [23] proposes a RVM model based on empirical model decomposition (EMD) to predict wind speed. The EMD algorithm is used to decompose wind speed signal in order to lessen the influence of uncertainty and nonlinearity on the model. This decomposition process results in a series of intrinsic mode functions (IMF) and RVM algorithm is applied to each IMF to construct a partial prediction model. The final prediction is obtained by superposition of all partial prediction models obtained for the IMFs. The authors in [23] claim that this method gives better forecasting results in terms of approximation accuracy that BP and RVM models alone. The reasons for applying combined fuzzy logic and neural network techniques for wind speed prediction in this work are discussed below.

A NEURO-FUZZY MODEL FOR WIND SPEED PREDICTION

Very often the real-world problems are extremely non-linear, or time-varying, or too com-

plex all together to be described with precise mathematical means. In addition, they might be

unfamiliar, uncertain, imprecise and/or vague. In all those cases, the conventional modelling techniques do not perform well and other approaches are needed in modelling such systems. Fuzzy logic and artificial neural networks are two scientific fields that provide unconventional modelling techniques proven to be very important and successful tools for modelling this kind of systems. The fuzzy logic models alone, called fuzzy inference systems (FIS) are very effective tools for modelling of nonlinear dynamic systems, but they have limitations. Their main disadvantages are lack of adaptability to different structural or behavioral changes in the modelled system and difficulties with extracting the necessary and accurate knowledge for building the rule base. On the other hand, the artificial neural networks (ANN) possess an inherent ability to adapt their parameters to changing conditions within or around the modelled system and automatically acquire the necessary knowledge. However, despite many of their advantages, ANN still have a number of weak points such as lack of interpretability, difficulties in choosing the number of hidden units, the problem of over-fitting etc. In order to overcome the disadvantages of the two modelling techniques, and to emphasize their advantages, Jang has proposed a hybrid neuro-fuzzy model, which acquires its knowledge from a given input-output data [24]. These models have been actively investigated and applied since [24–27]. The integration of learning capabilities of ANN and transparency of FIS results in a hybrid intelligent system capable of human-like reasoning, which learns its fuzzy if-then rules by some kind of learning algorithm from the field of ANN. However, the established classic and reliable ANN training methods have number of weak points, the existence of local minima solutions being one. Thus, further research has been conducted and different learning approaches have been attempted. A major breakthrough has been achieved by the advanced learning method for classification and regression called support vector machine (SVM), developed within the area of statistical learning theory [28]. Because of its excellent performance

in various applications, SVM has been widely acknowledged as one of the leading machine learning techniques. The main advantages of SVM learning method are that it possesses a very efficient mechanism for avoiding the over-fitting problem of ANNs, has proven itself to be a very good approximation tool, and is known to produce fairly sparse models. Yet, despite its widespread success, SVM still has some limitations. The main disadvantages of the SVM learning mechanism are that the number of required SVs increases proportionally with the size of the training data set, which in turn increases its computational complexity, the employed kernel functions must satisfy the Mercer's condition, and the SVM makes point predictions rather than generating predictive distributions. In order to obtain the posterior probability distribution of the output estimates in SVM, additional processing is required. To surpass the mentioned disadvantages of the SVM, Tipping has formulated the relevance vector machine (RVM) [29], which can be described as a probabilistic model with functional form equivalent to SVM. Compared to SVM, RVM has the following advantages: provides a full predictive distribution of the output since it is fully based on the statistical learning theory, performs generalization as well as the SVM, the applied kernel functions do not have to satisfy the Mercer's condition, and it typically employs significantly less kernel functions than the SVM, i.e. acquires significantly greater sparseness. To sum up, the RVM does not suffer from the SVM limitations and disadvantages, and its generalization performance and accuracy are comparable to the ones of the SVM with the advantage of employing fewer kernel functions than the SVM.

The neuro-fuzzy model for wind speed prediction presented here employs Tipping's RVM learning mechanism and is based on several excellent papers [29–31]. As most modern neuro-fuzzy systems, it is presented as a special multilayer feedforward neural network. The obtained results show a very good generalization feature of the applied modelling technique.

A BRIEF DESCRIPTION OF THE APPLIED FIS

The modelling of wind speed is based on the available input-output data $\{x_k, y_k\}; k = 1, 2, \dots, N$. The FIS implemented for modelling these data, as presented in [31], has the same structure as a Takagi-Sugeno (TS) fuzzy model [32]. The fuzzy IF-

THEN rules of this system have the following form:

$$\mathfrak{R}^i: \text{ IF } x_1 \text{ is } A_1^i \text{ and } x_2 \text{ is } A_2^i \text{ and } \dots \text{ and } x_M \text{ is } A_M^i \\ \text{ THEN } f_i = a_{i1}x_1 + \dots + a_{iM}x_M + a_{i0}; i = 1, \dots, n, \quad (1)$$

and they represent the relationships between the input \mathbf{x}_k and output y_k of the modeled system. The variable x_j in (1) defines the j -th feature of the k -th input variable \mathbf{x}_k , and at the same time it is the j input to the fuzzy rules \mathfrak{R}^i , A_j^i are appropriate fuzzy sets, a_{ij} are consequent parameters, f_i is the output of the i -th fuzzy rule, n is the number of fuzzy rules and M is the dimension of the input data vectors ($i = 1, 2, \dots, n$; $j = 1, 2, \dots, M$).

The fuzzy sets A_j^i ($i = 1, 2, \dots, n$; $j = 1, 2, \dots, M$) in ordinary TS fuzzy models are represented by their membership functions, which can belong to any of the widely accepted conventional forms (trigonal, trapezoidal, bell shaped, etc.). Here in this paper, the fuzzy sets A_j^i are represented by kernel functions, which have the following Gaussian form:

$$K(x_j, x_{ij}^*) = \exp\left[-\frac{(x_j - x_{ij}^*)^2}{2\theta_{ij}^2}\right]; \quad \begin{matrix} i = 1, 2, \dots, n \\ j = 1, 2, \dots, M \end{matrix} \quad (2)$$

The variable x_{ij}^* in (2) is the center and θ_{ij} is the variance of the Gaussian kernel function $K(x_j, x_{ij}^*)$; ($i = 1, 2, \dots, n$; $j = 1, 2, \dots, M$). In general, the kernel functions $K(x_j, x_{ij}^*)$ can be of many different types, but the Gaussian kernel function

(2) has the advantage of allowing exact computation of its parameters, the center and variance. The introduced kernel functions (2), in fact constitute the Gaussian membership functions of the input variables x_j in the applied FIS.

The fuzzy IF-THEN rules of the presented neuro-fuzzy model, which number is automatically determined by the employed extended relevance vector learning algorithm, have the following specific form:

$$\begin{aligned} \mathfrak{R}_i : & \text{IF } x_1 \text{ is } K(x_1, x_{i1}^*) \text{ and } \dots \text{ and } x_M \text{ is } K(x_M, x_{iM}^*) \\ & \text{THEN } f_i = a_{i1}x_1 + \dots + a_{iM}x_M + a_{i0}; \quad i = 1, \dots, n \end{aligned} \quad (3)$$

where each kernel function $K(x_j, x_{ij}^*)$ corresponds to one fuzzy set, $A_j^i = K(x_j, x_{ij}^*)$. The function $K(x_j, x_{ij}^*)$ in (3) represents the grade of membership of x_j with respect to the fuzzy set A_j^i , x_j is the j -th input to the fuzzy rules \mathfrak{R}^i , the kernel parameters x_{ij}^* are relevance vectors (RV), and together with the kernel parameters θ_{ij} represent parameters of the antecedent part of the fuzzy rules, f_i is the output variable of the i -th fuzzy rule, a_{ij} are parameters of the consequent part of the fuzzy rules, the number of fuzzy rules n equals the number of RVs and ($i = 1, 2, \dots, n$; $j = 1, 2, \dots, M$).

A BRIEF OVERVIEW OF RVM

A brief review of the most important features of RVM is presented next, and it is based on several distinguished papers [29, 30]. The input-output relationship of a given data set of input-output pairs $D = \{\mathbf{x}_k, y_k\}$; $k = 1, 2, \dots, N$, can be modeled by RVM as a weighted sum of N appropriately chosen basis functions $\phi_i(\mathbf{x}) = K(\mathbf{x}, \mathbf{x}_i)$:

$$f(\mathbf{x}) = f(\mathbf{x}, \mathbf{w}) = \sum_{i=1}^N w_i K(\mathbf{x}, \mathbf{x}_i). \quad (4)$$

Equation (4) establishes the relationship between the scalar outputs $\{y_k\}$; $k = 1, 2, \dots, N$ and the input vectors $\mathbf{x} = \{\mathbf{x}_k\}$; $k = 1, 2, \dots, N$; the model parameters w_i in (4) are called as weights, and the kernel functions $K(\mathbf{x}, \mathbf{x}_i)$ define one basis

function for each example in the training data set D . Learning the function $f(\mathbf{x})$ means learning its parameters, i.e. the weights w_i , and the fact that the model (4) is linear in the parameters makes the process of its learning easier.

The modelling process is done in a Bayesian probabilistic framework, because of the presence of noise and uncertainty in data in real world situations. So, it can be said that RVM is a Bayesian approach to efficient estimation of the model (4) parameters, i.e. the elements of the parameter vector $\mathbf{w} = [w_1 \ w_2 \ \dots \ w_N]^T$. It has the same functional form as SVM, but it is not to be concluded that RVM is a Bayesian version of SVM; it is rather an independent method of its own.

Assuming that the outputs of the modelled system are noisy which can be expressed as follows

$$y_k = f(\mathbf{x}_k, \mathbf{w}) + \varepsilon_k; \quad k = 1, 2, \dots, N, \quad (5)$$

an explicit probabilistic model over the output noise component ε_k is defined firstly. This model is a Gaussian distribution with zero mean and variance σ^2 ,

$$p(\varepsilon_k | \sigma^2) = N(0, \sigma^2). \quad (6)$$

Then, it follows that the probability distribution of the output y_k over the input data is

$$p(y_k | \mathbf{x}_k, \mathbf{w}, \sigma^2) = N[f(\mathbf{x}_k, \mathbf{w}), \sigma^2]. \quad (7)$$

The mean and the variance of this Gaussian distribution are $f(\mathbf{x}_k, \mathbf{w})$ and σ^2 , respectively. For independently generated examples of the training data set, the likelihood of the complete data set is given by

$$\begin{aligned} p(\mathbf{y} | \mathbf{w}, \sigma^2) &= p(\mathbf{y} | \mathbf{x}, \mathbf{w}, \sigma^2) = \\ &= \frac{\exp\left(-\frac{1}{2\sigma^2} \|\mathbf{y} - \Phi\mathbf{w}\|^2\right)}{\sqrt{(2\pi\sigma^2)^N}}. \end{aligned} \quad (8)$$

The matrix Φ in (8) is a design matrix of dimension $N \times N$, and N is the number of training data; \mathbf{w} is parameter vector of dimension N , and its elements are chosen to maximize the likelihood (8). The number of model parameters in (4) equals the number of training examples N , which yields severe over-fitting. This can be avoided, and the number of parameters in (4) can be limited, by introducing an explicit prior probability distribution over \mathbf{w} of the following form:

$$p(\mathbf{w}, \mathbf{a}) = \prod_{i=1}^N N(w_i | 0, \alpha_i^{-1}) = \prod_{i=1}^N \left(\frac{\alpha_i}{2\pi}\right)^{\frac{1}{2}} \exp\left(-\frac{\alpha_i}{2} w_i^2\right). \quad (9)$$

The imposed constraint on model parameters (9) is a zero-mean Gaussian distribution with a variance $1/\mathbf{a}$, $\mathbf{a} = [\alpha_1 \ \alpha_2 \ \dots \ \alpha_N]^T$ being the appropriate vector of N new parameters. The parameters α_i are called as hyperparameters, and by adjoining independently each hyperparameter with one of the weights, they moderate the strength of the prior by controlling the inverse variance of the associated weight. The adopted Gaussian distribu-

tion of the prior in (9) indicates that smaller weights are a priori more probable, and leads to smoother and less complex models, thus encoding the preference for smoother (simpler) models into the learning algorithm.

Although the model (4) already possesses too many parameters, the addition of N new parameters does not impose additional problem, since during the learning process based completely on the Bayesian probabilistic framework, many of the hyperparameters α_i become extremely large, which in turn leads to very small values for the appropriate weights w_i . As a consequence, the corresponding terms of the sum in (4) are eliminated as irrelevant. In this way, the number of parameters of the model (4) is drastically reduced, which leads to the desired sparseness. The RVM learning procedure is extremely effective in selecting only the relevant basis functions leading to good generalization.

In addition to the prior distribution over \mathbf{w} , hyperpriors over the hyperparameters \mathbf{a} and the noise variance σ^2 must be defined as well, which is done by assuming a Gamma distribution as follows.

$$\begin{aligned} p(\mathbf{a}) &= \prod_{i=1}^N \text{Gamma}(\alpha_i | a, b) \\ p(\beta) &= \text{Gamma}(\beta | c, d); \quad \beta = \sigma^{-2} \end{aligned} \quad (10)$$

The introduction of hierarchical priors over the parameters of the model \mathbf{w} , the hyperparameters \mathbf{a} , and the noise variance σ^2 , is a crucial feature of the relevance vector machine which ultimately results in desired sparse models. By fixing the parameters a, b, c , and d in (10) equal to zero, the hyperpriors become uniform over a logarithmic scale, which has a very pleasing consequence that the model output does not depend on the measurement units of the training output data.

Having introduced all the priors, including the priors over \mathbf{w} and the hyperpriors over \mathbf{a} and σ^2 , and following the Bayesian framework, for each given input data \mathbf{x}_k , a correct prediction of the corresponding output y_k is performed:

$$p(\hat{y}_k | \mathbf{y}) = \int p(\hat{y}_k | \mathbf{w}, \mathbf{a}, \sigma^2) \cdot p(\mathbf{w}, \mathbf{a}, \sigma^2 | \mathbf{y}) d\mathbf{w} d\mathbf{a} d\sigma^2, \quad (11)$$

where $p(\mathbf{w}, \mathbf{a}, \sigma^2 | \mathbf{y})$ is the posterior probability distribution over all unknown model parameters \mathbf{w} ,

$$p(\mathbf{w}, \boldsymbol{\alpha}, \sigma^2 | \mathbf{y}) = p(\mathbf{w} | \mathbf{y}, \boldsymbol{\alpha}, \sigma^2) p(\boldsymbol{\alpha}, \sigma^2 | \mathbf{y}). \quad (12)$$

The weight posterior distribution

$$p(\mathbf{w} | \mathbf{y}, \boldsymbol{\alpha}, \sigma^2)$$

can be estimated as

$$\begin{aligned} p(\mathbf{w} | \mathbf{y}, \boldsymbol{\alpha}, \sigma^2) &= N(\mathbf{w} | \boldsymbol{\mu}, \boldsymbol{\Sigma}) = \\ &= (2\pi)^{-\frac{N+1}{2}} |\boldsymbol{\Sigma}|^{-\frac{1}{2}} \exp\left[-\frac{(\mathbf{w} - \boldsymbol{\mu})^T \boldsymbol{\Sigma}^{-1} (\mathbf{w} - \boldsymbol{\mu})}{2}\right], \end{aligned} \quad (13)$$

$$\boldsymbol{\Sigma} = (\sigma^{-2} \boldsymbol{\Phi}^T \boldsymbol{\Phi} + \mathbf{A})^{-1}, \mathbf{A} = \text{diag}(\alpha_1, \alpha_2, \dots, \alpha_N), \quad (14)$$

$$\boldsymbol{\mu} = \sigma^{-2} \boldsymbol{\Sigma} \boldsymbol{\Phi}^T \mathbf{y}, \quad (15)$$

where $\boldsymbol{\Sigma}$ and $\boldsymbol{\mu}$ are the covariance and mean of this weight posterior distribution, respectively. It should be noted that $\mu_i \rightarrow 0$ whenever $\alpha_i \rightarrow \infty$.

Unfortunately, the posterior distribution

$$p(\boldsymbol{\alpha}, \sigma^2 | \mathbf{y})$$

of the hyper parameters cannot be computed analytically and must be approximated, which leads to maximization of

$$p(\boldsymbol{\alpha}, \sigma^2 | \mathbf{y}) \propto p(\mathbf{y} | \boldsymbol{\alpha}, \sigma^2) p(\boldsymbol{\alpha}) p(\sigma^2) \quad (16)$$

with respect to $\boldsymbol{\alpha}$ and σ^2 . In case of uniform hyperpriors only the term $p(\mathbf{y} | \boldsymbol{\alpha}, \sigma^2)$ with covariance \mathbf{C} , known as marginal likelihood,

$$p(\mathbf{y} | \boldsymbol{\alpha}, \sigma^2) = (2\pi)^{-\frac{N}{2}} |\mathbf{C}|^{-\frac{1}{2}} \exp\left(-\frac{1}{2} \mathbf{y}^T \mathbf{C}^{-1} \mathbf{y}\right) \quad (17)$$

$$\mathbf{C} = \sigma^2 \mathbf{I} + \boldsymbol{\Phi} \mathbf{A}^{-1} \boldsymbol{\Phi}^T$$

needs to be maximized, which is named as type-II maximum likelihood method [33].

The optimal values of α_i and σ^2 that maximize the marginal likelihood (17), i.e. its logarithm with respect to the hyperparameters α_i , cannot be obtained in a closed form. Instead, they are computed iteratively [34]

$$\alpha_{i, \text{new}} = \frac{\gamma_i}{\mu_i^2}; \quad \gamma_i = 1 - \alpha_i \Sigma_{ii}, \quad \sigma_{\text{new}}^2 = \frac{\|\mathbf{y} - \boldsymbol{\Phi} \boldsymbol{\mu}\|^2}{N - \sum_i \gamma_i}. \quad (18)$$

The parameter μ_i in (18) is the i -th posterior mean weight from (15), Σ_{ii} is the i -th diagonal element of the posterior weight covariance in (14), computed with the current values of parameters $\boldsymbol{\alpha}$ and σ^2 . Each parameter $\gamma_i \in [0, 1]$ can be considered a measure of how well its corresponding parameter w_i is determined by the given training data. For large values of α_i , $\Sigma_{ii} \approx \alpha_i^{-1}$ and it follows that $\gamma_i \approx 0$. On the other hand, when α_i is small, $\gamma_i \approx 1$ and w_i fits the data. It should be noted that N in the denominator of (18) refers to the number of data examples and not the number of basis functions.

The RVM learning algorithm is of an iterative type. The parameters α_i and σ^2 are repeatedly estimated every iteration step until the desired convergence criterion is achieved. At the same time, at each step of iteration the newly calculated values for α_i and σ^2 are used for updating the posterior statistics $\boldsymbol{\Sigma}$ and $\boldsymbol{\mu}$. During this iteration process, many of the hyperparameters become very large approaching infinity, which indicates that the appropriate posterior distributions $p(w_i | \mathbf{y}, \boldsymbol{\alpha}, \sigma^2)$ become very large at zero. This further means that the adjacent weights w_i are zero with a posteriori certainty. The zero valued weights result in pruning the corresponding basis functions in (4), thus reducing considerably the number of model parameters. The vectors from the training data set associated with the remaining nonzero weights are called the relevance vectors (RV).

THE STRUCTURE OF THE FIS WITH EXTENDED RVM

The structure of the neuro-fuzzy system is shown in Figure 1. It represents a neural network with six different layers. The first layer is called the input layer. It consists of nodes that represent

the input variables to the model. There is one node in this layer for each input variable. Thus, the input layer has a total of M nodes, M being the number of elements in the training input vector

$\mathbf{x}_k = (x_{k1}, x_{k2}, \dots, x_{kM})$. This layer has the sole role of transmitting the upcoming input data to the second layer. It does not perform any operations over the training input data.

The second layer is the fuzzification layer, since it performs fuzzification over the training input data by projecting the input space into a high-dimension feature space. This nonlinear projection is defined by the chosen kernel functions. Each node in this layer has exactly M inputs, M being the dimension of the input vector $\mathbf{x}_k = (x_{k1}, x_{k2}, \dots, x_{kM})$, i.e. the number of nodes in the input layer. The second layer consists of n nodes that represent the adequate kernel functions. These kernel functions are not required to satisfy the Mercer's condition as in the case of SVM learning mechanism. Therefore they can have a different shape: triangular, trapezoidal, bell, Gaussian, polynomial, Fourier series etc. The neuro-fuzzy model in Figure 1 uses the Gaussian kernel functions defined by (2). The choice of Gaussian kernel functions is very convenient because their parameters can be learned easily and computed precisely.

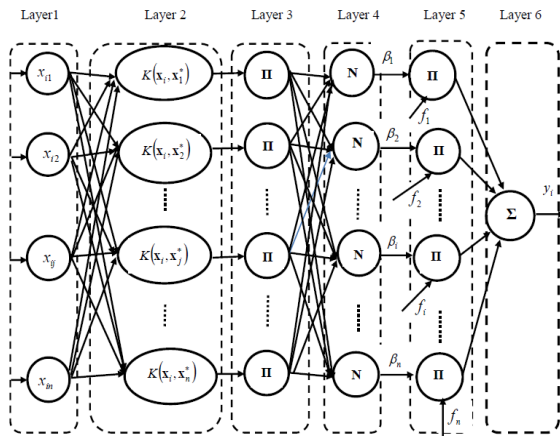


Fig. 1. The structure of the neuro-fuzzy model used for modelling the wind speed

From the fuzzy modelling perspective, the terms in (2) can be interpreted as follows: x_j is the j -th input to the fuzzy model, $K(x_j, x_{ij}^*)$ is the membership function $\mu_{ij} = \mu_{A_j^i}(x_j)$ of the j -th fuzzy input x_j with respect to the i -th fuzzy rule, the parameters x_{ij}^* and θ_{ij} of $K(x_j, x_{ij}^*)$ are the premise parameters of the corresponding fuzzy

rule, M is the number of fuzzy inputs to the neuro-fuzzy model, and the number n of kernel functions $K(x_j, x_{ij}^*)$ is the number of fuzzy rules, i.e. the number of nodes in the second layer. Because of the Gaussian shape of the selected kernel functions, the membership functions of the antecedent part of the fuzzy rules are Gaussian membership functions. From the RVM prospective, the center x_{ij}^* of $K(x_j, x_{ij}^*)$ is a relevance vector, the variance θ_{ij} , i.e. the width of the Gaussian kernel, is a kernel parameter, and n is the number of relevance vectors.

The third layer can be called as the rule layer, since a node in this layer generates the IF part of each fuzzy rule. The nodes in this layer can be called as the rule nodes, accordingly. This layer has n nodes, one for each fuzzy rule, and they compute the firing strength of the associated fuzzy rules. For each node the following T-norm operator is used:

$$K(\mathbf{x}, \mathbf{x}_i^*) = \prod_{j=1}^M K(x_j, x_{ij}^*); \quad i = 1, 2, \dots, n. \tag{19}$$

The vector $\mathbf{x}_i = (x_{i1}, x_{i2}, \dots, x_{iM})$ in (19) represents the i -th input vector to the model of dimension M , and $\mathbf{x}_i^* = (x_{i1}^*, x_{i2}^*, \dots, x_{iM}^*)$ is the RV of the i -th input vector. Instead of the product of membership functions in (19), any other T-norm operator could be used to perform the fuzzy AND operation. The first three layers in Figure 1 belong to the antecedent part of the FIS. The next layers belong to the consequent part of the FIS.

The fourth layer is the normalization layer. It consists of n nodes and each node performs normalization of the firing strength of the associated fuzzy rule. This normalization is done with respect to the sum of the firing strengths of all the fuzzy rules, and the output of each node in this layer is the normalized firing strength, i.e. weight β_i of the corresponding fuzzy rule, computed as the following ratio:

$$\beta_i = \frac{K(\mathbf{x}, \mathbf{x}_i^*)}{\sum_{j=1}^n K(\mathbf{x}, \mathbf{x}_j^*)}; \quad i = 1, 2, \dots, n. \tag{20}$$

Each node i in the fifth layer calculates the product of the normalized weight β_i for the i -th

rule and the local output variable f_i of the fuzzy system. The output variables v_i of the nodes in this layer are:

$$v_i = \beta_i f_i = \beta_i (a_{i1} x_{i1} + \dots + a_{iM} x_{iM} + a_{i0}). \quad (21)$$

The parameters $(a_{i0}, a_{i1}, \dots, a_{iM})$ in (21) can be called as consequent parameters, since they represent the parameters of the consequent part of the correspondent fuzzy rules.

The sixth and the last layer is the output layer. The single node in this layer computes the overall output $f(\mathbf{x})$ of the neuro-fuzzy model as the sum of all incoming signals,

$$f(\mathbf{x}) = \sum_{i=1}^n \beta_i f_i. \quad (22)$$

MODELLING AND SIMULATION RESULTS

The neuro-fuzzy model for wind speed prediction was built upon the available meteorological data for Mauna Loa (MOA), Hawaii, US, for year 2015, available at [35]. The measured input-output data points were randomly permuted and divided into two sets – training and evaluation data. The proposed neuro-fuzzy model for wind speed prediction was built and evaluated on 10 such randomizations between training and test data containing $\frac{3}{4}$ and $\frac{1}{4}$ data points, accordingly. After training with the training data set, 48 relevance vectors were generated, thus yielding a neuro-fuzzy model of wind speed with 48 fuzzy rules. The learning algorithm of the FIS with extended RVM according to [31] is shown in Figure. 2.

The output of the neuro-fuzzy model for wind speed forecasting with the obtained relevance vectors is shown in Figure. 3, compared to the actual measured output. It can be easily seen that the model output practically coincides with the measured output.

In order to evaluate the performance of the built neuro-fuzzy model for wind speed prediction, the root mean square error (RMSE) of the model output y_{model} is calculated

$$PI = \sqrt{\frac{1}{n} \sum_{i=1}^n (y_{\text{real}}^i - y_{\text{model}}^i)^2}. \quad (23)$$

The structure of this adaptive neural network is not unique. For example, last two layers can be easily combined to form one defuzzification layer, which computes the overall output $f(\mathbf{x})$ of the neuro-fuzzy model using the center of gravity defuzzification method. Similarly, the third and the fourth layers can be combined together as one layer, to obtain an equivalent five layers neural network, as in [31].

The system in Figure 1 performs system optimization and generalization simultaneously. The number of fuzzy rules and the parameters of the membership functions are generated automatically by the extended relevance vector learning machine algorithm [31]. The parameters of the kernel functions are adjusted by the gradient ascent method (GAM) [31]. The coefficients in the consequent part of the fuzzy rules are determined by the least square method (LSE) [31].

It is compared to several unconventional models based on Sugeno-Yasukawa fuzzy identification [36], and extreme learning machine ELM [37], and the comparison results are shown in Table 3.

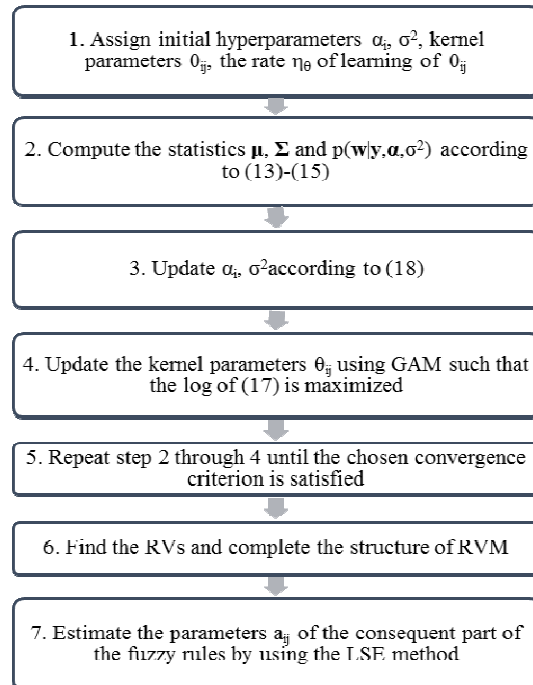


Fig. 2. The learning algorithm of the neuro-fuzzy model with extended RVM

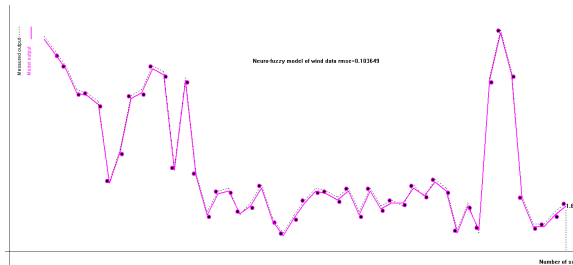


Fig. 3. The output of the neuro-fuzzy model for wind speed prediction with relevance vectors, compared to the actual measured output.

Table 3

Comparison of wind speed prediction models obtained by different modelling techniques

Model	RMSE
Position type fuzzy model	0.40438
Position-gradient type fuzzy model	0.33537
Neuro-fuzzy model based on extended RVM	0.103649
NN model based on ELM	0.162942

CONCLUSION

The simulation results proved the built FIS very effective in modelling the wind speed. The main advantages of the RVM learning algorithm are: the ability to provide accurate prediction model with fewer basis functions, automatic estimation of “nuisance” parameters, and the facility to utilize arbitrary basis functions.

Acknowledgment; The meteorological data used in this research are part of the meteorology measurements from NOAA/ESRL/GMD, where NOAA stands for National Oceanic and Atmospheric Administration, ESRL stands for Earth System Research Laboratory and GMD stands for Global monitoring division. They can be accessed at National Renewable Energy Laboratory NREL web-site [35], which is operated for the US Department of Energy by the Alliance for Sustainable Energy LLC.

REFERENCES

- [1] R. Ehrlich: *Renewable Energy: A first course*, 1st Edition, CRC Press, 2013.
- [2] R. P. Walker, A. Swift: *Wind Energy Essentials: Societal, Economic, and Environmental Impacts*, 1st Edition, Wiley, 2015.
- [3] L. R. Brown, E. Adams, J. Larsen, J. M. Roney: *The Great Transition: Shifting from Fossil Fuels to Solar and Wind Energy*, 1st Edition, W. W. Norton & Company, 2015.
- [4] Global Wind Energy Council: *Global wind statistics 2015*, GWEC, 2015. Available at: http://www.gwec.net/wp-content/uploads/vip/GWEC-PRstats-2015_LR_corrected.pdf.
- [5] R. Gasch, J. Twele: *Wind Power Plants: Fundamentals, Design, Construction and Operation*, 2nd edition, Springer, 2012.
- [6] Y. Tamura, K. Suda, A. Sasaki, Y. Iwatani, K. Fujii, R. Ishibashi, K. Hibi: Simultaneous measurements of wind speed profiles at two sites using Doppler sodars, *Journal of Wind Engineering and Industrial Aerodynamics*, **89**, 3–4, 325–335 (March 2001).
- [7] S. Soisuvarn, Z. Jelenak, P. S. S. O. Cheng, Q. Zhu: CMOD5.H.Q. – A high wind geophysical model function for c-band vertically polarized satellite scatterometer measurements, *IEEE Transactions on Geoscience and Remotesensing*, **51**, 6, 3741–3760 (June 2013).
- [8] S. Yang, E. McKeogh: LIDAR and SODAR measurements of wind speed and direction in upland terrain for wind energy purposes, *Remote Sensing*, **3**, 9, 1871–1901 (2011).
- [9] A. Kusiak, W. Li: Estimation of wind speed: a data-driven approach, *Journal of Wind Engineering and Industrial Aerodynamics*, **98**, 10–11, 559–567 (Oct.–Nov. 2010).
- [10] M. Mohandes, S. Rehman, S. M. Rahman: Estimation of wind speed profile using adaptive neuro-fuzzy inference system (ANFIS), *Applied Energy*, **88**, 11, 4024–4032 (Nov. 2011).
- [11] J. L. Torres, A. García, M. De Blas, A. De Francisco: Forecast of hourly average wind speed with ARMA models in Navarre (Spain), *Solar Energy*, **79**, 1, 65–77 (July 2005).
- [12] R. G. Kavasseri, K. Seetharaman: Day-ahead wind speed forecasting using f-ARIMA models, *IEEE Transactions on Renewable Energy*, **34**, 5, 1388–1393 (May 2009).
- [13] T. M. H. El-Fouly, E. F. El-Saadany: Grey predictor for hourly wind speed and power forecasting, *IEEE Transactions on Power Systems*, **21**, 3, 1450–1452 (August 2006).
- [14] I. G. Damousis, P. Dokopoulos: A fuzzy expert system for the forecasting of wind speed and power generation in wind farms, In: *Wind Energy Conversion Systems: Technology and Trends*, S. M. Mayeen ed., London: Springer, 2012, pp. 197–226.
- [15] T. G. Barbounis, J. B. Theocharis, M. C. Alexadis, P. S. Dokopoulos: Long term wind speed and powercasting using local recurrent neural network models, *IEEE Transactions on Energy Conversion*, **21**, 1, 273–284 (March 2006).
- [16] M. A. Mohandes, T. O. Halawani, S. Rehman, A. A. Hussain: Support vector machine for wind speed prediction, *Renewable Energy*, **29**, 6, 939–947 (May 2004).
- [17] A. U. Haque, P. Mandal, J. Meng, M. E. Kaye, L. Chang: A new strategy for wind speed forecasting using hybrid

- intelligent models, *25th IEEE Canadian Conference on Electrical and Computer Engineering, CCECE*, 2012, pp. 1–4.
- [18] S. S. Soman, H. Zareipour, O. Malik, P. Mandal: A review of wind power and wind speed forecasting methods with different time horizons, *Nort American Power*, **2**, 5, 8–16 (2010).
- [19] M. Bhaskar, A. Jain, N. V. Srinath: Wind speed forecasting: Present Status, *International Conference on Power System Technology (POWERCON)*, 24–28 Oct. 2010, pp. 1–6.
- [20] S. M. Lawan, W. A. W. Z. Abidin, W. Y. Chai, A. Baharun, T. Maasri: Different models of wind speed prediction: A comprehensive review, *International Journal of Scientific and Engineering Research*, **5**, 1, 1760–1768 (2014).
- [21] M. Lei, L. Shiyan, J. Chuanwen, L. Hongling, Z. Yan: A review on the forecasting of wind speed and generated power, *Renewable and Sustainable Energy Reviews*, **13**, 4, 915–920 (May 2009).
- [22] G. Sun, Y. Chen, Z. Wei, X. Li, K. W. Cheung: Day-ahead wind speed forecasting using relevance vector machine, *Journal of Applied Mathematics*, Volume **2014**, Article ID 437592, available on-line at: <http://dx.doi.org/10.1155/2014/437592>.
- [23] G. Yang, Z. Hu, X. Liu: A novel strategy for wind speed prediction in Wind farm, *Telkommika*, **11**, 12, 7007–7013 (Dec. 2013). (2004).
- [24] J.-S. R. Jang: ANFIS: Adaptive-network-based fuzzy inference systems, *IEEE Trans. Sys. Man. Cybern.*, **23**, pp. 665–685 (1993).
- [25] C. T. Lin: A Neural fuzzy control systems with structure and parameter learning, *Fuzzy Sets and Systems*, **70**, pp. 183–212 (1995).
- [26] C. T. Lin, C. S. G. Lee.: *Neural fuzzy systems: A neural fuzzy synergism to intelligent systems*, Prentice-Hall, Englewood Cliffs, 1996.
- [27] C. F. Yang, C. T. Lin: An on-line self-constructing neural fuzzy inference network and its applications, *IEEE Trans. Fuzzy Syst.*, **6**, pp. 12–32 (1998).
- [28] V. N. Vapnik: *Statistical Learning Theory*, Wiley, N. Y., 1998.
- [29] M. E. Tipping: The relevance vector machine. In: S. A. Sola, T. K. Leen and K.-R. Muller, editors, *Advances in Neural Processing Systems* **12**, MIT Press, pp. 652–658 (2000).
- [30] M. E. Tipping: Sparse Bayesian learning and the relevance vector machine, *J. Mach. Learn. Res.*, **1**, pp. 211–244 (2001).
- [31] J. Kim, Y. Suga, S. Won: A new approach to fuzzy modelling of nonlinear dynamic systems with noise: relevance vector learning mechanism, *IEEE Trans. on Fuzzy Systems*, **14**, pp. 222–231 (2006).
- [32] T. Takagi, M. Sugeno: Fuzzy identification of systems and its applications to modelling and control, *IEEE Trans. Syst. Man. Cybern.* **15**, pp. 116–132 (1985).
- [33] J. O. Berger: *Statistical Decision Theory and Bayesian Analysis*, Springer, 2nd edition, 1985.
- [34] D. J. C. MacKey: Bayesian interpolation, *Neural Computation*, **4**, pp. 415–445 (1992).
- [35] http://www.nrel.gov/gis/data_wind.html
- [36] M. Sugeno, T. Yasukawa: A fuzzy-logic-based approach to qualitative modelling, *IEEE Trans. on Fuzzy Syst.*, **1**, pp. 7–33 (1993).
- [37] G.-B. Huang, Q.-Y. Zhu, C.-K. Siew, Extreme learning machine: A new learning scheme of feedforward neural networks, *Proceedings of the IEEE International Joint Conference on Neural Networks (IJCNN2004)*, 25–29 July, Budapest, Hungary, 2004, pp. 985–990.

WIRELESS INFORMATION AND ENERGY TRANSFER: TRADEOFF FOR FAIR RESOURCE ALLOCATION

Hristina Čingoska, Zoran Hadži-Velkov, Ivana Nikoloska

*Faculty of Electrical Engineering and Information Technologies,
"Ss. Cyril and Methodius" University in Skopje,
Rugjer Bošković bb, P.O. box 574, 1001 Skopje, Republic of Macedonia
zoranhv@feit.ukim.edu.mk*

A b s t r a c t: In this paper, we study two schemes for the fair resource allocation in wireless powered communication networks (WPCNs): a non-orthogonal multiple access (NOMA) scheme, and a proportional fair (PF) scheduling scheme. The considered WPCN consists of a base station (BS) that broadcast radio frequency (RF) energy over the downlink, and N energy harvesting users (EHUs). If NOMA is employed, all EHUs concurrently transmit information over the uplink with successive interference cancellation employed at the BS. If PF scheduling is employed, a single EHU is selected for uplink transmission in each frame. For both schemes, we arrive at optimal allocations for the BS transmit power and the time sharing between uplink and downlink transmissions that maximize the uplink sum-rate, while maintaining high level of system fairness. For the PF scheme, we also derive the optimal scheduling policy. Compared to the state-of-the art schemes based upon time division multiple access (TDMA), both schemes significantly improve the system fairness at the expense of minor (or nonexistent) rate degradation.

Key words: energy harvesting; wireless powered communication networks; non-orthogonal multiple access; successive interference cancelation; proportional fair scheduling

БЕЗЖИЧЕН ПРЕНОС НА ИНФОРМАЦИЈА И ЕНЕРГИЈА СО ПРАВИЧНА РАСПРЕДЕЛБА НА РЕСУРСИ

А п с т р а к т: Во овој труд се проучени две шеми за фер распределба на ресурсите во безжично напојувани телекомуникациски мрежи (WPCN): шема со не-ортогонален повеќекратен пристап (NOMA) и шема со пропорционално опслужување (PF). Во разгледуваната мрежа базната станица емитува радиофреквенциско зрачење кон повеќе крајни корисници, кои ја прифаќаат енергијата од тоа зрачење. Ако се примени шемата NOMA, сите крајни корисници истовремено праќаат информација кон базната станица, а таа врши последователно поништување на интерференцијата предизвикана од примените сигнали. Ако се примени шемата PF, само една избрана станица во еден момент праќа информација кон базната станица. За двете шеми е определена оптимална распределба на излезната моќност на базната станица и оптимална распределба помеѓу времињата за праќање информација и енергијата, со цел да се максимира вкупната податочна брзина кон базната станица, а истовремено да се зачува принципот за фер искористување на системските ресурси. Во случајот на шемата PF, исто така е определена полсата за оптимално опслужување. Во споредба со познатите шеми со временски ортогонален повеќекратен пристап (TDMA), двете предложени шеми значително ја подобруваат рамноправноста меѓу крајните корисници, на сметка на незначително намалување на вкупната податочна брзина кон базната станица.

Клучни зборови: прифаќање енергија; безжично напојувани телекомуникациски мрежи (WPCN); неортогонален повеќекратен пристап; последователно поништување на интерференција; шема со пропорционално опслужување (PF)

INTRODUCTION

Recent advances in ultra-low power wireless communications and energy harvesting (EH) technologies have made self-sustainable devices fea-

sible. Typically, the major concern for these devices is battery life and replacement. Applying energy harvesting techniques to these devices can significantly extend battery life and sometimes even entirely eliminate the need for a battery [1, 2].

However, energy harvesting from the environment (such as, solar or wind) may not provide a stable and continuous power supply to the communication system. Instead, energy may be harvested from a radio frequency (RF) radiation from dedicated power sources. Therefore, the RF energy harvesting has emerged as a revolutionary technology for the energy-constrained wireless networks, such as the sensor and ad hoc networks [1–3].

Networks of nodes that utilize both information transmission and energy transmission are known as wireless-powered communication networks (WPCNs) [4–6]. The design optimization of WPCNs so far typically focuses on maximization of the sum-rate over the uplink, which is a spectrally efficient method, but yet biased and unfair in terms of resource sharing among the EHUs. In particular, due to the large-scale fading, the EHUs at closer distances to the BS can transmit at much higher rates compared to the more distant EHUs. Thus, conventional sum-rate maximization allows only EHUs close to the BS to achieve a much higher aggregate rate compared to the cell-edge EHUs.

In order to tackle this issue, this paper proposes two different schemes that facilitate fair resource allocation in the WPCNs: (a) non-orthogonal multiple access (NOMA), and (b) proportionally fair (PF) scheduling. When NOMA is employed, all network users simultaneously transmit their codewords towards a common receiver, which decodes them by successive interference cancellation (SIC) [7–9]. [10] solves an weighted sum-rate maximization problem in order to derive achievable rate regions and compares the performances between the approach with joint resource allocation and the one when only optimal time allocation is considered. On the other hand, PF scheduling is widely applied to today's conventional cellular systems [11]. In the context of EH communications, [12] determines the optimum offline resource allocation on an EH downlink [13] studies uplink sum-rate maximization with short-term energy harvesting and the applicability of a proposed suboptimal online algorithm, while [14] studies uplink sum-rate maximization with long-term energy harvesting with a complex battery model and processing cost.

In this paper, we study WPCN that employs short-term energy harvesting with a simple battery model. For both of these schemes, by solving a sum-rate maximization problem we derive the expressions for optimal allocations for the BS transmit power and the time sharing between the uplink

and downlink transmissions. For the PF scheme, we also derive the optimal online scheduling policy.

SYSTEM AND CHANNEL MODEL

The WPCN is assumed to operate in a random fading environment, consisting of a base station (BS) and N EHUs, all equipped with a single antenna. The EHUs are equipped with rechargeable EH batteries that store the harvested energy. Let the time be divided into epochs of equal duration T . Each epoch is subdivided into two consecutive phases: an EH phase, during which the BS broadcasts RF energy to the EHUs, and an IT phase (Figure 1). In the case of the NOMA scheme, the IT phase consists of multiple concurrent transmissions from all the EHUs (Figure 2), whereas, in the case of the PF scheduling, the IT phase consists of a single transmission of the scheduled EHU (Figure 3). In epoch i , the duration of the EH phase is τT , whereas the duration of the IT phase is $(1 - \tau)T$. During the IT phase, the EHUs consume the total amount of energy harvested during the preceding EH phase.

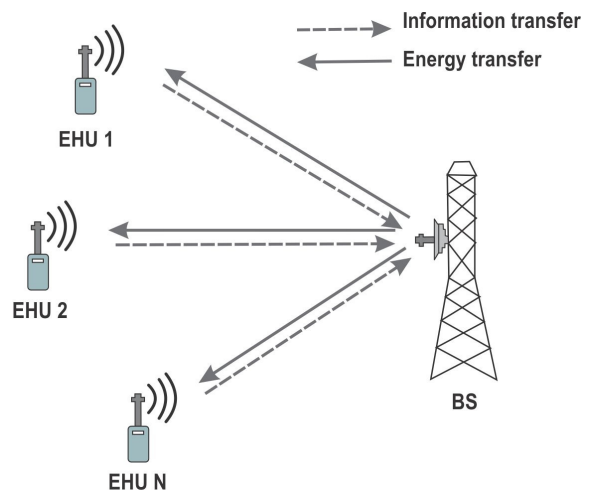


Fig. 1. System model

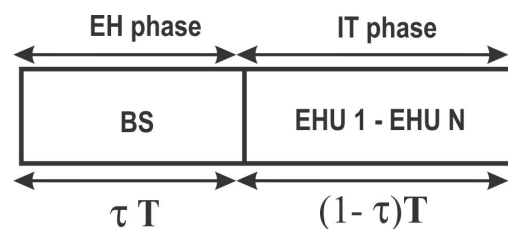


Fig. 2. NOMA epoch

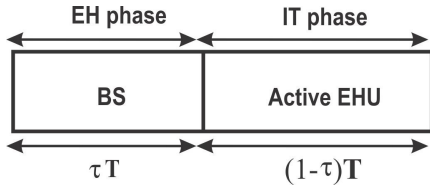


Fig. 3. Epoch with PF scheduling

The fading between the BS and EHU n ($1 \leq n \leq N$) is assumed to be stationary and ergodic random process, which follows the block fading model (i.e. the channel is constant during a single block but changes independently from one block to the next). We assume that the duration of each fading block is equal to T , and coincides with a single epoch. In epoch i , let the fading power gain of the BS-EHU $_n$ channel be denoted by $x_n(i)$. For convenience, the corresponding downlink (BS-EHU $_n$) and uplink (EHU $_n$ -BS) channels are assumed to be reciprocal, although the generality of our results is unaffected by this assumption. These gains are normalized by the additive white gaussian noise (AWGN) at the receiver N_0 , yielding $x_n(i) = x_n(i)/N_0$. The average value of $x_n(i)$ is denoted by $\Omega_n = E[x_n(i)]/N_0$, where $E[\cdot]$ denotes expectation. The BS is assumed to control and coordinate the uplink and downlink transmissions, and therefore is assumed to have perfect channel state information (CSI) of all N fading links, $\{x_n(i)\}_{n=1}^N$, in each epoch. The transmit power of the BS in epoch i is denoted by p_i . We assume that the power of the BS has to satisfy an average power constraint, P_{avg} (i.e. $E[p_i] \leq P_{avg}$), and a maximum power constraint, P_{max} (i.e. $0 \leq p_i \leq P_{max}$).

FAIR RESOURCE ALLOCATION

In the following subsections we derive expressions for the optimal BS transmit power and the duration of the EH and IT phase for two scenarios: (a) when NOMA is employed in the WPCN, and all of the EHUs transmit simultaneously over the uplink; (b) when PF scheduler selects a single EHU for uplink transmission.

Non-orthogonal multiple access

In case of NOMA, the harvested energy by n th EHU is $E_n(i) = \eta_n x_n(i) N_0 p_i \tau_i T$, where η_n

is the energy harvesting efficiency of n -th EHU. Using the notations, we can obtain the transmit power of n -th EHU during the successive IT phase in epoch i as

$$P_n(i) = \frac{E_n(i)}{(1-\tau_i)T} = \frac{\eta_n x_n(i) N_0 p_i \tau_i}{1-\tau_i}. \quad (1)$$

On the other hand, the rate of n -th EHU, denoted by $R_n(i)$, depends on the decoding order at the BS. Without loss of generality, we enumerate the EHUs according to the order of increasing average fading gains (i.e. $\Omega_1 \leq \Omega_2 \leq \dots \leq \Omega_N$).

Given τ_i , $P_n(i)$, $\forall n$, the n -th EHU in epoch i transmits a Gaussian distributed codeword (comprised of infinitely many symbols during the time $(1-\tau_i)T$). The actual achievable rate of n -th EHU, $\forall n$, in epoch i is given by

$$R_n(i) = (1-\tau_i) \log \left(1 + \frac{P_n(i)x_n(i)}{1 + \sum_{k=1}^{n-1} P_k(i)x_k(i)} \right). \quad (2)$$

The decoding order of the proposed NOMA scheme is based upon the long-term channel statistics, with fixed decoding order at the BS that is inverse to the distances of the EHUs from the BS. Please note that, compared to the duration of a single epoch, the time to decode information of all EHUs at the BS (employing SIC) is negligible, which is a reasonable assumption. The BS decodes the EHUs' codewords in the order $N, N-1, \dots, 2, 1$ and uses SIC: The EHU N is decoded first while experiencing interference from the remaining $N-1$ EHUs. The EHU $N-1$ is decoded second while experiencing interference from EHUs $N-2, N-3, \dots, 2, 1$. Finally, the EHU with smallest average fading power, the EHU 1 is decoded last in the absence of interference. It is worth mentioning that the decoding order does not affect the sum-rate of the EHUs. It only affects the value of the individual rates of the EHUs, and consequently the system fairness.

Using (2) the average achievable rate of EHU n , $\forall n$, over M epochs is given by

$$\bar{R}_n = \lim_{M \rightarrow \infty} \frac{1}{M} \sum_{i=1}^M (1-\tau_i) \log \left(1 + \frac{P_n(i)x_n(i)}{1 + \sum_{k=1}^{n-1} P_k(i)x_k(i)} \right), \quad (3)$$

Assuming $M \rightarrow \infty$ epochs we can formulate the following sum-rate maximization problem:

$$\text{Maximize } \sum_{n=1}^N \bar{R}_n$$

s.t.

$$\begin{aligned} C1: & \frac{1}{M} \sum_{i=1}^M p_i \tau_i \leq P_{avg} \\ C2: & 0 \leq p_i \leq P_{max}, \\ C3: & 0 < \tau_i < 1, \end{aligned} \quad (4)$$

where \bar{R}_n is given by (3).

The solution of (4) is given by the following theorem.

Theorem 1. The optimal BS transmit power, p_i^* , is given by

$$p_i^* = \begin{cases} P_{max}, & \lambda < b(i) \\ 0, & \text{otherwise,} \end{cases} \quad (5)$$

The optimal duration of the EH phase $\tau_i^* T$, is found as the root of the following transcendental equation,

$$\begin{aligned} \log \left(1 + \frac{b(i) P_{max} \tau_i^*}{1 - \tau_i^*} \right) + \lambda P_{max} &= \\ = \frac{b(i) P_{max}}{1 - \tau_i^* + b(i) P_{max} \tau_i^*} & \end{aligned} \quad (6)$$

where

$$b(i) = N_0 \sum_{n=1}^N \eta_n x_n^2(i). \quad (7)$$

The constant λ is found from

$$(1/M) \sum_{i=1}^M p_i^* \tau_i^* = P_{avg}.$$

Proof: Please refer to Appendix A. ■

Proportional fair scheduling

We aim at determining an opportunistic scheduling policy that achieve proportional fairness in the considered WPCN. Let the EHU s_i be the scheduled user in epoch i , which is selected opportunistically from among the EHUs. The remaining $N-1$ EHUs are silent (i.e. they neither harvest energy nor transmit information). The

amount of harvested energy by EHU s_i during the EH period is given by

$$E_{s_i}(i) = \eta_{s_i} x_{s_i}(i) N_0 p_i \tau_i T, \quad (8)$$

where η_{s_i} is the energy harvesting efficiency of the scheduled EHU, and $x_{s_i}(i)$ is the normalized fading power gain of the channel between the scheduled EHU and the BS. During the IT phase, EHU s_i spends all of its harvested energy, E_{s_i} , for transmitting information to the BS. In particular, the EHU s_i in epoch i can transmit a codeword of duration $(1-\tau_i)T$ with an output power,

$$P_{s_i}(i) = \frac{E_{s_i}(i)}{(1-\tau_i)T} = \frac{\eta_{s_i} x_{s_i}(i) N_0 p_i \tau_i}{(1-\tau_i)} \quad (9)$$

and an information rate $\log(1 + P_{s_i}(i) x_{s_i}(i))$. The actual achievable rate of the scheduled EHU s_i in that epoch is given by:

$$r_{s_i}(i) = (1-\tau_i) \log(1 + P_{s_i}(i) x_{s_i}(i)). \quad (10)$$

Let us now define the indicator variable

$$I_n(i) = \begin{cases} 1, & \text{if } n = s_i \\ 0, & \text{if } n \neq s_i \end{cases} \quad (11)$$

denoting whether EHU n is activated or not. Using (10) and (11) the average achievable rate of EHU n over M epochs is given by

$$\bar{R}_n = \lim_{M \rightarrow \infty} \frac{1}{M} \sum_{i=1}^M I_n(i) r_n(i). \quad (12)$$

By definition, PF scheduling is aimed at maximizing the product of the achievable rates of all users, or, equivalently the sum of the logarithms of the individual rates [12, 15]. Following this approach, we aim at maximizing the objective function $\sum_{n=1}^N \log \bar{R}_n$ and the PF optimization problem is defined as follows:

$$\text{Maximize } \sum_{n=1}^N \log \bar{R}_n$$

s.t.

$$\begin{aligned} C1': & \frac{1}{M} \sum_{i=1}^M p_i \tau_i \leq P_{avg} \\ C2': & 0 \leq p_i \leq P_{max}, \forall i \end{aligned}$$

$$\begin{aligned}
C3': & 0 < \tau_i < 1, \forall i \\
C4': & I_n(i) \in \{0, 1\}, \forall i, n, \\
C5': & \sum_{n=1}^N I_n(i) \leq 1, \forall i.
\end{aligned} \tag{13}$$

Theorem 2. The solution of (13) is given by

$$s_i = \arg \max_n \frac{r_n(i)}{\bar{R}_n}. \tag{14}$$

Moreover, the optimal allocations of the BS transmit power and the duration of the EH phase are respectively given by

$$p_i^* = \begin{cases} P_{max}, & a_{s_i}(i) > \lambda \bar{R}_{s_i} \\ 0, & \text{otherwise,} \end{cases} \tag{15}$$

$$\tau_i^* = 1 - \frac{a_{s_i}(i) P_{max}}{a_{s_i}(i) P_{max} - 1} \left(1 + \frac{1}{W \left(\frac{a_{s_i}(i) P_{max} - 1}{e^{1 - \bar{R}_{s_i} \lambda P_{max}}} \right)} \right)^{-1}, \tag{16}$$

where $a_{s_i}(i) = N_0 \eta_{s_i} x_{s_i}^2(i)$. Note that $W(\cdot)$ denotes the Lambert W function. The constant λ is found from $(1/M) \sum_{i=1}^M p_i^* \tau_i^* = P_{avg}$.

Proof: Please refer to Appendix B. ■

NUMERICAL RESULTS

In this section, we provide simulation results to complement the analysis above. Since Rayleigh fading is considered, $x_n(i)$ follow an exponential distribution. The deterministic path loss is calculated as $E[x_n(i)] = 10^{-3} D_n^{-\alpha}$, where D_n is the distance of the n -th EHU to the BS. The pathloss at a reference distance of 1 m is set to 30 dB, and the pathloss exponent is set to $\alpha = 3$. We assume an AWGN power equal to $N_0 = 2 \cdot 10^{-12}$ W. Thus, $\Omega_n = 10^{-3} D_n^{-3} / N_0$. We consider that one half (i.e. $N/2$) of the EHUs are placed at a distance of $D_1 = 10$ m, yielding to $\Omega_n = 10^6$ and the other half (i.e. $N/2$) of the EHUs at a distance of $D_2 = 12.5$ m from the BS, yielding to $\Omega_n = 10^6/2$. The average output power of the BS, P_{avg} , is set to either one of

the following values: 1 W and 2 W. We set $P_{max} = 5P_{avg}$, and $\eta_n = 0.5 \forall n$. We consider $M = 10^5$ epochs, and we depict the average achievable rates for the EHUs for this simulation setup. With these calculated average achievable rates, $\bar{R}_n, \forall n$, we can calculate the desirable metrics-sum-rate and fairness index for this system.

Figure 4 depicts the sum-rate over the uplink when NOMA or PF scheduling is employed in the WPCN with respect to the number of EHUs and the average BS power, P_{avg} . As a baseline we use TDMA-based WPCN proposed in [16], where the sum-rate is maximized by optimizing the durations of the EH and IT phases and the BS output power. It can be observed that NOMA achieves the same sum-rate for the same number of EHUs as TDMA, and PF scheduling achieves much smaller sum-rate due to the selection of a single EHU for uplink transmission in each epoch.

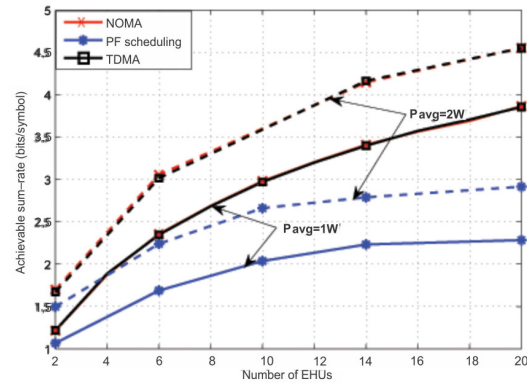


Fig. 4. Achievable sum-rate vs. number of EHUs

In Figure 5, we show the system fairness for the schemes with respect to the number of EHUs and the average BS power, P_{avg} . The system fairness is described by the Jain's fairness index, defined by [17]:

$$J(\bar{R}_n) = \frac{(\sum_{n=1}^N \bar{R}_n)^2}{N \sum_{n=1}^N \bar{R}_n^2}, \tag{17}$$

where \bar{R}_n is the achievable rate, defined by (3). Note that a higher value of $J(\bar{R}_n)$ indicates a higher degree of system fairness. It can be observed that both NOMA and PF schemes provide substan-

tial fairness enhancement compared to the baseline TDMA scheme.

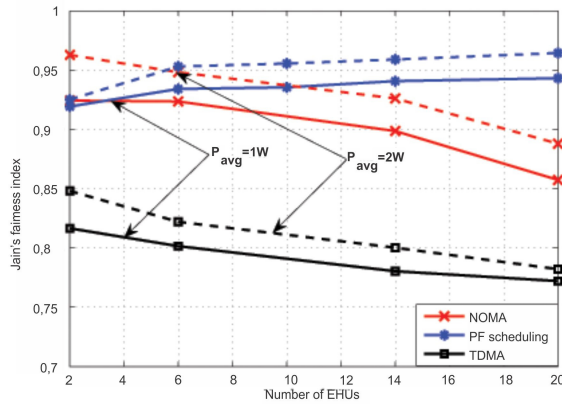


Fig. 5. System fairness vs. number of EHU

The proposed schemes achieve greater fairness for the same number of EHU when the average BS power P_{avg} increases. On the other hand, TDMA attains smaller improvement of the fairness for larger P_{avg} . Although NOMA achieves great level of fairness, it can be observed that the level of fairness decreases with the number of EHU. On the other hand, the number of EHU has positive impact for the fairness when PF scheduling is employed, and the results show that PF scheduling outperforms NOMA in terms of system fairness for larger number of EHU.

CONCLUSION

In this paper, we propose two schemes that tackle the tradeoff between the uplink sum-rate and system fairness in the WPCNs. Compared to the WPCNs employing TDMA scheme, both proposed schemes significantly enhance the system fairness. The NOMA scheme preserves identical sum-rate as compared to TDMA scheme, and outperforms PF scheduling in terms of achievable sum-rate, thus delivers balanced trade-off between sum-rate maximization and fair resource allocation among the EHU.

APPENDIX A PROOF OF THEOREM 1

By interchanging the order of summation and using the properties of the logarithmic function the objective function of (4) is transformed as

$$\frac{1}{M} \sum_{i=1}^M (1 - \tau_i) \log \left(1 + \frac{p_i \tau_i b(i)}{1 - \tau_i} \right), \quad (18)$$

where $b(i)$ is given by (7). The optimization problem (4) with the new objective function (18) is non-convex due to the products and ratios of the optimization variables p_i and τ_i . Therefore, we reformulate the problem by introducing the change of variable $e_i = p_i \tau_i$, and transform (4) into convex problem in terms of e_i and τ_i , as

$$\text{Maximize}_{e_i, \tau_i, \forall i} \frac{1}{M} \sum_{i=1}^M (1 - \tau_i) \log \left(1 + \frac{e_i b(i)}{1 - \tau_i} \right),$$

s.t.

$$\bar{C}1: \frac{1}{M} \sum_{i=1}^M e_i \leq P_{avg}$$

$$\bar{C}2: 0 \leq e_i \leq P_{max} \tau_i, \forall i$$

$$\bar{C}3: 0 < \tau_i < 1, \forall i. \quad (19)$$

The Lagrangian of (19) is given by

$$L = \frac{1}{M} \sum_{i=1}^M (1 - \tau_i) \log \left(1 + \frac{e_i b(i)}{1 - \tau_i} \right) - \lambda \left(\frac{1}{M} \sum_{i=1}^M e_i - P_{avg} \right) + \sum_{i=1}^M \alpha_i e_i - \sum_{i=1}^M \beta_i (e_i - P_{max} \tau_i). \quad (20)$$

In (20), the non-negative Lagrange multipliers λ , α_i and β_i are associated with the constraints $\bar{C}1$, the left-hand side of $\bar{C}2$ and the right-hand side of $\bar{C}2$, respectively, which satisfy the corresponding complementary slackness conditions $\alpha_i e_i = 0, \forall i$, and $\beta_i (e_i - P_{max} \tau_i) = 0, \forall i$.

By differentiating (20) with respect to e_i and τ_i , we obtain:

$$\frac{\partial L}{\partial e_i} = \frac{b(i)}{1 + b(i) \frac{e_i}{1 - \tau_i}} - \lambda + \alpha_i - \beta_i = 0. \quad (21)$$

$$\frac{\partial L}{\partial \tau_i} = \beta_i P_{max} + \frac{b(i) e_i}{1 - \tau_i + b(i) e_i}$$

$$- \log \left(1 + \frac{b(i) e_i}{1 - \tau_i} \right) = 0. \quad (22)$$

We now consider the following 2 cases.

Case 1: If $\tau_i = 0$, then $e_i = 0$ and no power is allocated to epoch i , i.e. $p_i^* = 0$. Since $e_i = 0$, the slackness conditions require $\alpha_i > 0$ and $\beta_i = 0$. From (21) we obtain the condition:

$$\alpha_i = \lambda - b(i) > 0. \quad (23)$$

After introducing (7) into (23), we obtain the following condition for the occurrence of this case:

$$\lambda > N_0 \sum_{n=1}^N \eta_n x_n^2(i).$$

Case 2: Let us assume $0 < \tau_i < 1$ and $e_i = P_{\max} \tau_i$. This case corresponds to $p_i^* = P_{\max}$. The slackness conditions require $\alpha_i = 0$ and $\beta_i > 0$. From (21) we obtain the condition:

$$\beta_i = \frac{b(i)}{1 + b(i) \frac{P_{\max} \tau_i}{1 - \tau_i}} - \lambda > 0. \quad (24)$$

Introducing (24) and $e_i = P_{\max} \tau_i$ into (22), we obtain (6). Based upon (6) and (24), it can be shown that the sufficient condition for the occurrence of this case is given by

$$\lambda < N_0 \sum_{n=1}^N \eta_n x_n^2(i).$$

APPENDIX B PROOF OF THEOREM 2

Although $I_n(i)$ is a binary variable, we can relax the constraint C4 as $0 \leq I_n(i) \leq 1$ in order to make the PF optimization problem tractable. After relaxing C4' and introducing the change of variables $e_i = p_i \tau_i$, we obtain the following optimization problem:

$$\text{Maximize}_{e_i, \tau_i, I_n(i)} \sum_{n=1}^N \log \left[\frac{1}{M} \sum_{i=1}^M I_n(i) (1 - \tau_i) \log \left(1 + \frac{e_i a_n(i)}{1 - \tau_i} \right) \right]$$

s.t.

$$\begin{aligned} \bar{C}1' : & \frac{1}{M} \sum_{i=1}^M e_i \leq P_{\text{avg}} \\ \bar{C}2' : & 0 \leq e_i \leq P_{\max} \tau_i, \forall i \\ \bar{C}3' : & 0 < \tau_i < 1, \forall i \\ \bar{C}4' : & I_n(i) \geq 0, \forall i, n, \\ \bar{C}5' : & \sum_{n=1}^N I_n(i) \leq 1, \forall i. \end{aligned} \quad (25)$$

However, the optimization problem (25) is still non-convex, because of the product $I_n(i)(1 - \tau_i)$ which appears in the objective function. Nevertheless, similarly to [19, (P4)], we can still apply the Lagrange duality method to solve (13) based on [18, Theorem 1]. In particular, (25) is in the form of [18, Eq. (4)]. For any fixed τ_i and $I_n(i)$, the objective function is concave in e_i . Therefore, for any fixed set of $\tau_i, \forall i$ and $I_n(i), \forall i$, the objective function of (25) is concave in (e_1, e_2, \dots, e_M) and the constraint C1 is affine (i.e. convex) in (e_1, e_2, \dots, e_M) . According to [18, Definition 1], the time-sharing condition is thus satisfied, implying zero duality gap.

The Lagrangian of (25) is as follows:

$$\begin{aligned} L = & \sum_{n=1}^N \log \left[\frac{1}{M} \sum_{i=1}^M I_n(i) (1 - \tau_i) \log \left(1 + a_n(i) \frac{e_i}{1 - \tau_i} \right) \right] \\ & - \lambda \left(\frac{1}{M} \sum_{i=1}^M e_i - P_{\text{avg}} \right) + \sum_{i=1}^M q_i e_i - \sum_{i=1}^M \mu_i (e_i - P_{\max} \tau_i) \\ & + \alpha_{n,i} I_n(i) - \beta_i \left(\sum_{n=1}^N I_n(i) - 1 \right), \end{aligned} \quad (26)$$

where the Lagrange multiplier $\lambda > 0$ is associated with the constraint $\bar{C}1'$, whereas the non-negative Lagrange multipliers q_i and μ_i correspond to the left-hand side and the right-hand side of $\bar{C}2'$, respectively, and Lagrange multipliers $\alpha_{k,i}$ and β_i correspond to $\bar{C}4'$ and $\bar{C}5'$, respectively.

By differentiating L with respect to $I_n(i)$, τ_i and e_i , we obtain the following system of 3 equations:

$$\frac{\partial L}{\partial I_n(i)} = \frac{r_n(i)}{R_n} + \alpha_{n,i} - \beta_i = 0, \quad (27)$$

$$\begin{aligned} \frac{\partial L}{\partial \tau_i} = & \sum_{n=1}^N \frac{I_n(i)}{R_n} \left(-\log \left(1 + \frac{a_n(i) e_i}{1 - \tau_i} \right) - \frac{\frac{a_n(i) e_i}{1 - \tau_i}}{1 + \frac{a_n(i) e_i}{1 - \tau_i}} \right) \\ & + \mu_i P_{\max} = 0, \end{aligned} \quad (28)$$

$$\begin{aligned} \frac{\partial L}{\partial e_i} = & \sum_{n=1}^N \frac{I_n(i) a_n(i)}{R_n} \frac{1 + a_n(i) \frac{e_i}{1 - \tau_i}}{1 - \tau_i} - \lambda + q_i - \mu_i = 0. \end{aligned} \quad (29)$$

The complementary slackness are given by

$$\lambda \left(\frac{1}{M} \sum_{i=1}^M e_i - P_{avg} \right) = 0, \quad (30)$$

$$q_i e_i = 0, \forall i, \quad (31)$$

$$\mu_i (e_i - P_{max} \tau_i) = 0, \forall i, \quad (32)$$

$$\alpha_{n,i} I_n(i) = 0, \forall i, n, \quad (33)$$

$$\beta_i \left(\sum_{n=1}^N I_n(i) - 1 \right) = 0, \forall i, \quad (34)$$

where $q_i \geq 0$, $\mu_i \geq 0$, $\alpha_{n,i} \geq 0$, and $\beta_i \geq 0$.

We divide the rest of the proof in two parts: Scheduling policy (part 1) and optimal power and time allocation (part 2).

Part 1

First, let us focus only on (27) and its corresponding slackness conditions (33)–(34). Without loss of generality, let us assume a WPCN consisting of 2 EHUs (a and b). From (27), we have:

$$\frac{\partial L}{\partial I_a(i)} - \frac{\partial L}{\partial I_b(i)} = \frac{r_a(i)}{R_a} - \frac{r_b(i)}{R_b} = -\alpha_{ai} + \alpha_{bi} \quad (35)$$

Case 1: If the IT phase is not allocated to any user from complementary slackness it follows that $\alpha_{a,i} > 0$ and $\alpha_{b,i} > 0$. From (35) we obtain:

$$\frac{\partial L}{\partial I_a(i)} - \frac{\partial L}{\partial I_b(i)} = \frac{r_a(i)}{R_a} - \frac{r_b(i)}{R_b} = \alpha_{b,i} - \alpha_{a,i} = 0, \quad (36)$$

thus $\alpha_{a,i} = \alpha_{b,i}$ and the probability for it to happen tends to zero. We conclude that the IT phase must be allocated in each epoch.

Case 2: If $0 < I_a(i)$ and $0 < I_b(i)$, then $\alpha_{a,i} = 0$ and $\alpha_{b,i} = 0$. Now we derive:

$$\frac{\partial L}{\partial I_a(i)} - \frac{\partial L}{\partial I_b(i)} = \frac{r_a(i)}{R_a} - \frac{r_b(i)}{R_b} = 0, \quad (37)$$

or $\frac{r_a(i)}{R_a} = \frac{r_b(i)}{R_b}$, which also has probability tending to zero.

Case 3: Lastly, if the IT phase is allocated to user a only, then $I_a(i) = 1$ and $I_b(i) = 0$, which in turn implies that $\alpha_{a,i} = 0$ and $\alpha_{b,i} > 0$ due to the complimentary slackness condition. From (35) it follows:

$$\frac{\partial L}{\partial I_a(i)} - \frac{\partial L}{\partial I_b(i)} = \frac{r_a(i)}{R_a} - \frac{r_b(i)}{R_b} = \alpha_{b,i} > 0. \quad (38)$$

From the fact that $\log x$ is a strictly concave function and the previous equation it follows that the optimal scheduling policy is thus given by (14).

Part 2

Let EHU s_i be the scheduled user in epoch i . Now, (28) and (29) become:

$$\begin{aligned} \frac{\partial L}{\partial \tau_i} = \frac{I_{s_i}(i)}{R_s} & \left(-\log \left(1 + \frac{a_{s_i}(i)e_i}{1-\tau_i} \right) - \frac{\frac{a_{s_i}e_i}{1-\tau_i}}{1 + \frac{a_{s_i}e_i}{1-\tau_i}} \right) + \\ & + \mu_i P_{max} = 0 \end{aligned} \quad (39)$$

$$\frac{\partial L}{\partial e_i} = \frac{I_{s_i}(i)a_{s_i}}{R_{s_i}} \frac{1 + a_{s_i} \frac{e_i}{1-\tau_i}}{1-\tau_i} - \lambda + q_i - \mu_i = 0. \quad (40)$$

We consider the following 2 cases:

Case 1: If $\tau_i = 0$, then $e_i = 0$ and $I_{s_i}(i) = 0$ and no power is allocated to epoch i , i.e. $p_i^* = 0$.

Case 2: Let us assume $0 < \tau_i < 1$, also $e_i = P_{max} \tau_{0i}$ and $I_{s_i}(i) = 1$. This case corresponds to $p_i^* = P_{max}$. The slackness conditions require $q_i = \alpha_{s,i} = 0$, $\mu_i > 0$ and $\beta_i > 0$. From (40), we obtain the inequality condition

$$\mu_i = \frac{a_{s_i}}{1 + \frac{a_{s_i} P_{max} \tau_i}{1-\tau_i}} - \lambda R_{s_i} > 0,$$

or, equivalently,

$$\frac{1-\tau_i}{\tau_i} \left(\frac{1}{\lambda R_{s_i}} - \frac{1}{a_{s_i}} \right) > P_{max}.$$

In order to satisfy the constraint $0 < \tau_{0i} < 1$, $\lambda R_{s_i} < a_{s_i}$ must be satisfied. Introducing μ_i and $e_i = P_{\max} \tau_{0i}$ into (39), we obtain (16).

REFERENCES

- [1] P. Grover, A. Sahai: Shannon meets Tesla: wireless information and power transfer, *Proc. IEEE ISIT 2010*, pp. 2363–2367, Austin, USA, June 2010.
- [2] D. Gunduz, K. Stamatiou, N. Michelusi, M. Zorzi: Designing intelligent energy harvesting communication systems, *IEEE Commun. Magazine*, **52**, 1, 210–216 (Jan. 2014).
- [3] C. K. Ho, R. Zhang: Optimal energy allocation for wireless communications with energy harvesting constraints, *IEEE Trans. Signal Processing*, **60**, 9, 4808–4818 (May 2012).
- [4] H. Ju, R. Zhang: Throughput maximization in wireless powered communication networks, *IEEE Trans. Wireless Commun.*, **13**, 1, 418–428 (Jan. 2014).
- [5] X. Kang, C. Ho Keong, S. Sun: Optimal time allocation for dynamic-TDMA-based wireless powered communication networks, *Proc. IEEE Globecom 2014*, Austin, USA, Dec. 2014.
- [6] H. Ju, R. Zhang: Optimal resource allocation in full-duplex wireless-powered communication network, *IEEE Trans. on Commun.*, **62**, 10, 3528–3540 (Oct. 2014).
- [7] T. Takeda, K. Higuchi: Enhanced user fairness using non-orthogonal access with SIC in cellular uplink, *VTC 2011*, San Francisco, USA, pp. 1–5, 2011.
- [8] Z. Ding, Z. Yang, P. Fan, H. V. Poor: On the performance of non-orthogonal multiple access in 5G systems with randomly deployed users, *IEEE Signal Process. Lett.*, **21**, 12, 1501–1505 (2014).
- [9] S. Timotheou, I. Krikidis: Fairness for non-orthogonal multiple access in 5G systems, *IEEE Signal Process. Lett.*, **22**, 10, 1462–1465 (2015).
- [10] H. Chingoska, Z. Hadzi-Velkov, I. Nikoloska, N. Zlatanov: Resource Allocation in Wireless Powered Communication Networks with Non-Orthogonal Multiple Access, *IEEE Wireless Communications Letters*, **5** (6), 684–687 (2016).
- [11] P. Viswanath, D. N. Tse, R. Laroia: Opportunistic beamforming using dumb antennas, *IEEE Trans. Information Theory*, **46**, 6, 1277–1294 (June 2002).
- [12] N. Tekbiyik, T. Girici, E. Uysal-Biyikoglu, K. Leblebicioglu: Proportional fair resource allocation on an energy harvesting downlink, *IEEE Trans. Wireless Communications*, **12**, 4, 1699–1711 (April 2013).
- [13] H. Chingoska, I. Nikoloska, Z. Hadzi-Velkov, N. Zlatanov: Proportional fair scheduling in wireless powered communication networks, *23rd International Conference on Telecommunications (ICT)*, May 2013.
- [14] Z. Hadzi-Velkov, I. Nikoloska, H. Chingoska, N. Zlatanov, Proportional fair scheduling in wireless networks with RF energy harvesting and processing cost, *IEEE Comm. Letters*, **20**, 10, 2107–2110 (2016).
- [15] T.-D. Nguyen, Y. Han: A Proportional Fairness Algorithm with QoS Provision in Downlink OFDMA Systems, *IEEE Comm. Letters*, **10**, 11 (Nov. 2006).
- [16] Z. Hadzi-Velkov, I. Nikoloska, G. K. Karagiannidis, T. Q. Duong: Wireless networks with energy harvesting and power transfer: joint power and time allocation, *IEEE Signal Process. Letters*, **23**, 1, 50–54 (Jan. 2016).
- [17] R. Jain, D. Chiu, W. Hawe: A Quantitative measure of fairness and discrimination for resource allocation in shared computer systems, *Tech. Rep. TR-301, DEC*, September 1984.
- [18] W. Yu, R. Lui: Dual methods for nonconvex spectrum optimization of multicarrier systems, *IEEE Trans. Commun.*, **54**, 7, 1310–1322 (Jul. 2006).
- [19] L. Liu, R. Zhang, K.-C. Chua: Wireless information transfer with opportunistic energy harvesting, *IEEE Trans. Wireless. Commun.*, **12**, 1, 288–300 (Jan. 2013).

METHODS FOR RADIO SPECTRUM EVALUATION AND MONITORING

Liljana Gavrilovska, Pero Latkoski, Vladimir Atanasovski

Faculty of Electrical Engineering and Information Technologies,

"Ss. Cyril and Methodius" University in Skopje,

Rugjer Bošković bb, P.O. box 574, 1001 Skopje, Republic of Macedonia

liljana@feit.ukim.edu.mk

A b s t r a c t: Due to the extensive growth of wireless communications, the usage of radio bands requires a substantial optimized approach and rational treatment. Many new emerged communication scenarios necessitate techniques for optimal spectrum evaluation and monitoring. This paper discusses various such approaches and particularly focuses on spectrum sharing and coexistence presenting several case studies. It offers insights into simulation, modeling and measurement-based methodologies related to spectrum evaluation and utilization, focusing on the effects before and after the digital switchover (DSO) of the TV systems. We investigate the usability of the different propagation models in current wireless systems modeling, including the measurement-based validation of their precision for different scenarios. The article, furthermore, presents laboratory experiments on DVB-T and LTE-800 coexistence. Finally, it discusses a designed example of a nationwide monitoring system for intruder detection, comparing several applied methods and their precision.

Key words: radio spectrum; measurement; modeling; LTE; DTV; intruder detection

МЕТОДИ ЗА ЕВАЛУАЦИЈА И МОНИТОРИНГ НА РАДИОСПЕКТАР

А п с т р а к т: Со развојот на безжичните комуникации се јавува потреба од постојано оптимизирање и рационално користење на опсезите на радиофреквенциите. Многуге нови комуникациски сценарија бараат техники за евалуација и мониторинг на спектарот. Во трудот се разгледуваат повеќе пристапи поврзани со овој проблем со посебен фокус на неколку разработени примери за делење на спектарот и коегзистенција на технологии. Трудот дава детали поврзани со евалуацијата на спектарот преку симулации, моделирање и мерење, фокусирајќи се на ефектите пред и по дигитализацијата на телевизискиот систем. Се испитува користењето на различни пропагандиски модели и се прави нивна валидација со мерење. Дополнително се дадени резултати од лабораториски експерименти поврзани со коегзистенција на DVB-T и LTE технологии. На крајот е опишан систем за мониторинг на натрапници во спектарот кој функционира на целата територија на една држава. Испитувани се различни методи за детекција од аспект на нивната прецизност.

Клучни зборови: радиоспектар; мерење; моделирање; LTE; DTV; детекција на натрапници

1. INTRODUCTION

The continuous increase in data rates and the number of people using mobile communications has been a trend over the last decade. Successful implementation of digital television (DTV) and the emergence of the digital dividend (DD), increases significantly the demand for wireless services, stimulated by new applications and the push towards the Internet of Things (IoT) [1], 5G mobile communications [2] and small cells [3]. The higher

number of users, as well as the diversity of the services operating in the same or adjacent bands, contributes to the increased spectrum evaluation and optimization problems. This is why the planning and managing of the spectrum imposes a necessity for international regulations on global, regional and national levels. The global radio services are regulated coherently for all countries worldwide under the auspices of the International Telecommunication Union. The regulation of the spectrum requires clear approaches, rational usage and opti-

mization, which is not a trivial task and needs some comprehensive research, with variety of applied methodologies. Furthermore, the local regulators need accurate results for the specific problems of spectrum management, caused by the coexistence of wireless technologies. Some examples are: the coexistence of DVB-T and LTE-800 or WiFi-like devices operating within the TV band. Such results can be obtained by focused measurement campaigns, laboratory experiments and comprehensive calculations. Finally, the maintenance and the protection of the spectrum impose a necessity of nationwide monitoring systems.

In this context, the reminder of this article is organized as follows: Section II describes the targeted scenarios; Section III presents several case studies on spectrum evaluation, detailing the results based on modeling and measurements. Section IV contains the laboratory experiments on DVB-T and LTE-800 coexistence. In Section V, the article provides solutions for radio interference and intruder detection on a nationwide operational level and finally, Section VI concludes the article.

2. USAGE SCENARIOS

The implementation of DSO leads to TV White Spaces (TVWS), i.e. chunks of available spectrum that can be used for a plethora of applications and services. First and foremost, it is targeted for the *mobile broadband services such as LTE-800*, as witnessed by the adoption of the DD 1, as well as the adoption of the DD 2 [4]. However, other potential scenarios are also viable, e.g.:

- *Cellular use of white spaces* where cellular systems are secondary users of the TV bands and they get access to the available spectrum in addition to the licensed mobile bands.
- *WiFi-like usage of TVWS* where the secondary system is a fixed network operator, i.e. a WLAN service provider, which deploys opportunistic spectrum access for WLAN-like devices operating in the TV bands.

Both of the envisioned scenarios require a clear and distinct technical and business feasibility study for practical deployment.

3. DTV SPECTRUM MODELING AND MEASUREMENT

Multiple interleaved methodologies and approaches should be engaged to obtain relevant results and conclusions regarding the coexistence of

different wireless technologies. A full list of utilized methodologies involves: numerical calculations performed by multiple software packages, simulations of behavior prediction, laboratory setup measurements, as well as field measurements. The methodology also includes validation of results, obtained by comparison between the predictions and the measurements. This section provides details in spectrum modeling and measurement. The main focus is on the UHF TV band, pinpointing the most suitable propagation models and measurement setup for DTV spectrum evaluation.

a) Modeling approach

The process of spectrum modeling for any foreseen spectrum sharing scenario requires usage of (as accurate as possible) radio propagation models. Propagation models in general are divided into *empirical-statistical* models and *physical-analytical* models. Empirical models are better adapted to a quick and approximate coverage calculation, while physical-analytical models may be computationally-intensive but they are much more accurate.

In order to verify the relevance of this methodology for assessing TVWS, this section investigates the influence of the used propagation model on the channel availability, taking the territory of the Republic of Macedonia as an example study area [5]. The following figures (Figure 1 and Figure 2) present the number of free TV channels for each location (pixel size 100×100 m) within the target territory, when applying two different propagation models. Figure 1 presents the estimated available channels when the calculations include the statistical ITU propagation model [6], without taking into consideration the real geographical terrain in the area. Figure 2 uses the Longley-Rice propagation model [7] and the actual terrain. Both cases apply same regulatory criteria for channels availability.

The figures reveal that due to the highly mountainous geographical characteristics of the target area, the results significantly differ from each other. In particular, the most common number of available channels per location in the first case is one or two, while in the second case this number varies between five and ten. In the first case, the maximum number of free channels is 20, while in the second case this number is 40. Obviously the second approach involving actual terrain plus Longley-Rice propagation model provides more realistic white space availability.

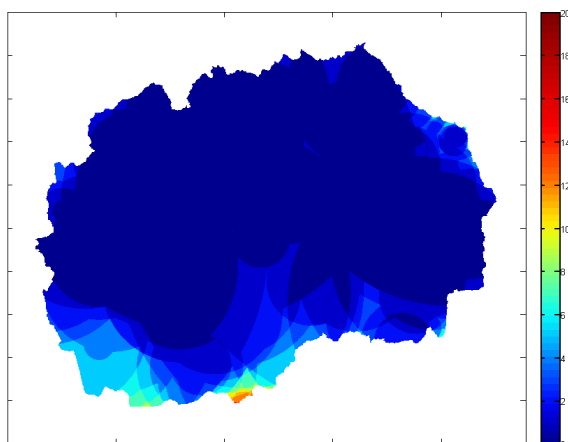


Fig. 1. TV channels availability (ITU propagation model)

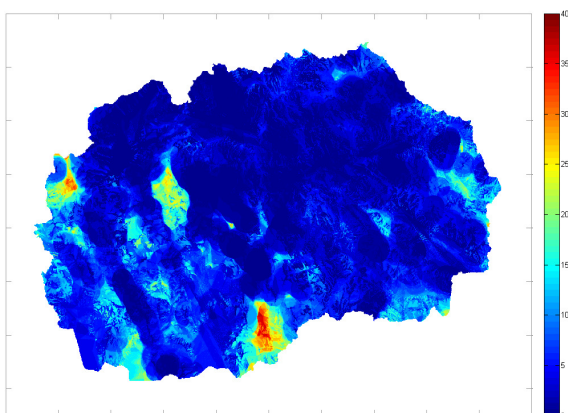


Fig. 2. TV channels availability (Longley-Rice propagation model)

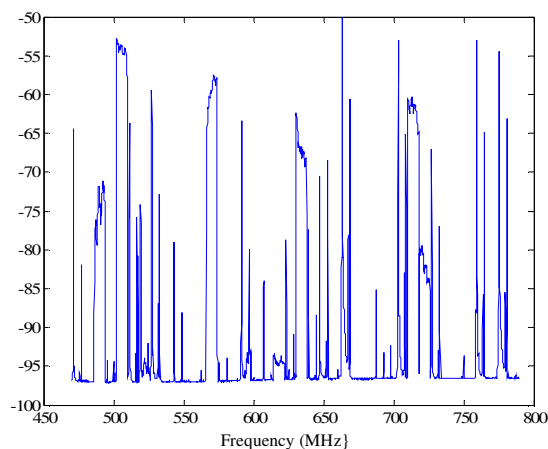
b) Spectrum availability before and after DSO

The majority of the European countries have completed the process of DSO for their television systems [8]. The major DTV advantages are: increased number of television programs, excellent visual and audio quality, possible mobile and portable reception, plethora of new services and applications on demand, reflection-free picture and constant signal quality.

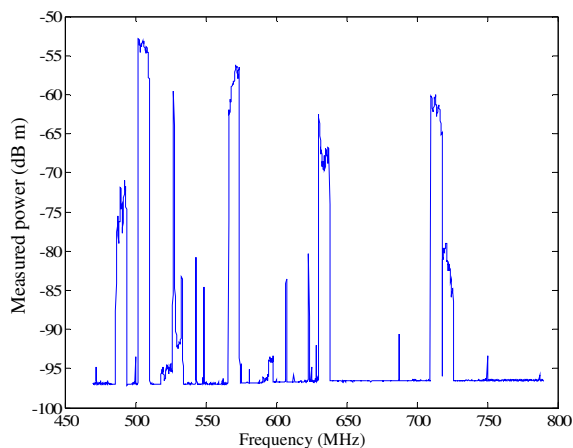
This sub-section showcases the spectrum availability obtained by measurements, before and after the DSO in Macedonia. Furthermore, the analysis provides an evaluation of the available spectrum usability when assuming WiFi-like secondary users operating in TVWS.

The measurement setup was customized towards an accurate estimation of the TV signals and it involved an Anritsu MS2690A spectrum ana-

lyzer and a Sachwarzbeck bi-conical antenna. The results revealed the primary system activities during the DSO transition in terms of frequency spectrum utilization. Figure 3 shows the frequency utilization of the 470 – 790 MHz band that is foreseen as the main TVWS provider. A visual comparison of the two figures (Fig.3-a and Fig.3-b) proves the expansion of the TVWS after the DSO.



a) before DSO



b) after DSO

Fig. 3. Spectrum occupancy in Macedonia

In order to calculate the real usable frequency chunks for secondary communication that will not degrade the operation of the primary TV reception, the analysis firstly needs to determine the maximum received power for each TV channel. These values represent an input to the calculation process, which implements the ECC rules for operation of the White Space Devices (WSD) in the TV band

based on the SE43 Report 154. According to the SE43, the implementation of any WSD should not violate certain limits related to the degradation of the TV reception location probability. Additionally, the calculation of the secondary spectrum availability needs a precise specification of the WSD transmission power and the required channel bandwidth. One important parameter is the number of adjacent TV channels, which will be protected from the WSD transmissions in terms of the interference produced towards the TV receivers operating on the same channels. The requirement to protect a higher number of adjacent TV channels reduces the secondary spectrum availability.

In terms of TVWS usability, the continuity of the available frequency channels for the WSD operation also represents an important parameter. The blocks of the available channels, also known as *available frequency chunks*, are multiples of 8-MHz frequency channels. The size of these frequency chunks determines the operational WSD channel bandwidth. According to the results, the most promising scenario in terms of spectrum availability is the one immediately after the DSO, protecting ± 1 adjacent TV channels, due to the number of available chunks with a size of 8 MHz.

A quantitative study on the TVWS availability prior and after the DSO would require a comparison of the secondary system performance in terms of throughput achieved by the WSDs. In order to obtain this performance metric, the calculation process requires an even more detailed description of the secondary system and its capabilities.

The results reveal that the scenario involving the TV band after the DSO, where the secondary system operates over 8 MHz frequency chunks, provides the best performance in terms of achievable throughput. The organization in 16 MHz chunks is less efficient mainly because of the spectrum utilization efficiency. The achievable throughput prior the DSO is much lower for both cases (8 MHz and 16 MHz).

4. LABORATORY EVALUATION OF LTE-800 AND DVB-T COEXISTENCE

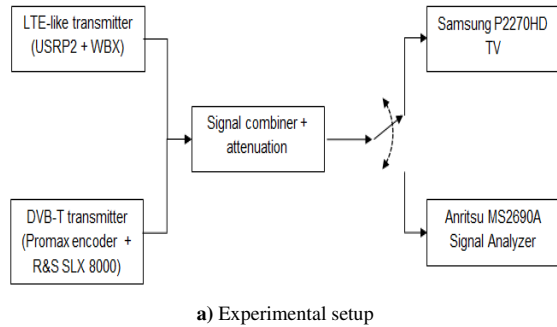
The recent DSO and the release of the upper UHF bands for LTE services, has led to coexistence issues between LTE-800 and DVB-T transmissions. This is a significant problem especially for the DTV service degradation because the DTV receivers are still manufactured to receive signals

in the upper UHF bands. Therefore, the regulatory bodies have been particularly active in this area performing tests and deriving the DTV service protection ratios for different types of commercial receivers.

The performed laboratory evaluation predicts the LTE interference on DVB-T system performance. The analysis considers the current regulatory recommendations. It numerically and experimentally derives the DTV protection ratios, comprising an USRP2-based [9] implementation of an LTE-like signal generator, a DVB-T transmitter and receiver, and a video encoder. The performance analyses consider different LTE transmission configurations in terms of the transmit/receive power, the bandwidth and the DTV frequency proximity [10].

The LTE-like signal generated with the USRP2 and the WBX daughterboard is combined with a real DVB-T signal (generated with an R&S transmitter, and video encoded by a Promax H264 encoder) and input directly to a Samsung P2270HD TV. The practical setup and analyses are presented in Figure 4-a). The desired signal levels are achieved using adjustable attenuators and measured using an Anritsu MS2690A signal analyzer. The LTE-like transmission uses a central frequency of 786MHz, while the DVB-T transmission/reception is switched between channels 52-60 to evaluate the adjacent and co-channel DTV protection ratios. The equipment used in the demo setup is listed in the table within Figure 4-b).

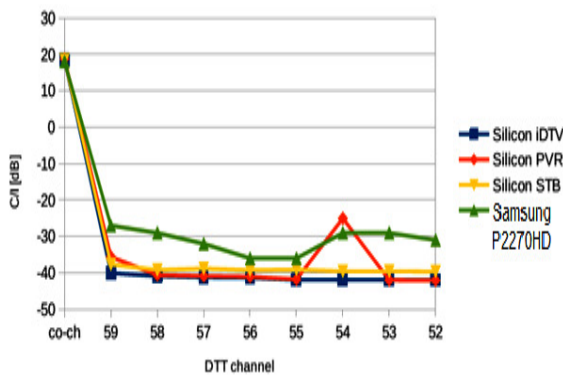
Figure 4-c) presents the numerically and experimentally derived protection ratios for the LTE-like transmitter and the four different DTV receivers, i.e. three typical Silicon receivers [11] and one Samsung P2270HD TV. The LTE-like transmitter uses 5 MHz bandwidth. The results consider a scenario when the required signal level of the DTV reception is -50 dBm. It is important to notice that the practically obtained (with Samsung P2270HD) and the numerically obtained (with the Silicon receivers from [11]) protection ratios experience increased differences (up to 10 dB). This is due to the non-linearity of the signals attenuation caused by the used attenuators and the combiner in the demo. In particular, some frequency chunks of the DVB-T signal are more attenuated than others. Based on the results, the USRP-based LTE-like transmitter is a satisfying LTE emulator, since there are only minor differences in the protection ratios with the results in [11].



a) Experimental setup

Equipment	Hardware
LTE-like signal generator	USRP2 with WBX daughterboard
DVB-T transmitter	Rohde & Schwarz SLX 8000 low power DVB-T transmitter
Video encoder	Promax DVB-H-264 Encoder and Transcoder
DVB-T receiver	Samsung P2270HD TV
Signal Analyser	Anritsu MS2690A

b) Demo equipment



c) Derived protection ratios

Fig. 4. Demo setup and results for the practical evaluation of DTV protection ratio with the LTE-like transmitter

5. ANALYSIS OF INTERFERENCE AND INTRUDER DETECTION

The coexistence of DVB-T and LTE-800 may often lead to undesirable consequences such as *interference* and *service outage*. All national regulatory bodies perform radiomonitoring in order to ensure quality reception by the end users. The scope of their work targets continuous radiomonitoring of interference, control of technical and exploitation conditions (usual for operation of licensed wireless transmitters), discovery of unauthorized wireless transmitters as well as monitoring of the spectrum usage.

Modern radiomonitoring encompasses wireless signal receptions by fixed, remote and mobile radiomonitoring stations and sensors. The received signals are then subjected to analysis by *Direction Finding* (DF), *Time Difference of Arrival* (TDoA), *Angle of Arrival* (AoA) and/or hybrid (combination of TDoA and AoA) methods for geolocation of wireless transmitters.

The TDoA method determines the location of a wireless transmitter by using a relative time difference of the received signal by several radiomonitoring stations and sensors. The AoA method determines the direction of arrival of a wireless transmission using a receive antenna array. The hybrid method combines TDoA and AoA characteristics, in order to improve the precision. It exploits parabolic curves and DF lines stemming from the TDoA and AoA methods and analyzes their intersections to precisely find the geolocation of a wireless transmitter [12].

This sub-section focuses on the practical (empirical) evaluation and validation of the TDoA, AoA and hybrid geolocation methods using the nationwide spectrum monitoring system of the Agency of Electronic Communications (AEC) in Macedonia (see Figure 5-a). The empirical results prove the validity and the precision of the designed system and pave the way towards the modern radiomonitoring for effective spectrum usage regulations [13].

The empirical analysis exploits the operational radiomonitoring system of AEC and a fixed wireless transmitter (signal generator Anritsu MS2690A) with a variable output power. The transmitter is used to generate controllable transmissions of different wireless signals (e.g. DVB-T, FM, TETRA, GSM, UMTS) under five distinct measurement scenarios:

1. TDoA geolocation using three sensors closely located to the position of the wireless transmitter.
2. TDoA geolocation using three sensors located far from the position of the wireless transmitter.
3. TDoA geolocation using five sensors.
4. Hybrid geolocation three TDoA sensors (closely located to the actual position of the wireless transmitter) and a DF receiver.
5. Hybrid geolocation three TDoA sensors (located far from the actual position of the wireless transmitter) and a DF receiver

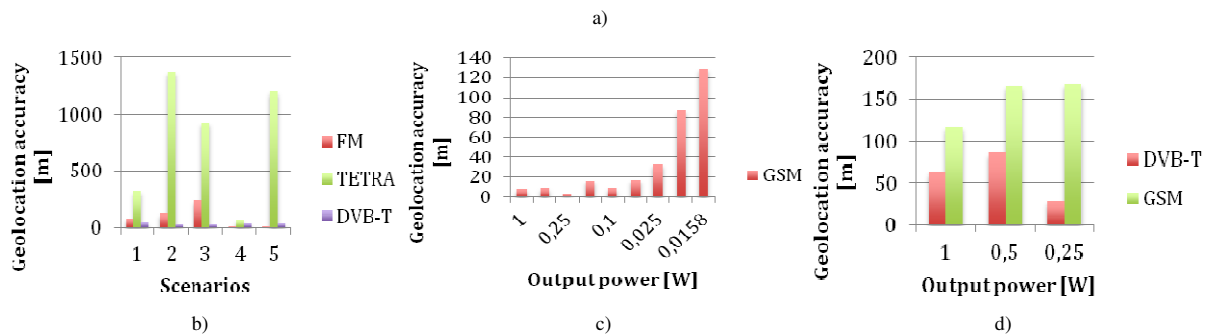
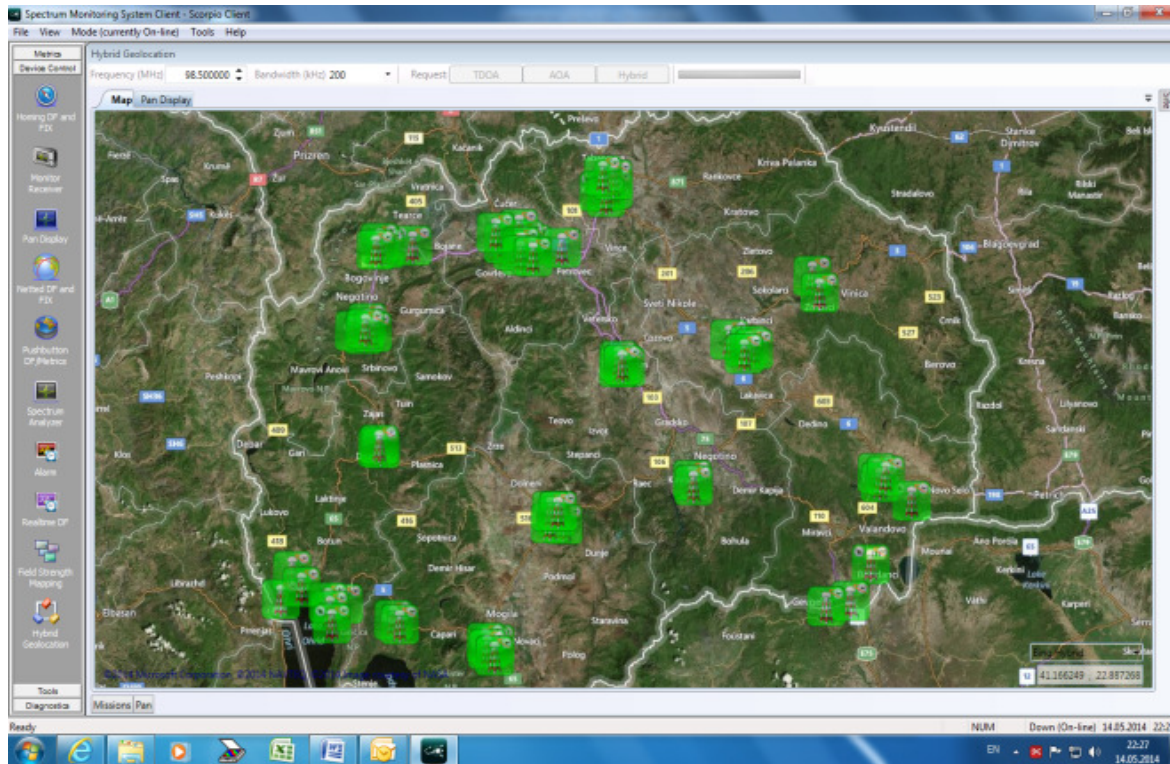


Fig. 5. Transmitter localization using a nationwide monitoring system in the Republic of Macedonia
a) Distribution of TDoA sensors (AEC spectrum monitoring solution); **b)** Geolocation accuracy of the hybrid method for FM, TETRA and DVB-T signals; **c)** Geolocation accuracy of the hybrid method for GSM signal with variable output power; **d)** Geolocation accuracy of the AoA method for DVB-T and GSM signals with variable output power

The scenarios are chosen to reflect the effect of the geometry and the number of used sensors on the system performance having in mind the actual operational characteristics of the wireless systems. Measurements were conducted with variable output power of the controlled wireless transmitter in order to analyze the minimum transmitter power that can be detected by the system. The metrics of interest is the *geolocation accuracy* expressed in the coordinate difference between the actual location of the transmitter and the output of the chosen geolocation method.

Figure 5-b shows that the accuracy for the hybrid method is improved when the signal being

located has wider bandwidth (DVB-T as opposed to FM and TETRA signals). Figure 5-c shows that the accuracy of the hybrid method is the highest for a GSM signal with lower power (higher powers lead to interferences that affect the accuracy of the system). Finally, Figure 5-d shows that the geolocation TDoA for a DVB-T signal does not necessitate TDoA sensors for high accuracy (as opposed to a GSM signal).

The empirical evaluation in this analysis gives a detailed insight into the performance of an operational nationwide radiomonitoring system that incorporates different radiomonitoring stations and different geolocation methods.

One of the main findings is that the hybrid method offers the best performance in terms of geolocation accuracy. The reason lies in the unique combination of both TDoA and AoA benefits within.

6. CONCLUSION

This article discussed a plethora of possible methodologies and approaches in radio spectrum evaluation. These methods (including laboratory and field measurements, numerical and analytical calculations, simulations and modeling) need to be applied in combined manner in order to provide accurate results and mutual validations. The spectrum re-usage and co-existence are hot topics and above all an obvious necessity in the radio-communications today and it requires careful selection of tools and means when estimating the secondary system characteristics. Furthermore, the applied settings of each particular approach must be customized according to the primary and secondary systems. This article elaborated several case studies on spectrum availability, pinpointing to possible issues that may emerge by the coexistence of wireless technologies.

Acknowledgment: The Public Diplomacy Division of NATO in the framework of Science supported this work for Peace through the SFP-984409 Optimization and Rational Use of Wireless Communication Bands (ORCA) project. The authors would like to thank to all partners and participants in the project.

REFERENCES

- [1] P. K. Agyapong, et al.: Design considerations for a 5G network architecture, *IEEE Communications Magazine*, **52**, 11, 65–75 (2014).
- [2] Horizon 2020 Advanced 5G Network Infrastructure for Future Internet PPP – Creating a Smart Network that is Flexible, Robust and Cost Effective, <http://ec.europa.eu/digital-agenda/futurium/en/content/horizon-2020-advanced-5g-network-infrastructure-future-internet-ppp-creating-smart-network>, accessed, Oct. 2014.
- [3] A. Ichkov, V. Atanasovski, L. Gavrilovska: Analysis of Two-Tier LTE Network with Randomized Resource Allocation and Proactive Offloading, *Mobile Networks and Applications*, 2016, pp. 1–8, DOI: 10.1007/s11036-016-0754-0.
- [4] *ITU World Radiocommunications Conference 2015*. <http://www.itu.int/en/ITU-R/conferences/wrc/2015/Pages/default.aspx>.
- [5] P. Latkoski, J. Karamacoski, L. Gavrilovska.: Availability assessment of TVWS for Wi-Fi-like secondary system: A case study, *7th International Conference on Cognitive Radio Oriented Wireless Networks – CROWN-COM 2012*, Stockholm, Sweden, June 18–20, 2012.
- [6] Method for point-to-area predictions for terrestrial services in the frequency range 30 MHz to 3000 MHz, *International Telecommunications Commission (ITU)*, Rec. ITU-R P. 1546–3, 2007.
- [7] P. Rice, A. Longley, K. Norton, A. Barsis: Transmission Loss Predictions for Tropospheric Communication Circuits, Volume I, *National Bureau of Standards, Technical Note*, vol. **101**, 1967.
- [8] Bernard Pauchon: Digital Switch Over Experiences across Europe, *ITU International Symposium – Digital Switchover*, Geneva, June 17th, 2015.
- [9] Universal Software Radio Peripheral 2 (USRP2). Information available: http://www.ece.umn.edu/users/ravi0022/class/ee4505/ettus_ds_usrp2_v5.pdf.
- [10] D. Denkovski, V. Atanasovski, L. Gavrilovska: Practical evaluation of LTE-800 and DVB-T coexistence, *IEEE International Symposium on Broadband Multimedia Systems and Broadcasting (BMSB)*, Ghent, Belgium, June 17–19, 2015.
- [11] OFCOM Technical Report: *Technical analysis of interference from mobile network base stations in the 800 MHz band to digital terrestrial television*, June, 2011.
- [12] A. Grambozov, V. Atanasovski, L. Gavrilovska: Practical evaluation of TDoA, AoA and hybrid methods for geolocation of wireless transmitters, *IEEE International Symposium on Broadband Multimedia Systems and Broadcasting (BMSB)*, Ghent, Belgium, June 17–19, 2015.
- [13] <http://orca.feit.ukim.edu.mk>

BILLING SYSTEM FOR OTT SERVICES

Marko Porjazoski, Pero Latkoski, Borislav Popovski

*Faculty of Electrical Engineering and Information Technologies,
"Ss. Cyril and Methodius" University in Skopje,
Rugjer Bošković bb, P.O. box 574, 1001 Skopje, Republic of Macedonia
{markop, pero, borop}@feit.ukim.edu.mk*

Abstract: In this paper we propose a functional architecture of billing system for Over the Top services. Since OTT services are very diverse provided over different access technologies, on different user devices, legacy billing systems designed for support of unique services in closed provider networks are no longer suitable for new OTT environment. So we propose more flexible approach in building billing systems.

Key words: billing system; OTT services; video streaming

СИСТЕМ НА НАПЛАТА ЗА OTT СЕРВИСИ

Апстракт: Во овој труд е предложена функционална архитектура на систем за наплата (биллинг систем) за OTT (Over the Top) сервиси. Бидејќи OTT-сервисите се обезбедуваат преку различни пристапни технологии, различни кориснички уреди, постојните системи преку кои се врши наплатата се дизајнирани за поддршка на само поединечни сервиси во блиските провајдерски мрежи, па не се соодветни за новата OTT околина. Во решението е предложен пофлексибилен пристап во развојот на системите за наплата.

Клучни зборови: систем за наплата; OTT сервиси; поток на видеоподатоци

INTRODUCTION

Over-the-top (OTT) refers to delivery of video, audio and other media over the Internet without having Internet service provider involved in the control or distribution of the content [1]. Content is transited over the ISP network and he may be aware of the contents of the Internet Protocol packets but it is not responsible for, nor able to control, the viewing abilities, copyrights, and/or other redistribution of the content. One example of system architecture for provisioning of OTT services is presented in Fig 1.

Furthermore, OTT services are meant to be device independent. It means that user should obtain same service on any device like smart phone, smart TV, laptop, set-top box, PC, etc.

One of the major backend functionalities of OTT system certainly are charging and billing. It

should provide great flexibility to the service provider in the way how it will offer and charge different services to the end user.

The simplest form of charging the user is to ask him to pay prior for the certain service that he wants to subscribe too. The second form of charging is prepaid concept where user has certain credit on his account and he spends it whenever he subscribe to some OTT service. These two solutions are suitable for users who do not want or are unable to sign a contract with the service provider [2, 3].

Third possible solution for charging of OTT services is postpaid solution, where user signs contract with service provider and receives a bill once a month for delivered services.

Prepaid and postpaid billing system is easy to implement in closed network where network provider is also a service provider. Having in

mind the diverse of possible OTT services, as well as diverse of possible access technologies and end user devices, it is obvious that legacy billing systems based on Call Data Record (CDR) and Usage Data Records (UDR) are not suitable for new OTT environment. So we need a new more flexible approach in building billing systems [4]. In paper [5] authors have stated that billing systems has to be more flexible in order to meet demands

of new services. In [6], architecture to realize a flexible charging system is proposed for 3G networks, but this solution only supports legacy voice and data services.

In this paper we propose a functional architecture of billing system for OTT services which is already implemented and running within the OTT solution of one service provider in R. Macedonia.

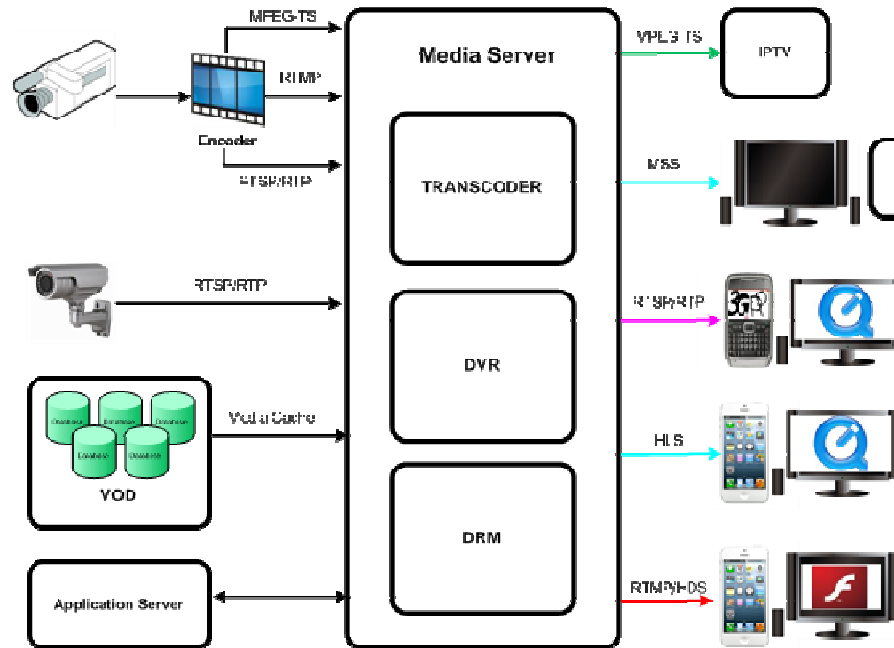


Fig. 1. System architecture for OTT services [1]

DEFINITIONS OF TERMS

Before explaining proposed billing system architecture, we will define some terms used in this paper and objects that are managed with this system.

OTT reseller is a partner that will use OTT service provider infrastructure to sale/resell OTT services to their customers are defined as OTT resellers. Proposed OTT solution enables creation of reseller specific content that will be available only to their customers.

User is an individual or company that registers at OTT service provider or its resellers billing system. One user can have multiple accounts.

Each **account** has its one credentials, i.e. username and password. Accounts are entities that

are actually subscribed to some service. Single account can be used to get services on multiple devices. Two types of accounts are provided: pre-paid or postpaid. User can have multiple accounts of different type.

Service plan is a set of OTT services that are offered to customers as a whole. Services belonging to one service plan do not need to be homogeneous, i.e. services in one service plan can be of different type.

Offer is a set of conditions under which service plane is offered to a customer like duration of subscription, payment type, price, promotional discounts etc.

Service is a basic unit provided to end users. Some examples of different services are: streaming of live TV or radio program, streaming of video or audio content on demand, available min-

utes for content recording, or available number of devices aloud per account etc.

Functional architecture of billing system for OTT services

Proposed functional architecture of billing system for OTT services is presented in Fig. 2, and it consist of several functional blocks:

- **Partners/resellers management** functional block is responsible for definition and control of partner companies access and service definition rights. This will allow partner companies to resell services provided by service provider, owner of this system, or to use service provider infrastructure to provide their own services to their customers.
- **Users and accounts management** functional block is responsible for user registration and management of accounts and their credentials. As an option this functional block may allow creation of temporary users and accounts meant for testing of OTT services before customers makes their final decision to subscribe.
- **Service management** is a functional block that should provide functionalities for service definition, service provisioning, creation of service plans and service plan's offers. Depending on his rights, reseller can have access to these functionalities in orders to define their own services and services plans for their customers.
- **Subscription management** functionalities should allow flexible assignment of subscriptions of different service plans to prepaid and postpaid accounts.
- **Billing engine** is meant to calculate total subscription cost for postpaid accounts and to generate invoices.
- **Credit control** should check prepaid accounts credit each time before user is subscribed to new service plan in order to verify whether there are sufficient funds to cover the cost of subscription.
- **Payment processing** functional block should check timely payment of invoices and provide functionalities to enable alternative methods for payment of invoice such as m-banking or e-banking.
- **Report generation** should enable creation of different kind reports related to all aspect of OTT billing system. For an example timely reports on user subscriptions or reports for outstanding invoices, etc.
- **Notification engine** should enable sending notifications to users about some promotions, about expiration date of its subscription, notification about credit left to prepaid account, etc.
- **OTT mediation** is a functional block that will provide communication interfaces and APIs for integration of OTT billing system with other entities involved in OTT services delivery like OTT headed, DRM systems, server for control of partners/resellers licenses, etc.

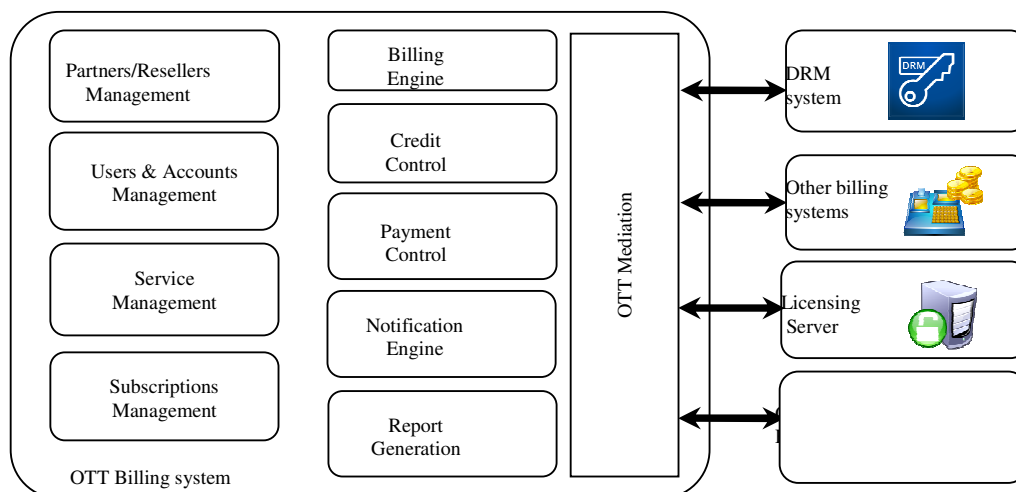


Fig. 2. Functional architecture of billing system for OTT services

SOFTWARE IMPLEMENTATION OF BILLING SYSTEM FOR OTT SERVICE PROVIDERS

All the functionalities of the proposed billing solution can be implemented in software. Components of the software implementation of billing system for OTT services are presented in Figure 3.

Main part of this implementation are databases where all the records about resellers, users, accounts, services, service plans, offers etc. are stored.

Administrative Graphical User Interface (GUI) is a modular solution providing access to different databases and records depending on administrative privileges of the logged user. In order to provide access to administrative stuff any ware at any time we recommend administrative GUI to be web based, i.e. it can be access over secured HTTP(S). For that reason HTTP server has to be engaged. Databases can be hosted on single or multiple machines or in the cloud depending on provider's infrastructure and number of expected customers and subscriptions.

OTT mediation software should provide communication interfaces and APIs with other entities involved in OTT services provisioning. It consists of several modules also, each responsible to respond to particular request sent by peering entity.

OTT mediation Billing Module is responsible for communication between OTT billing sys-

tem with OTT headend and other billing systems. OTT mediation will push some information to OTT headend necessary for the proper functioning of the system, like services definition for example, or it will respond to paired systems requests.

Upon incoming request Billing Module will share subscription information of users registered in OTT billing system.

Notification module should generate notification about user subscriptions, for example subscription expiration date, or credit limit, or some promotions, and send them to users through OTT headend.

DRM module should communicate with the third party DRM management system to implement appropriate security mechanisms for content protected by DRM.

Licensing module is meant to communicate with licensing server in order to find out details about partner/reseller's access rights and privileges.

Depending on the incoming request OTT mediation should construct its response based on the information that he found in the OTT billing databases.

We recommend usage of secured HTTP(S) for communication between OTT mediation and other OTT system entities with json (Java Script Object Notation) formatting of request and response messages sent or received, form or to OTT mediation.

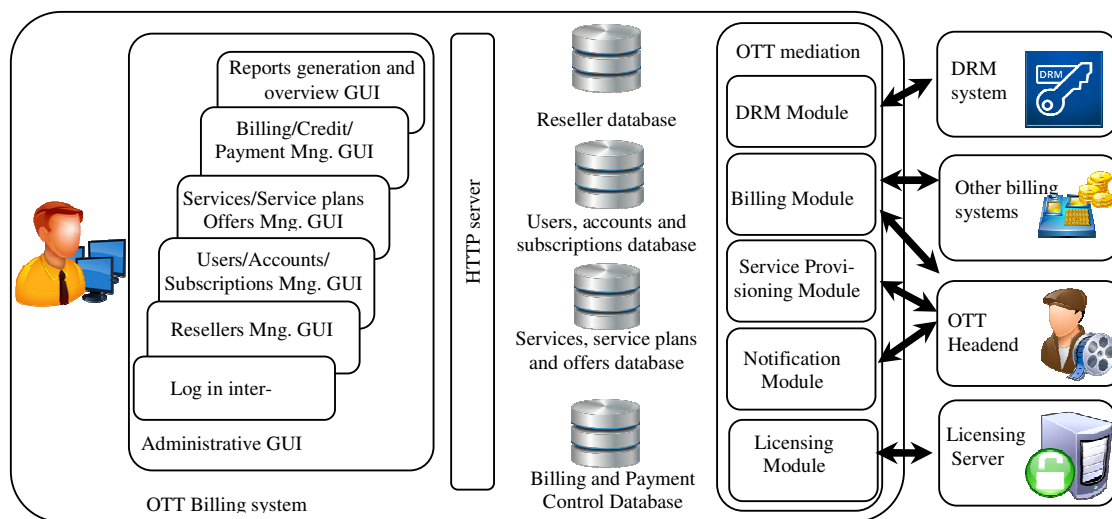


Fig. 3. Software implementation of billing system for OTT services

Some example request and response messages sent or received by OTT mediation in order to get data from billing system are:

- Get(BillingData) – request sent by OTT head end in order to find out service plans that user is subscribed to and which services should be provided. OTT mediation billing module should respond with response (BillingData) message containing information about user data subscriptions.
- Get(ServicePlans) – request sent by OTT headend to find out a set of services included in each service plan. OTT mediation billing module should send response (ServicePlans) with service plans content defined in OTT billing system.
- Post(Notification) – request sent by OTT mediation notification module to OTT headend containing notification message that should be delivered to users. OTT mediation notification module should expect response on the outcome of notification delivery.
- Get(LicenseInfo) request sent by OTT mediation licensing module in order to find out reseller's access rights and privileges.

Since OTT billing system will use DRM system services, mediation software should adopt messaging format provided by the third party DRM solution. Usually messaging format used for this purposes are based on SOAP (Simple Object Access Protocol) and WSDL (Web Services Description Language) [7].

SERVICES, SERVICE PLANS AND OFFERS DEFINITION AND PROVISIONING

Parameters required for service definition are following:

- ResellerID – unique reseller identifier, that will be used to associate service to appropriate reseller;
- ServiceType – some of the supported service types like TV channel, radio channel, number of recording minutes etc.;
- ServiceName – name of defined service;
- ServiceURL – Unified resource location where service can be reached;
- SupportedBitrates – in case of streaming service type this parameter defines list of available bitrates for different streaming quality.

After definition service info is stored in local database and then sent to OTT headend by request through communication interface between OTT mediation and OTT headend. Service data is sent to OTT headend in json format presented in Figure. 4.

```
{
  "TimeStamp": "2016-10-02T21:20:07Z",
  "ResellerID": "FEIT",
  "services": [
    {
      "ServiceType": "TVchannel", "servicesName":
      "MTV 1", "serviceURL":
      "http://server/streaming/mtv1", "SupportedBitrates":
      [{"Bitrate": "500kbps"}, {"Bitrate": "1000
      kbps"}, {"Bitrate": "2000kbps"}], },
    {
      "ServiceType": "RadioChannel", "servicesName":
      "MR 1", "serviceURL":
      "http://server/streaming/mr1", "SupportedBitrates":
      [{"Bitrate1": "4kbps"}, {"Bitrate2": "8kbps"}, {"Bi-
      trate3": "16kbps"}], }}

```

Fig. 4. Service data in json format.

In Figure 4 definition for two services is presented. The first service is a TV channel named as MTV1, which streaming URL is "http://server/streaming/mtv1" and it has three different streaming bitrates 500, 1000 and 2000 kbps. The second service is a streaming service for radio channel MR1. "http://server/streaming/mr1" is a URL to reach this streaming service and it has also three supported streaming bitrates 4, 8 and 16 kbps.

Service plan is a set of services offered to users as a whole. The conditions under which customers subscribe to service plan are defined in service plan offers. Parameters defining offers are following:

- ResellerID – unique reseller identifier;
- ServicePlanName – name of service plan which offer is defined;
- OfferName – name of the offer;
- ValidityPeriod – Time period in days for how long offer is valid;
- Price – Offer price;
- Discount – price discount in some promotional period;
- PromotionPeriod – Duration of promotional period in days.

After defining service plans and their offers in OTT billing, they are forwarded to OTT headend using messages structured in json format as shown in Figure 5:

```
{
  "TimeStamp": "2016-10-02T21:20:07Z",
  "ResellerID": "FEIT",
  "ServicePlans": [
    {
      "ServicePlanName": "NationalTVs",
      "services": [
        { "servicesName": "MTV 1" },
        { "servicesName": "MTV 2" }
      ],
      "offers": [
        {
          "OfferName": "OfferNationalTV1",
          "ValidityPeriod": "365",
          "Price": "400 MKD",
          "Discount": "100 MKD",
          "PromotionPeriod": "30"
        },
        {
          "OfferName": "OfferNationalTV2",
          "ValidityPeriod": "730",
          "Price": "300 MKD",
          "Discount": "100 MKD",
          "PromotionPeriod": "90"
        }
      ]
    },
    {
      "ServicePlanName": "LocalTVs",
      "services": [
        { "servicesName": "ATV" },
        { "servicesName": "BTV" }
      ],
      "offers": [
        {
          "OfferName": "OfferLocalTV1",
          "ValidityPeriod": "180",
          "Price": "250 MKD",
          "Discount": "0",
          "PromotionPeriod": "0"
        },
        {
          "OfferName": "OfferLocalTV2",
          "ValidityPeriod": "365",
          "Price": "200 MKD",
          "Discount": "50 MKD",
          "PromotionPeriod": "30"
        }
      ]
    }
  ]
}
```

Fig. 5. Service plan's and their offers data in json format.

Data presented in Figure 5 defines two service plans, each with two different offers. First service plan names as "NationalTVs" consists of two services: MTV1 and MTV2. This service plan has two offers named as "OfferNationalTV1" and "OfferNationalTV2". The first offer have validity period of 355 days, its monthly price is 300 MKD, promotion period is 30 days and discount for this period is 100 MKD. The second offer for service plan "NationalTVs" is named as "OfferNationalTV2". It has validity period of 730 days, monthly price of 300 MKD, promotion period of 90 days with monthly discount of 100 MKD. The second service plan defined with json structure in Figure 5 is named as "LocalTVs". It has also two offers named as "OfferLocalTV1" and "OfferLocalTV2". The first one have validity period of 180 days while the second have validity period of 365 days. Price for the first offer is 250 MKD with no promotion and discount, while validity period for the second offer is 365 days with monthly price of 200 MKD and discount of 50 MKD within 30 days promotion period.

USERS, SUBSCRIPTIONS AND LICENSING

One way to protect OTT system from illegal and unauthorized use is implementation of so called licensing server. Licensing server holds the records about number of users and number of subscriptions allowed for some reseller. During the process of user creation and subscription assignment, OTT billing checks the reseller's license status at licensing server to ensure that there is a free license that can be assigned to new user and user's subscription. If there is no free license for particular reseller, creation of new user and its subscriptions will be discarded.

Upon successful user creation and subscription assignment, data are saved to local database. In order to enable automatic and instant service provisioning, user data is sent to OTT headend to allow user access to particular service.

A format of message with user data sent to OTT headend is presented in Figure 6.

```
{
  "TimeStamp": "2016-10-02T21:20:07Z",
  "ResellerID": "FEIT",
  "users": [
    {
      "UserName": "user1",
      "subscriptions": [
        {
          "OfferName": "OfferNationalTV1",
          "StartDate": "2016-10-01T00:00:00Z",
          "EndDate": "2018-10-01T00:00:00Z"
        },
        {
          "OfferName": "OfferLocalTV2",
          "StartDate": "2016-10-01T00:00:00Z",
          "EndDate": "2018-10-01T00:00:00Z"
        }
      ]
    },
    {
      "UserName": "user2",
      "subscriptions": [
        {
          "OfferName": "OfferNationalTV2",
          "StartDate": "2016-12-15T00:00:00Z",
          "EndDate": "2018-12-15T00:00:00Z"
        },
        {
          "OfferName": "OfferLocalTV1",
          "StartDate": "2016-12-15T00:00:00Z",
          "EndDate": "2018-12-15T00:00:00Z"
        }
      ]
    }
  ]
}
```

Fig. 6. User subscriptions data in json format.

Data presented in Figure 6 are subscription information for two different users identified by their user names: "user1" and "user2". User1 is subscribed to "OfferNationalTV1" and "OfferLocalTV2", offers defined for service plans "NationalTVs" and "LocalTVs" respectively. User2 is subscribed to "OfferNationalTV2" and "OfferLocalTV1". Subscription period is defined with "StartDate" and "EndDate" values. OTT headend should provide user access to services included in each service plan that he is subscribed to within

subscription period. Outside of this period access to services should be blocked for that particular user.

CONCLUSIONS

Considering the fact that the existing billing systems are not flexible enough to be engaged in provisioning of OTT services, it is clear that we need a new billing system that will meet the requirements. In this paper we have proposed a flexible modular architecture of OTT billing system that should meet current and future requirements of OTT services.

Proposed OTT billing architecture can be easily implemented by using standard programming languages (php, ASP.NET, or Java), well established database systems (mySQL, ORACLE, or Microsoft SQL) and HTTP servers (IIS, Apache etc).

This solution can be easily integrated with other billing and DRM systems through appropriate communication and AP interfaces.

REFERENCES

- [1] Wowza Media Systems, <https://www.wowza.com/>.
- [2] Robert Törnkvist, Ralph Schubert: *Ericsson convergent charging and billing*, https://www.ericsson.com/ericsson/corpinfo/publications/review/2009_01/files/Charging.pdf.
- [3] Ericson White Paper: *Prepaid postpaid convergent charging*, http://www.idc-online.com/technical_references/pdfs/data_communications/PREPAID_POSTPAID_CONVERGENT.pdf
- [4] Xie Qingrui: Reshape your billing support system Huawei, *Huawei Technologies*, APR 2008, Issue 40, pp 43–46, <http://www1.huawei.com/en/static/HW-079821.pdf>.
- [5] Cliff Lui, Hui Ka Yu, Richard Shi, Jacky Pang: *Telecommunications Billing in the Competitive Wireline Arena*, May 2007, <http://www.viperfusion.com/wordpress/wpcontent/uploads/2007/11/2007PaperTelecommunicationsBillingandStrategy.pdf>
- [6] R. Kühne, U. Reimer, M. Schläger, F. Dressler, C. Fan, A. Fessi, A. Klenk, G. Carle: *Architecture for a Service-Oriented and Convergent Charging in 3G Mobile Networks and Beyond*, 2005, <https://www.net.in.tum.de/fileadmin/bibtex/publications/papers/kuehne05architecture.pdf>
- [7] Verimatrix, <http://www.verimatrix.com/>

CONSUMER'S "LOCK-IN" – A KEY ELEMENT OF THE SWITCHING COSTS IN MOBILE TELEPHONY IN THE REPUBLIC OF MACEDONIA

Slavica Nasteska¹, Liljana Gavrilovska²

¹Agency for Electronic Communications, Kej "Dimitar Vlahov" 21, 1000 Skopje, Republic of Macedonia

²Faculty of Electrical Engineering and Information Technologies,

"Ss. Cyril and Methodius" University in Skopje,

Rugjer Bošković bb, P.O. box 574, 1001 Skopje, Republic of Macedonia

nasteslavica@gmail.com

Abstract: This paper presents the calculation of the switching costs based on the previously developed model providing analysis for the mobile telephony market in the Republic of Macedonia for period from 2005 to 2015. Based on an administered questionnaire to various customers of the mobile telecommunication industry in the country, we find that the so called "Lock-in" affects the switching costs, being in close relation to the market competition. The analysis shows different stages of the competition on the mobile market and proposes some appropriate regulatory tasks.

Key words: switching costs empirical model; regulation; consumer behavior; loyalty; competition

„ЗАКЛУЧУВАЊЕ“ ОД КОРИСНИЦИТЕ – КЛУЧЕН ЕЛЕМЕНТ ВО ТРОШОЦИТЕ ЗА ПРОМЕНА НА МОБИЛЕН ОПЕРАТОР ВО РЕПУБЛИКА МАКЕДОНИЈА

Апстракт: Во овој труд се презентира претходно развиен модел за пресметка на трошоците за промена на оператор, надграден со анализа на пазарот за мобилна телефонија во Република Македонија во периодот од 2005 до 2015 година. Врз основа на прашалник што беше дистрибуиран до различни корисници на мобилните комуникациски услуги во државата, констатиравме дека таканареченото „заклучување“ на корисниците влијае врз трошоците за промена на оператор, што пак е во тесна релација со конкуренцијата на пазарот. Анализата ги покажува различните нивоа на конкуренцијата на пазарот на мобилни комуникации, при што се предлагаат и соодветни регулаторни активности.

Клучни зборови: трошоци за промена на оператор; емпириски модел; регулатива; однесување на корисниците; верност; конкуренција

1. INTRODUCTION

Consumers on many markets for particular products or services face significant costs when moving to the product or service offered by a competing company. The most general feature related to the products or services offered on particular market is the so called consumer's "Lock-in", which occurs when the consumer continues to use the product or service of a certain brand even when the same product or service offered by a competitive brand is cheaper [1]. An important benefit of

"Lock-in" the consumer is that the companies are allowed to charge the prices above the marginal costs. A basic way to "Lock-in" the consumer is through the switching costs expressed in the form of human and physical capital that each customer invests to purchase a certain brand. It is necessary to highlight the fact that each brand operates on a standard that may not be compatible with the standards embedded among the competing brands.

This paper relies on the empirical research developed by Shy [2] that offers a model to precisely calculate the *switching costs* through the

observed prices and market share. Even there are vast of theoretical works in different industries related to this problem [3], empirical works are difficult to find. The empirical model is presented in Section 2. It is then tested with the actual data for the mobile market in the Republic of Macedonia for the period 2005–2015, when different stages on the market can be easily recognized. Section 3 presents the results and provides the appropriate discussion. Finally, section 4 examines the calculated switching costs based on the customer behavior with respect to “Lock-in” and provides some appropriate recommendations for activities in the future. Section 5 concludes the paper on how consumers can benefit from the competition.

The goal of the work is not only to calculate the consumers’ switching costs for the existing mobile operators on the market in different stages of market development, but also to identify the rational behind the numerical values and the particular calculated switching costs. Also, the work locates some switching barriers and proposes appropriate regulatory activities.

2. EMPIRICAL MODEL

Direct measurement of the switching costs is a complex procedure. The implemented *Shy’s model* offers a “*quick and easy*” methodology for estimation based on the observed variables [2]. His innovative approach allows the calculations of the switching cost without using any econometrics. The methodology enables calculation solely as a function of the prices / fees and market share. The methodology assumes that the companies involved in the price competition recognize the switching cost for the consumers and therefore maximize their prices. These prices are subject to the restriction that no other company will decide it is profitable to lower its prices in order to subsidize the switching cost of its consumers. Thus, the switching cost specific for that brand is calculated as a function of the observed prices and market share.

The model starts with the assumption that the prices of each company satisfy the Undercut-proof Property [2], so no company can increase its revenues by undercutting the rival company and no company can increase its price without being profitably undercut by the competing company. This model was adjusted to different developing phases, specifics and parameters of the mobile telephony market in the Republic of Macedonia and was

validated through calculation of the switching costs based on real data, leading to relevant conclusions.

If we define S_i to be a switching cost of a i -company consumer and assume that all S_i ($I = 1, \dots, I$) are known to all companies and consumers, then each company $i \neq I$ takes the price charged by i -company p_i as known and sets maximal p_i to satisfy

$$\pi_i = p_i N_i \geq (p_i - S_i)(N_i + N_I), \quad (1)$$

where:

π_i stands for the revenues of i -company,

π_I stands for the revenues of I -company,

S_i is a cost of i -company’s customer to switch into I -company,

p_i is a price charged by i -company,

p_I is a price charged by I -company,

N_i denotes the number of i -company’s customers,

N_I denotes the number of I -company’s customers.

Therefore, every i -company maximizes its price p_i so that I -company will not find undercutting as profitable. Because all prices are observed, unobserved switching costs of the consumers of each company can be calculated. By solving (1) as equality, S_i becomes

$$S_i = p_i - N_i p_I / (N_i + N_I), \quad I \in \{1, \dots, I-1\}. \quad (2)$$

Equation (2) represents the switching cost for i -company’s consumers as a function of the prices set by i -company and I -company and the size of the market share of each company. This determines the switching costs of I -company’s consumers. The company with the lowest market share (the I -company) assumes that it is the target of company 1, who first appeared on the market. Therefore, the I -company sets the price p_I that would make undercutting its price by company 1 unprofitable:

$$\pi_i = p_i N_i \geq (p_i - S_i)(N_i + N_I). \quad (3)$$

Since the price p_I is observed, the unobserved switching cost S_I is calculated from (3) in the case of equality as:

$$S_I = p_I - N_I p_1 / (N_I + N_1). \quad (4)$$

However, in reality consumers may not have the same switching costs. If the switching costs reflex the training or learning by doing, then the switching costs will be higher for those customers who have high *value of time* (they use the same brand for longer time), probably as result of higher income.

3. FITTING THE MODEL INTO ACTUAL MARKET CONDITION

In this section we use the model presented in the previous section to calculate the switching costs for the mobile telephony market in the Republic of Macedonia. The calculations reflex different phases on the mobile telephony market during a decade. Only the market shares of the mobile operators existing on the market in the specific period are used for the calculation. Particularly, the calculations use as input data the market shares in subscriber number and revenues.

3.1. The period of monopoly

Mobile telephony as a service in the Republic of Macedonia was offered in September 1996 by organizational unit "Center for mobile telephony" which functioned within the Public Enterprise "PTT Macedonia". After the separation of the postal activities from the telegraph and telecommunications, within the JSC (Joint Stock Company) owned by the state, it started to prepare for privatization named "Makedonski telekomunikacii". On January 15, 2000, the Government of the Republic of Macedonia and the consortium led by the Hungarian telecommunication operator "MATAV" signed a contract for sale of shares of JSC "Makedonski telekomunikacii", making "MATAV" in the register of shareholders of JSC "Makedonski telekomunikacii" as the owner of 51% of the shares. Today "MATAV" is Magyar Telekom Group and is a part of the international Deutsche Telekom.

The mobile activity center of JSC "Makedonski telekomunikacii" was transferred to JSC "Mobimak" on June 4, 2001. The new company provided only mobile telephony services and data transmission over a cellular communication network, based on signed concession agreement. In 2006, JSC "Mobimak" rebranded into "T-Mobile Macedonia" and became part of the international group "T-Mobile".

3.2. Entry of a second mobile operator

The period of monopoly was terminated on November 22, 2001, when the Minister of Transport and Communications of the Republic of Macedonia grant a concession for the provision of public mobile telecommunications services and networks to "MTS" Mobile Telecommunications

Services Inc., which was wholly owned by the Greek Telecommunications Company SA "OTE".

The commercial launch of the mobile services was in June 2003 under the brand "Cosmofon". In April 2009 the Greek Telecommunications Company SA "OTE" totally sold the company in Macedonia to Slovenian telecommunications company "Telekom Slovenia", which continued to provide mobile communications networks and services. Since November 11, 2009, the company started to provide also fixed telephony services and digital broadcasting DVB-T on under the brand "ONE".

Switching costs in a period of duopoly. The presented empirical model in section 2 is used to calculate the switching costs for each of the two mobile operators "Mobimak" and "Cosmofon". Table 1 presents the calculated results based on the Cullen International Report 2 – Country Comparative Report "Supply of services in monitoring of South East Europe – telecommunications services sector and related aspects", June 26, 2006 [4]. It was used to observe the market share (by subscriber data base – where N stands for number of subscribers) and the revenues π (in Euros) of each company existing on the market. The calculated price p set by each company and the switching cost S are presented in euros.

Table 1

Status on mobile market (31. 12. 2005)

	N	π (€)	p (€)	S (€)
"Mobimak"	877,142	70,443,528.45	80.31	64.45
"Cosmofon"	384,186	20,007,406.50	52.07	-3.77

The estimated switching costs for the operator "Mobimak" consumers are higher than the switching costs for the operator "Cosmofon" consumers, since the former already uses network effects of its realized subscriber pool in contrast to the latter, as presented in Figure 1.

In order to check the validity of the estimated switching costs, it is necessary to identify the costs a subscriber faces when he/she replaces operator "Mobimak" with operator "Cosmofon" and vice versa. In the observed period, the subscriber had the following costs:

- costs in the amount of one-time fee for service usage and
- costs because of his lost time due to the change of subscriber's calling phone number.

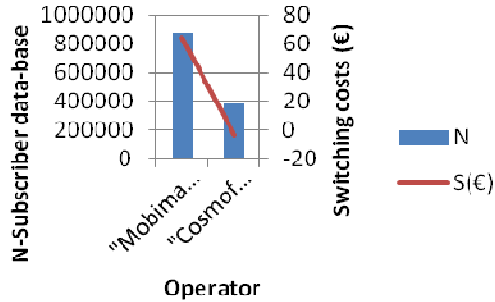


Fig. 1. Switching costs in period of duopoly

Given the pricelist of the operators, the calculated value of the switching costs are within the applicable prices and market conditions.

The negative value of the switching cost for the operator "Cosmofon" subscribers only confirms that in the observed period the number of the pre-paid subscribers is dominant in the total number of the subscribers. It is a consequence of the operator's business model and policies and resulted in low costs for switching from this operator.

3.3. The third mobile operator

The use of radio frequencies for the third mobile operator in the Republic of Macedonia was published in October 2006 through. The Agency for Electronic Communications in March 2007 issued an approval to "Mobilkom Austria" for usage of radio frequencies for mobile telephony for a period of 10 years with a possible extension of the approval at least once for a period of 10 years. The third mobile operator in Macedonia began its commercial operation in September 2007 under the brand "VIP operator".

All three mobile operators began their commercial launch on the GSM (2G) technology platform. By decision of the Agency for Electronic Communications from 1.12.2013, all three mobile operators have gained approval for radio frequencies for LTE valid for 20 years and an obligation for commercial launch of 4G technology services within 9 months of authorization receipt.

Switching costs in the beginning of the work of the 3rd operator. The switching costs for each of the three mobile operators "T-Mobile", "ONE" and "VIP", only 3 months after the commercial launch of the third operator on the market and the relevant network parameters are presented in Table 2. The market share observations are based on source [5] from 31.12.2007. The price p set by

each company and the switching cost S for the customers of each company, are calculated using the empirical model from section 2 and are presented in euros. The results show that the customers of each company have different values of switching costs when moving to other operator from the existing two companies.

Table 2

Status on mobile market (31.12.2007)

Operator	"T-Mobile"	"ONE"	"VIP"
N	1,212,610	592,970	141,136
π (€)	152,876,032.14	57,681,066.36	1,463,232.93
p (€)	126.00	97.27	10.36
S (€)	(T->V) 124.92 (T->O) 94.05	(O->V) 95.28 (O->T) 12.65	(V->T) -102.50 (V->O) -68.20

It is obvious that immediately after the entry of a new operator on the market, the highest switching costs have subscribers who choose to exit operators "T-Mobile" and "Cosmofon" and switch to the new operator "VIP", as shown in Figure 2.

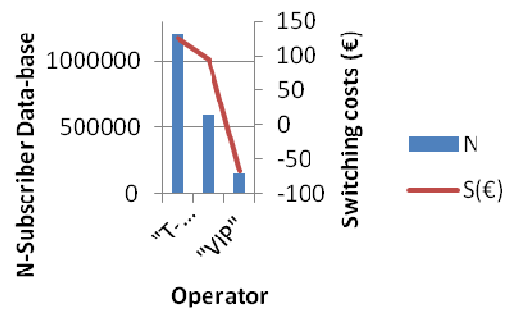


Fig. 2. Switching costs on the beginning of the work of the 3rd operator

This is confirmed by the results of the empirical model. So, the cost of switching the second operator appeared on the market (i.e. "Cosmofon") into the newest operator "VIP" are higher than the switching cost of the oldest operator "T-Mobile". This explicitly shows the impact of the network effect (the size of the subscriber base of the "T-Mobile").

In the period of observation, two older operators on the market have started to conclude subscriber agreements with their consumers. These agreements included subsidies for mobile handsets.

The amount of the calculated switching cost is increased compared to the one of 31.12.2005 due to the following costs:

- costs in the amount of one-time fee for service usage,
- costs because of lost time due to the change of subscriber's calling phone number, and
- costs because of the difference to the full value of the purchased mobile handset.

In the observed period, the "number portability", as a subscriber's right to keep the existing number when changing operator, has not been implemented, so we have considered the cost related to the time lost due to change of the subscriber number.

Switching costs with 3 operators. The market parameters for three mobile operators "T-Mobile", "ONE" and "VIP" are shown in Table 3. The analysis was based on the observations of the market share and relevant data from Report 3 – Enlargement Countries Monitoring Report: „Supply of services in monitoring Regulatory and Market developments for electronic communications and information society services in Enlargement countries“, from April 2013 [6].

Table 3
Status on mobile market (31.12.2011)

Operator	“T-Mobile”	“ONE”	“VIP”
N	1,151,761	494,877	566,585
π (€)	143,941,153.97	34,655,651.76	34,145,071.25
p (€)	124.90	70.00	60.26
S (€)	(T->V) 96.90	(O->V) 37.84	(V->T) -58.78
	(T->O) 103.90	(O->T) -17.36	(V->O) 27.63

Four years after the entrance on the market of the third operator for mobile communication services in the country, a decrease in the switching cost is noticed for the subscribers of all three existing mobile operators, as presented in Figure 3.

A strong impact of the network effect on the switching costs is obvious. Namely, with increasing of the subscriber base of the operator "VIP" closer to the number of subscribers of the operator "ONE", the costs for "T-Mobile" subscriber (when switching into one of two other operators) are al-

most equal. Switching costs for the subscribers of the oldest operator on the market of mobile communications, "T-Mobile", remain the highest due to the impact of the network effect.

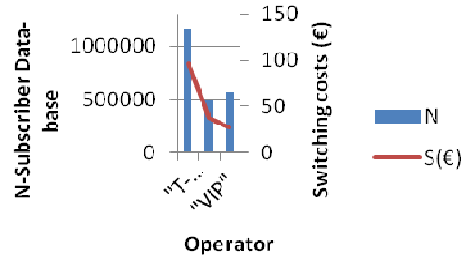


Fig. 3. Switching costs on market with 3 operators

In general, subscribers are faced with the following costs:

- costs in the amount of one-time fee for services usage;
- costs in the amount of one-time fee for service "number portability";
- costs because of the difference to the full value of the purchased mobile handset, and
- costs due to early termination of a subscriber agreement.

In the observed period, the operators in the country begun the procedure named "Lock-in" for their subscribers, by offering *loyalty contract* with duration of two or three years in return to favorable offer of service packages (benefits with included call minutes, SMSs and volume of internet traffic into the monthly subscription) and favorable offers for mobile handsets. The "number portability" starts from 1.9.2008, as a subscriber's right to retain the existing number when changing the operator. The Agency for Electronic Communications, with its decision from June 2009, calculates the amount of one-time fee for number portability as 200.00 denars (3.25 euros, excluding VAT).

3.4. Market's developments in 2015

The shareholders of the companies "Makedonski telekom" and "T-Mobile" have agreed to merge "T-Mobile" with "Makedonski telekom" on their meeting in June 2015. So, starting July 1st, 2015, "Makedonski telekom" and "T-mobile" became officially one company called "Makedonski Telekom" AD, which also provides mobile communication services.

The group "Telekom Austria" - owner of the "VIP operator" and the group "Telekom Slovenia" – owner of the operator "ONE" concluded an agreement to merge their daughter companies in October 2014. According to that agreement, the group "Telekom Austria" has 55% share capital and control over a newly created company, while the group "Telekom Slovenia" has 45% of the stakes. The newly created company called "one.Vip" has started October 1st, 2015, providing mobile communications services in the country, as a legal successor of the operators "ONE" and "VIP".

Table 4

Status on mobile market (31.12.2015)

	N	π (€)	P (€)	S (€)
Makedonski telekom	1,001,578	46,291,596.00	46.22	13.88
one.Vip	1,082,005	67,403,023.00	62.29	40.07

At the end of 2015, only two mobile operators, "Macedonian Telecom" and "one.Vip", were on the market. Table 4 presents the relevant market parameters based on the "Annual report for market developments in the Republic of Macedonia in 2015" [7].

After the merging, the new mobile operator "one.Vip" continued to supply the same packages and services that the both operators offered before the merging. This had an effect of doubled offers. The calculated results show the true effect of customer's "Lock-in" through loyalty agreements with duration of one or two years in return to the favorable offer for the service packages (benefits in included call minutes, SMSs and volume of Internet traffic into the monthly subscription) and for the mobile handsets.

The fact that even after the merging, the operator "one.Vip" impacts the market (as two separate operators versus its competitive operator), reflects in significantly higher switching costs with relatively small differences in the subscriber base. Therefore, the merging of the operators has a negative effect on the development and encouragement of the competition. From regulatory aspect, the case is trivial since it is step back instead of step forward.

3.5. Analysis of switching costs for "T-Mobile"

Since mobile operator "T-Mobile" is present on Macedonian mobile market for almost 20 years, it is interesting to analyze the behaviour of the switching costs for its subscribers in relation to its subscriber data-base over the studied period. The trends are shown in Figure 4.

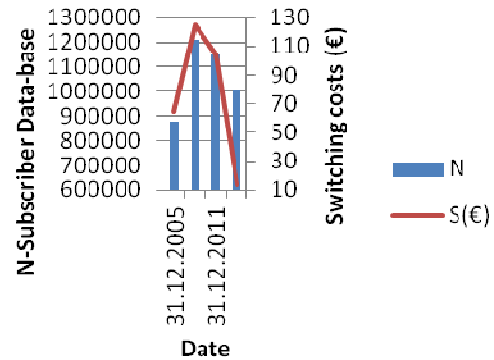


Fig. 4. Subscriber data-base vs. switching costs for "T-Mobile"

The graph shows that the network effect has a great influence over the switching costs for consumers of "T-Mobile". Also, the graph clearly presents a distinction between those costs which may arise from legitimate commercial customer retention strategies (period 2005–2014) and those that may arise due to the market failure, as it happened in the middle of 2015.

4. SWITCHING COSTS AND CUSTOMER'S "LOCK-IN"

The presented market characteristics and performed calculations for realistic scenarios defines the dependences and results for the switching trends and barriers. The following subsections provide some results and conclusions.

4.1. Materials and methods

We have used a survey with a structured questionnaire to test the relation between the switching costs and the customer's "Lock-in". Customers of all three mobile operators were sampled for the study. The study was performed during the distortion market period. The implemented research instrument was a *structured questionnaire*. The design of the questionnaire benefited from the

extant literature dealing with the effects of *switching costs* and *barrier on consumer retention* [8].

The research instrument attempted to isolate and emphasizes on consumer satisfaction and retention, as well as on switching barriers. The study has used a 5-points Likert's scale [9] ranging from "strongly agree" to "strongly disagree". The questionnaire was divided into three main sections. The first section dealt with the general demographic data, the second with the consumer behavior and satisfaction and the third section with the switching of an operator. The received data were analyzed using the SPSS (Statistical Package for the Social Sciences) computer package [10].

4.2. Results and discussion

The demographic data through the distribution of the respondents' age, sex and the number of members in the household are presented on Table 5.

Table 5

Demographic data

	Frequency	Percent (%)
Gender		
Male	23	38,3
Female	37	61,7
Age group (years)		
< 20	0	0,0
21 – 30	12	20,0
31 – 45	28	46,7
45 – 60	18	30,0
> 60	2	3,3
No. of members in the household		
1	1	1,7
2 – 4	54	90,0
> 4	5	8,3

The study uses a *convenient sample*, which has a total of 60 subjects (23 male and 37 female). All respondents were aged from 21 to over 60 years (mostly covered respondents are in the category of 31 to 45 years). Even though it is not a part of the goals of this research, it can be concluded that all of them belong to the working population

with regular sources of income. The sample includes respondents with secondary (4 cases) and higher education (56 respondents). Most of them work in private companies (44 respondents). Also, the survey includes respondents who work in different sectors (economy, health and education). According to the amount of the total household income, most of the respondents are in the category with turnover over 60,000.00 denars (27 respondents). Most of the respondents live in households with 2 to 4 members (54). Only 5 respondents live in family households where there are more than 4 members, while 1 respondent lives alone or in a household of 1 member.

All respondents use mobile communication services of all three mobile operators more than three years: 30% of the respondents are operator "ONE" consumers, 50% of the respondents are operator "T-Mobile" consumers and 20% of the respondents are operator "VIP" consumers.

The questionnaire analysis leads to some conclusions and observations:

- The number of post-paid customers prevail the number of pre-paid consumers (ratio 95:5 (%)), which also confirms the effect of customer's "Lock-in" since operators use loyalty agreements with duration of 1 or 2 years in return for favorable offer of service packages (benefits in included call minutes, included SMSs and included volume of Internet traffic into the monthly subscription) and favorable offers for products, such as mobile handsets, TV-sets, IT equipment, etc.
- Mobile communication services are used more for business (66.66% of the respondents) than for private purposes (31.67% of the respondents), which is in line with the dominance of post-paid customers related to the prepaid ones.
- Number of consumers of all three mobile operators who didn't switch their operator in the last two years is higher than the ones who did switched their mobile operator in the last two years. The ratio of frequencies of not switched compared to frequencies of did switched is 41:18.
- The largest number of respondents who answered negatively the question: "Have you tried to change your mobile operator in the last two years?" use mobile communication services of the same mobile operator as the members of their family. Consumers respond

positively to their mobile operator with a recommendation the same mobile operator to the members of their family, and thus potentially, increase the number of users of that mobile operator.

- The reasons for not switching the mobile operator vary and depend on the customer preferences. Table 6 shows the received answers on the question: "What was the main reason not to change mobile operator?"

Table 6

Responses on the question: "What was the main reason not to change mobile operator?"

Answer	Percent (%)
Subscriber agreement does not allow to switch the operator	7.5
The current operator has the best offer	42.5
Switching doesn't mean big benefit	20
Switching costs are too high	5
Hard to decide which operator is the cheapest	2.5
Other	22.5

Users do not change the operator of mobile communication services when they are satisfied with the offer of the current operator, as most of the participants answered, and when they have signed a subscriber agreement with mandatory duration with the current operator. Also, a significant number of the respondents believe that the benefits that they would have with the operator change is insignificant, pointing to the fact that operators use similar strategies in attracting and retaining the customers. Satisfied users return to their operator by re-selection of the same operator. Also, users shall respond positively to the mobile operator with their recommendation the same mobile operator to the members of their family, friends and relatives, and thus potentially increase the number of users of that mobile operator.

However, a valuable percent (5%) of the received answers is from the respondents who answered that they didn't changed their mobile operator because of the switching costs and because activities for changing the mobile operator are too long and complex. This should be a sign for the regulatory body in the country to take appropriate activities in a direction of revision of the current procedures for operator switching. Often, it is a

regulation for number portability, as well as regulation for end users rights protection and analysis and regulation for operator offers and prices on retail level. The focus should be on a duration of a procedure for number portability and in minimization of any barriers into subscribers' agreements that affect the user's right to switch the operator: determining the maximum duration of the mandatory period of duration for the subscriber contract, elimination the possibilities for automatic extension into a new commitment period after the expiration of the subscriber contract with mandatory duration, educating consumers about their rights.

The major contribution of this analysis is the conclusion related to the existence/absence of the possibility to switch the mobile operator for all customers on their free will. The switching costs have negative impact on customer's decision to switch the mobile provider. However, the customer's data base – network effect – has positive effects on the customer retention.

5. CONCLUSIONS

The level and complexity of changing the provider is a key indicator for the welfare and prosperity of customers and it is a significant factor influencing the overall development of competition on the retail markets [11]. The ability and the willingness of the consumers to switch the service provider is critically important because effective competition provides increased choice and lower prices for consumers, as well as adequate quality and innovation.

The paper shows the relation between the level of the competition and the switching costs on the mobile market in the country within the period of 10 years. Also, it stresses some weak points in the switching procedures and suggests appropriate regulatory activities in the near future. The presented analysis was based on analytical model and survey, which tests the results of the model.

To benefit from the competition, the consumers must be confident that they have a choice and that they can benefit from that choice. In cases where there is no such confidence, consumer may decide not to switch the provider. The reduction of the consumer's confidence in the switching procedure may additionally block the switching decision. This can weaken the process of the competition and consumers can not benefit from the competition as expected.

REFERENCES

- [1] *Monitoring consumer markets in the European Union in 2015 – Final Report*, January 2016, http://ec.europa.eu/consumers/consumer_evidence/consumer_scoreboard/market_monitoring/index_en.htm
- [2] O. Shy: A quick-and-easy method for estimating switching costs, *International Journal of Industrial Organization*, **20**, pp. 71–87 (2002).
- [3] J. Farrell, P. Klemperer: *Coordination and Lock-in: Competition with Switching Costs and Network Effect*, Handbook of Industrial Organization, Volume **3**, pp. 1970–2072, 2007.
- [4] Cullen International Report 2 – Country Comparative Report *Supply of services in monitoring of South-East Europe – telecommunications services and related aspects*, June 26, 2006, <http://www.cullen-international.com/asset/?location=/content/assets/research/studies/2005/08/report2comparative.pdf/report2comparative.pdf>
- [5] Cullen International Report 2 – Enlargement Countries Monitoring Report *Supply of services in monitoring regulatory and market developments for electronic communications and information society services in Enlargement countries*, September 30, 2008, <http://www.cullen-international.com/asset/?location=/content/assets/research/studies/2008/09/enlargement-countries-monitoring-report-1.pdf/enlargement-countries-monitoring-report-1.pdf>
- [6] Cullen International Report 3 – Enlargement Countries Monitoring Report *Supply of services in monitoring regulatory and market developments for electronic communications and information society services in Enlargement countries*, April, 2013, <http://www.cullen-international.com/asset/?location=/content/assets/research/studies/2011/11/enlargement-countries-monitoring-report-report-3.pdf/enlargement-countries-monitoring-report-report-3.pdf>
- [7] *Annual report for electronic communications market developments in the Republic of Macedonia*, <http://aek.mk/mk/dokumenti/izveshtai/godishni-izveshtai-za-analiza-na-pazar/item/1933-godisen-izvestaj-za-razvoj-na-pazarot-na-elektronski-komunikacii-vo-rm-za-2015>
- [8] V. Stan, B. Caemmerer, R. Cattani-Jallet: Customer loyalty development: The role of switching costs, *The Journal of Applied Business Research*, **29**, 5, 1541–1554 (September/October 2013), <http://cluteinstitute.com/ojs/index.php/jabr/article/viewfile/8069/8123>
- [9] Rensis Likert: A technique for the measurement of attitudes, *Archives of Psychology*, 140, 1–55 (1932),
- [10] SPSS (Statistical Package for the Social Sciences) computer package <http://www.ibm.com/analytics/us/en/technology/spss/>
- [11] “BEREC Report on the consultation on the best practices to facilitate switching”, BoR (10) 34, October 2010, http://www.berec.europa.eu/eng/document_register/subject_matter/berec/reports/186-berec-report-of-the-consultation-on-the-best-practices-to-facilitate-switching-bor-10-34

PROJECTING A HYDROGRAPHIC MAP OF THE REPUBLIC OF MACEDONIA

Vesna Andova, Sanja Atanasova, Elena Jovčevska, Viktorija Jordanova, Ilin Tolovski, Martin Rizov

*Faculty of Electrical Engineering and Information Technologies,
"Ss. Cyril and Methodius" University in Skopje,
Rugjer Bošković bb, P.O. box 574, 1001 Skopje, Republic of Macedonia
vesnaa@feit.ukim.edu.mk*

Abstract: Bezier and B-spline curves are among the most powerful tools used for complex graphical approximation. In this paper, we will use them to recreate the hydrographic map of the Republic of Macedonia. The results obtained in this paper show that cubic spline curves have smaller average deviation in respect to B-spline curves, in contrast to Bezier curves. The results and the images are obtained by using the software package Wolfram Mathematica.

Key words: Bezier curves; B-spline; cubic spline

МОДЕЛИРАЊЕ НА ХИДРОГРАФСКА МАПА НА РЕПУБЛИКА МАКЕДОНИЈА

Апстракт: Безиеовите и Б-кривите спаѓаат во групата најмоќни алатки кои се користат за апроксимација на комплексни графички прикази. Во трудот се користени овие криви за моделирање на хидрографска мапа на Р. Македонија. Резултатите во овој труд покажуваат дека кривите добиени со кубна крива имаат најмало просечно отстапување во однос на Б крива и Безиеовите криви. Резултатите и сликите се добиени со помош на софтверскиот пакет Математика.

Клучни зборови: Безиеови криви, Б-крива, кубна крива

1. INTRODUCTION

Since their introduction in the 1950's and 1960's, Bezier and B-spline curves have quickly become one of the most powerful and sought after tools in many fields where surface approximation is an imperative such as computer graphics, molecular and physical models, 3D animations and many more [7], [11].

This is the case, mostly because the idea behind these mathematical models is quite simple. They both rely on choosing set of control points which the curves will follow. Although the idea looks simple, the mathematical background is not. After choosing the control points, there are number of other properties that need to be set in order to get the desired outcome. Some of these properties are: degree of the curve, weight of the points, control knots etc.

The concept of Bezier curves was introduced in the 1910's by Charles Hermite and Sergei Bernstein. However, it was not until the 1950's when Pierre Bezier and Paul de Casteljaou brought this concept to life and introduced it to graphic specialists. These curves are based on the Bernstein polynomials, and can be calculated recursively either with developing the Bernstein polynomials or with the Casteljaou algorithm [8].

B-spline curve, on the other hand, represents a generalization of a Bezier curve. They are divided into multiple polynomial pieces and depending on the uniformity of these pieces there are two cases, uniform B-splines and NURBS (Non-uniform rational B-spline) [14], [10]. We will later consider both types.

In Section 2 we will explain the equations and all the steps of calculating both B-spline and Bezier curves. In Section 3 we use the B-spline,

Bezier and cubic spline curves to construct a hydrographic map of the Republic of Macedonia. Furthermore, we compare the curves, measure the percentage difference in lengths of the water areas (rivers, springs, not lakes and closed waters), in order to find out which curve will give the best approximation for this problem.

For the purposes of this project we use Matlab for obtaining the coordinates and Wolfram Mathematica for all of the modeling, approximations and calculations. Mathematica's built-in libraries and methods make it extremely powerful and pleasant to use for this sort of problems.

2. DEFINITIONS AND EQUATIONS

In this section we give the basic definitions and relations for Bezier and B-spline curves. For all the terms not defined here consult [15] or any other book from this field.

Bezier curve

As we mentioned, Bezier curves are based on Bernstein polynomials [12] of degree n , which are represented with

$$B_i^n(t) = n_i t^i (1-t)^{n-i}, \quad i = 0, \dots, n. \quad (1)$$

The computation of the Bernstein polynomials can be also displayed in triangular scheme, shown with equation (2):

$$\begin{array}{cccccc}
 B_0^n & B_1^n & B_2^n & \dots & B_n^n \\
 & B_1^n & B_2^n & \dots & B_n^n \\
 1 = & & B_2^n & \dots & B_n^n \\
 & & & \ddots & \vdots \\
 & & & & B_n^n
 \end{array} \quad (2)$$

These polynomials are defined for all $t \in \mathbb{R}$, but in practice they are usually restricted to $t \in [0,1]$. One of the most important properties of Bernstein polynomials is that they are linearly independent [1]. From relation [1] we can see that Bernstein polynomials are also symmetrical, i.e.

$$B_i^n(t) = B_{n-i}^n(1-t). \quad (3)$$

Moreover, the Bernstein polynomials can be calculated with a recursive formula, shown in equation (4).

$$B_i^n(t) = t B_{i-1}^{n-1}(t) + (1-t) B_i^{n-1}(t). \quad (4)$$

The main purpose of Bezier curves is modeling a whole curve or some part of it. When this is done in a Euclidean space, it is represented as a parametric polynomial defined in equation (5):

$$p(t) = \sum_{i=0}^n a_i t^i, \quad a_i \in \mathbb{R}^d. \quad (5)$$

Equation (5) also has a Bernstein representation:

$$p(t) = \sum_{i=0}^n c_i B_i^n(t), \quad c_i \in \mathbb{R}^d. \quad (6)$$

Equation (6) defines a Bezier curve with control points c_i . This curve is restricted to the parameter domain $[0,1]$ which makes p a parametric curve $p: [0,1] \rightarrow \mathbb{R}^d$. The control points c_i when connected are forming the control polygon of the curve. The shape of this polygon represents a shape that the Bezier curve will have when constructed. This property can easily be manipulated which is one of the reasons why Bezier curves are suitable for dynamic change of shape. Bezier curves inherit several properties of Bernstein polynomials, such as the symmetry. From the triangular scheme of the polynomials we have that they sum to 1, which means that every point $p(t)$ is an affine combination of the control points $c_i, i \in \{0, 1, \dots, n\}$ [3], [4]. Because the polynomials are also non-negative in the interval $[0,1]$, every point $p(t)$ is a convex combination of the control points $c_i, i \in \{0, 1, \dots, n\}$. Consequently, the Bezier curve p lies in the convex hull of its control points [6].

B-spline curves

B-spline curve $p(t)$ is analytically defined by

$$P(t) = \sum_{i=0}^n P_i N_{i,k}(t),$$

where $t \in [t_{k-1}, t_n]$, P_i are the control points, k is the order of the polynomial segments of the B-spline curve and $N_{i,k}(t)$ are normalized B-spline blending functions [5]. Order k means that the curve is made up of piecewise polynomial segments of degree $k - 1$. The $N_{i,k}$ functions are described by the order k and by a non-decreasing sequence of real numbers t_i , where $i \in \{0, 1, \dots, n+k\}$ which is referred as knot sequence [9]. The complete equations for $N_{i,k}$ are shown with (7) if $k = 1$ and with (8) if $k > 1$,

$$N_{i,1}(t) = \begin{cases} 1, & t \in [t_i, t_{i+1}) \\ 0, & \text{otherwise} \end{cases} \quad (7)$$

$$N_{i,k}(t) = \frac{t-t_i}{t_{i+k-1}-t_i} N_{i,k-1}(t) + \frac{t_{i+k}-t}{t_{i+k}-t_{i+1}} N_{i+k-1,k-1}(t) \quad (8)$$

A B-spline curve is geometrically defined by the relation (9), where the set of control points is $P_0, P_1, P_2, \dots, P_n$. Then the B-spline curve $P(t)$ is defined by

$$P(t) = P_l^{k-1}(t), \quad t \in [t_l, t_{l+1}) \quad (9)$$

where

$$P_i^{(j)}(t) = \begin{cases} (1-\tau_i^j)P_{i-1}^{j-1}(t) + \tau_i^j P_i^{j-1}(t), & j > 0 \\ P_i, & j = 0 \end{cases}$$

and

$$\tau_i^j = \frac{t-t_i}{t_{i+k-j}-t_i}.$$

3. COMPARISON BETWEEN THE CURVES

a) Bezier or B-spline curves?

In this section we state some of the main differences between Bezier and B-spline curves.

- 1) Bezier curves can be viewed as a parametric curve consisting of basic functions which are Bernstein polynomials, and on the other hand, B-splines are based on piecewise Bezier curves.
- 2) Bezier curves lacked in local control. This means that if we add or remove one control point, it will effect the hole curve. With B-splines we have more freedom and they provide more control flexibility.
- 3) Bezier curves are more suitable and give better approximation if the control points are nearly collinear. This means that when modeling some curve, we can make combination of both Bezier and B-spline curve depending on the choice of control points.
- 4) Bezier curves are special cases of B-spline curves. If $n = p$ (i.e. the degree of a B-spline curve is equal to n , the number of control points minus 1), and there are $2(p+1) = 2(n+1)$ knots with $p+1$ of them clamped at each end, this B-spline curve reduces to a Bezier curve. To simplify, any Bezier curve of arbitrary degree can be converted into a B-spline and

any B-spline can be converted in to one or more Bezier curves [13].

- 5) B-spline curves require more information and a more complex theory than Bezier curves, which means more time for running the code when modeling.
- 6) B-spline curves satisfy all important properties that Bezier curves have (affine invariance, positivity, variation Diminishing Property, the convex hull property any many others).
- 7) B-splines do not interpolate any of its control points, while the Bezier curve automatically clamps its end points. However, B-splines can be forced to interpolate any of its n control points without repeating it, which is not possible with the Bezier curve [2], [16].

b) Obtaining coordinates from the original hydrographic map

In order to be able to construct a hydrographic map with B-spline, Bezier and cubic spline curves, we needed to successfully select all of the water areas inside the Republic of Macedonia. We did just that by using an official 2600×1960 pixel hydrographic map (shown on Figure 1) designed by Prof. Dr. Ivica Milevski from the Institute of Geography at the Ss. Cyril and Methodius University in Skopje. For obtaining the coordinates, we used a custom Matlab script based on the *ginput* function. Even though bigger number of points would result in more precisely constructed map, we concentrated on selecting the right points, rather than every point. This way, the results would represent genuine differentiation between the B-spline, Bezier and cubic spline curves where we can clearly see the difference in the ways these curves are built. After obtaining the coordinates, all of the following analyses will be done in Wolfram Mathematica.

c) Constructing the model plots in Mathematica

Mathematica is among the most powerful software packages when it comes to solving geometrical modeling and calculation problems. It contains many built-in libraries and functions which make the coding cleaner, yet the results precise [17]. For constructing the models we used Mathematica's built-in methods BSplineCurve, BezierCurve and SplineFit. Figure 2 shows the plot constructed with B-spline curve.

On Fig. 3 and Fig. 4 you can see the maps constructed with Bezier and cubic spline curves respectively. Alongside these methods we also used some other methods along the course of this project, all of them that are relevant to the geometrical modeling are displayed in Table 1.

The outcome of these functions can be modified even more given the fact that they have many properties that can be tuned in a way that will give the best result for any given problem [18]. In this

case, by modifying the spline degree in the BSplineCurve method it was evident that B-spline with spline degree 2 had the smallest variation from the coordinates of the original hydrographic map compared to the maps plotted with Bezier-curve and spline fit methods, so B-spline of the second degree was chosen as a benchmark to which the other curves will be compared and measured.



Fig. 3. Hydrographic map of Macedonia plotted with Bezier curves

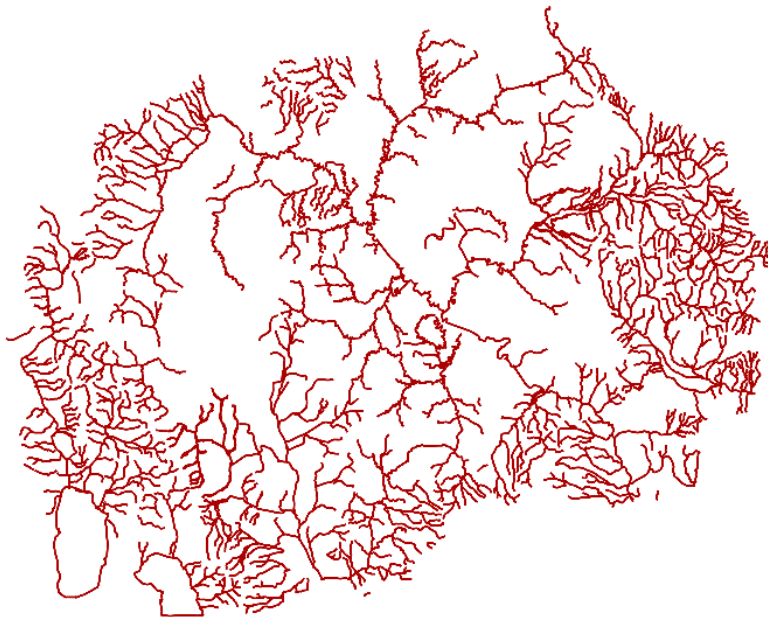


Fig. 4. Hydrographic map of Macedonia plotted with cubic spline curves

Table 1.

Methods used for modeling of the hydrographic map

Method	Description
BSplineCurve [$\{pt_1, pt_2, \dots\}$]	BSplineCurve is a graphics primitive that represents a non-uniform rational B-spline curve with control points p_{i_1}, \dots
BSplineFunction [$\{pt_1, pt_2, \dots\}$]	BSplineFunction represents a B-spline function for a curve defined by the control points p_{i_1}, \dots
BezierCurve [$\{pt_1, pt_2, \dots\}$]	BezierCurve is a graphics primitive that represents a Bezier curve with control points p_{i_1}, \dots
BezierFunction [$\{pt_1, pt_2, \dots\}$]	BezierFunction represents a Bezier function for a curve defined by the control points p_{i_1}, \dots
SplineFit [$\{pt_1, pt_2, \dots\}$, type]	SplineFit generates a SplineFunction object of the specified type from the points p_{i_1}, p_{i_2}, \dots
Spline [$\{pt_1, pt_2, \dots\}$, type]	Spline is a two-dimensional graphics primitive which represents a spline of type <i>type</i> through (or controlled by) points p_{i_1}, p_{i_2}, \dots
Discretize Graphics [<i>g</i>]	Discretizes a 2D or 3D graphic <i>g</i> into a MeshRegion.
ArcLength[<i>reg</i>]	ArcLength gives the length of the one-dimensional region <i>reg</i> .
ParametricPlot [$\{f_x, f_y\}$, <i>u</i> , u_{\max} , u_{\min}]	ParametricPlot generates a parametric plot of a curve with <i>x</i> and <i>y</i> coordinates f_x and f_y as a function of <i>u</i> .

d) Result measuring and comparison

In order to make a successful comparison with the original hydrographic map, or in this case our reference map which is the one that we construct with B-spline curves, we will measure the deviation in the lengths of all of the water areas that we constructed with B-spline, Bezier and cubic spline curves. First of all, for measuring the length of a single river or water area we use the method ArcLength that was mentioned and described in section *b*. After calculating the lengths of every water area, we calculate the deviation in percentages between the lengths of B-spline curve on one side and lengths of Bezier and cubic spline curves on the other. To do this we use the following formulas:

$$SRD_{CS}(\%) = \frac{|Len_{BS} - Len_{CS}|}{Len_{BS}} \cdot 100 \quad (10)$$

$$SRD_{BZ}(\%) = \frac{|Len_{BS} - Len_{BZ}|}{Len_{BS}} \cdot 100 \quad (11)$$

where Len_{BS} , Len_{CS} and Len_{BZ} represent the lengths of a single river constructed with B-spline, cubic spline and Bezier curves respectively. The result of (10) and (11) gives the percentage deviation for a single river. The smaller the percentage, the bigger the precision of the curve. Because there were big variations in the results for separate rivers, we also calculate the average deviation for all of the rivers. We do that by summing the absolute value of all of the differences between the rivers. Afterwards, we divide that with the sum of the lengths constructed with B-spline. The previous explanation is depicted with the following formulas:

$$ARD_{CS}(\%) = \frac{\sum_{i=1}^{870} |Len_{BS,i} - Len_{CS,i}|}{\sum_{i=1}^{870} Len_{BS}} \cdot 100 = 6.655\% \quad (12)$$

$$ARD_{BZ}(\%) = \frac{\sum_{i=1}^{870} |Len_{BS,i} - Len_{BZ,i}|}{\sum_{i=1}^{870} Len_{BS}} \cdot 100 = 11.027\% \quad (13)$$

Equations (12) and (13) are showing the average deviation when the calculation is done on all 870 water areas that exist in the Republic of Macedonia. From the results we can see that cubic spline curves have smaller average deviation in respect to B-spline curves, in contrast to Bezier curves. Given the fact that B-spline curves represent generalized Bezier curves and additionally cubic spline curves are special case of the B-spline curves this result is expected and logical.

This result was also confirmed by the data obtained when modeling a hydrographical map of Macedonia, for vast number of rivers the cubic spline method gave better results than Bezier curves. One such river is shown on Figure 5. In this case the deviation of the cubic spline is only 5%, while the Bezier curve's deviation is 16.92%.

These two methods are "equally" good for modeling short and smooth rivers. One such river is shown on Figure 6. As the river is short we used small number of points for the modeling. Our result show that the deviation of the Bezier curves is 2.06% and for the cubic spline 1.89% for the river on Figure 7.

When projecting a long river, we have to use a large number of points. At the same time, most of the "long" rivers have a lot of curves, and therefore

the deviation is big for the both methods. One such river is shown on Figure 7. For this river the deviation for the Bezier curves method and for the cubic spline is 12.98% and 11.91%, respectively.

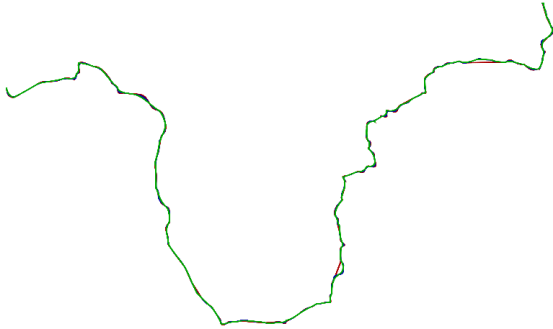


Fig. 5. A river projected by B-spline (blue), cubic spline (red) and Bezier curves (green). The deviation of the Bezier curve is much bigger than the deviation of the cubic spline



Fig. 6. A river projected by B-spline (blue), cubic spline (red) and Bezier curves (green). Bezier curves and cubic spline are "equally" good

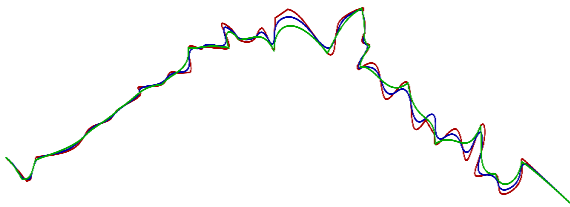


Fig. 7. A river projected by B-spline (blue), cubic spline (red) and Bezier curves (green). Both method have big deviation

Bezier curves gave better results only for "small" rivers (i.e. curves). These rivers are short, do not have many curves, and are modeled with several points which is the main reason for the obtained results. In total, cubic spline curves gave better approximation on 72.068% of the rivers, while Bezier curves gave better approximation on only 27.931% of all 870 measured water areas. The main reason for this gap is that most of the water areas measured are rather long and contain many curves, which given the analyses made for the

rivers shown on Figures 5, 6 and 7 it is intuitive that cubic spline curves will give more precise approximation for the water areas overall.

Despite the bigger precision, cubic spline curves take more time to be calculated, due to the fact that they have more properties and are more advanced than the Bezier curves.

CONCLUSION

When the first approaching this problem, it was straight-forward that it is an approximation problem. Since Bezier and B-spline curves are the cornerstones of geometrical approximation and modeling, we used them as building blocks on which we would construct a hydrographic map of the Republic of Macedonia. While the image manipulation and obtaining of coordinates was done in Matlab, all of the geometrical modeling and calculations were done in Wolfram Mathematica, due to its powerful and robust kernel tools. After plotting the map with B-spline, Bezier and cubic spline curves, we compared the coordinates of each curve with the original hydrographic map, and B-spline was the one whose coordinates were the closest. Therefore, it was taken as a reference curve. After measuring the percentage deviation length of each water area, and then also the average deviation on all of the areas, we concluded that cubic spline curves gave more precise length approximation of the water areas in the Republic of Macedonia compared to Bezier curves. This result was logical from the beginning, given the fact that cubic spline curves are much more flexible due to the bigger number of properties that can be modified in favor of getting a better solution. However, this benefits come with the price of speed, because the computer takes more time to process and calculate cubic spline curves rather than the ones obtained with the Bezier method.

Acknowledgment: The authors would like to thank Prof. Dr. Ivica Milevski from the Institute of Geography at the Ss. Cyril and Methodius University in Skopje for providing the map.

REFERENCES

- [1] Vera B. Anand: *Computer Graphics and Geometric Modeling for Engineers*, John Wiley & Sons Inc. 1996.
- [2] V. Andova, S. Atanasova, K. Bacev, Gj. Peev, G. Kostov: *Approximation of map borders using Mathematica*, *ETAI* (2015).

- [3] R. H. Bartels, J. C. Beatty, B. A. Barsky: *An Introduction to Splines for Use in Computer Graphics and Geometric Modeling*, Morgan Kaufmann Publishers Inc. 1987.
- [4] R. C. Beach: *An Introduction to the Curves and Surfaces of Computer-Aided Design*, Van Nostrand Reinhold, 1991.
- [5] E. Cohen: *Discrete B-splines and Subdivision Techniques in Computer Aided Geometric Design and Computer Graphics*, International Association for Bridge and Structural Engineering, 1979.
- [6] C. De Boor: *A Practical Guide to Splines*, Revised Edition, Springer, 1978.
- [7] G. Farin: *Curves and Surfaces for CAGD. A Practical Guide*, fifth edition, Academic Press, 2002.
- [8] G. Farin, J. Hoschek, M.-S. Kim: *Handbook of Computer Aided Geometric Design*, Elsevier, 2002.
- [9] G. Farin: *NURBS: From Projective Geometry to Practical Use*, 2nd edition, AK Peters, 1999.
- [10] J. Fiorot, P. Jeannin: *Rational Curves and Surfaces*, Wiley, 1992.
- [11] J. Gallier: Curves and Surfaces. In: *Geometric Modeling: Theory and Algorithms*, Morgan Kofman Publishers, 2000.
- [12] G. G. Lorentz: *Bernstein Polynomials*, University of Toronto Press, 1953.
- [13] R. F. Riesenfeld: *Applications of B-spline Approximation to Geometric Problems of Computer-Aided Design*, Syracuse University, 1973.
- [14] D. Rogers: *An Introduction to NURBS with Historical Perspective*, Elsevier, 2001.
- [15] W. Rudin: *Real and Complex Analysis*, McGraw-Hill Higher Education, 1986.
- [16] D. Salomon: *Curves and Surfaces for Computer Graphic*, Springer, 2006.
- [17] S. Wagon: *Mathematica in Action Problem Solving Through Visualization and Computation*, Springer, 2010.
- [18] S. Wolfram: *The Mathematica Book*, Fifth Edition, Wolfram Media, 2003.

INSTRUCTIONS FOR AUTHORS

The *Journal of Electrical Engineering and Information Technologies* is published twice yearly. The journal publishes **original scientific papers, short communications, reviews** and **professional papers** from all fields of electrical engineering.

The journal also publishes (continuously or occasionally) the bibliographies of the members of the Faculty, book reviews, reports on meetings, news of future meetings, important events and data, and various rubrics, which contribute to the development of the corresponding scientific field.

Original scientific papers should contain hitherto unpublished results of completed original scientific research. The number of pages (including tables and figures) should not exceed 15.

Short communications should also contain completed but briefly presented results of original scientific research. The number of pages should not exceed 5 (including tables and figures).

Reviews are submitted at the invitation of the Editorial Board. They should be surveys of the investigations and knowledge of several authors in a given research area. The competency of the authors should be assured by their own published results.

Professional papers report on useful practical results that are not original but help the results of the original scientific research to be adopted into scientific and production use. The number of pages (including tables and figures) should not exceed 10.

Acceptance for publication in the Journal obliges the authors not to publish the same results elsewhere.

SUBMISSION

The article and annexes should be written on A4 paper with margins of 2.5 cm on each side with a standard faint Times New Roman 11 points, and should be named with the surname of the first author and then if more and numbered. It is strongly recommended that on MS Word 2003 or MS Word 2007 and on PDF files of the manuscript be sent by e-mail:

JEEIT@feit.ukim.edu.mk.

A letter must accompany all submissions, clearly indicating the following: title, author(s), corresponding author's name, address and e-mail address, suggest-

ed category of the manuscript and a suggestion of five referees (their names, e-mail and affiliation).

THE REVIEW PROCESS

Articles received by the Editorial Board are sent to two referees (one in the case of professional papers). The suggestions of the referees and Editorial Board are sent to the author(s) for further action. The corrected text should be returned to the Editorial Board as soon as possible but in not more than 30 days.

PREPARATION OF MANUSCRIPT

The papers should be written in the shortest possible way and without unnecessary repetition.

The original scientific papers, short communications and reviews should be written in English, while the professional papers may be submitted also in Macedonian.

Only SI (Système Internationale d'Unites) quantities and units are to be used.

Double subscripts and superscripts should be avoided whenever possible. Thus it is better to write $v_3(\text{PO}_4)$ than $V_{3\text{PO}_4}$ or $\exp(-E/RT)$ than $e^{-E/RT}$. Strokes (/) should not be used instead of parentheses.

Figures (photographs, diagrams and sketches) and **mathematical formulae** should each be given on a separate sheet. Figures should also be inserted in the correct place in the manuscript, being horizontally reduced to 8 or 16 cm. The size of the symbols for the physical quantities and units as well as the size of the numbers and letters used in the reduced figures should be comparable with the size of the letters in the main text of the paper. Diagrams and structural formulae should be drawn in such a way (e.g. black Indian ink on white or tracing paper) as to permit high quality reproduction. The use of photographs should be avoided. The tables and the figures should be numbered in Arabic numerals (e.g. Table 1, Fig. 1). Tables and figures should be self-contained, i.e. should have captions making them legible without resort to the main text. The presentation of the same results in the form of tables and figures (diagrams) is not permitted.

Footnotes are also not permitted.

When a large number of compounds have been analyzed, the results should be given in tabular form.

Manuscript should contain: title, author(s) full-name(s), surname(s), address(es) and e-mail of the corresponding author, short abstract, key words, introduction, experimental or theoretical background, results and discussion, acknowledgment (if desired) and references.

The **title** should correspond to the contents of the manuscript. It should be brief and informative and include the majority of the key words.

Each paper should contain an **abstract** that should not exceed 150 words and **3–5 key words**. The abstract should include the purpose of the research, the most important results and conclusions.

The **title**, **abstract** and **key words** should be translated in Macedonian language. By the foreign authors Editorial Board will translate in Macedonian language.

In the **introduction** only the most important previous results related to the problem in hand should be briefly reviewed and the aim and importance of the research should be stated.

The **experimental** section should be written as a separate section and should contain a description of the materials used and methods employed – in form which makes the results reproducible, but without detailed description of already known methods.

Manuscripts that are related to **theoretical studies**, instead of experimental material, should contain a sub-heading and the **theoretical background** where the necessary details for verifying the results obtained should be stated.

The **results and discussion** should be given in the same section. The discussion should contain an analysis of the results and the conclusions that can be drawn.

The **reference** should be given in a separate section in the order in which they appear in the text. The surname of one or two authors may be given in the text, whereas in the case of more than two authors they should be quoted as, for example:

Examples of reference items of different categories shown in the References section include:

- example of a book in [1]
 - example of a book in a series in [2]
 - example of a journal article in [3]
 - example of a conference paper in [4]
 - example of a patent in [5]
 - example of a website in [6]
 - example of a web page in [7]
 - example of a databook as a manual in [8]
 - example of a datasheet in [9]
 - example of a master/Ph.D. thesis in [10]
 - example of a technical report in [11]
 - example of a standard in [12]
- All reference items must be in 9 pt font. Please use Regular and Italic styles to distinguish different fields as shown in the References section. Number the reference items consecutively in square brackets (e.g. [1]).

When referring to a reference item, please simply use the reference number, as in [2]. Do not use “Ref. [3]” or “Reference [3]” except at the beginning of a sentence, e.g. “Reference [3] shows ...”. Multiple references are each numbered with separate brackets (e.g. [2], [3], [4]–[6]).

The **category** of the paper is proposed by the author(s), but the Editorial Board reserves for itself the right, on the basis of the referees' opinion, to make the final choice.

Proofs are sent to the author(s) to correct printers' errors. Except for this, alterations to the text are not permitted. The proofs should be returned to the Editorial Board in 2 days.

The author(s) will receive, free of charge, 20 reprints of every paper published in the Journal.

REFERENCES

- [1] Surname, N(ame)., Surname, N(ame): *Name of the Book*, Publisher Year.
- [2] Surname, N(ame). Surname, N(ame): *Name of the Book*, Name of the Series. Publisher, **vol. XXX**, Year.
- [3] Surname, N(ame). Surname N(ame): *Title of the Article*, *Name of the Journal*, **vol. XX**, No. XX, pp. XXX–XXX (Year).
- [4] Surname, N(ame). Surname N(ame): *Title of the Article*, *Proceedings of the Name of the Conference*, vol. XX, pp. XXX–XXX. Year.
- [5] Surname, N(ame). Surname N(ame): *Name of the Patent*, Institution that issued the patent & Number of the patent (Date dd. mm. yyyy).
- [6] N.N.: *The XXX web site*, web address, Year.
- [7] N. Surname (Year): *XXX homepage on XXX*, web address
- [8] N.N.: *Title of the Manual*, Name of the Organization, Year.
- [9] N.N.: *XXX data sheet*, Name of the Organization.
- [10] N. Surname (Year): *Title of the Thesis*, Master/Ph.D. thesis (in Language), Institution. Year.
- [11] Surname, N(ame)., N(ame) Surname (Year): *Title of the Report*, Organization that issued the Report, Number of the Report.
- [12] Surname, N(ame). Surname N(ame). *Name of the Standard*, Institution that Issued the Standard & Number of the Standard (Year):.

**SURVEY
OF THE ARTICLES PUBLISHED IN THE PROCEEDINGS
OF THE FACULTY OF ELECTRICAL ENGINEERING IN SKOPJE
ISSUES FROM Vol. 1. No. 1 (1977) TO Vol. 22, No. 1–2 (2006)**

Vladimir Dimčev, Blagoja Bogatinoski

*Faculty of Electrical Engineering and Informations Technology,
"Ss. Cyril and Methodius" University in Skopje,
Karpoš II bb, P.O. box 574, 1001 Skopje, Republic of Macedonia
vladim@feit.ukim.edu.mk*

A b s t r a c t. A survey of the articles published in the Faculty of Electrical Engineering Proceedings for the period between 1977 up to 2006 is given. The first volume of the Proceedings was published in 1977, when the Faculty of Electrical Engineering has started to work as independent high education and research institution, and the last volume was published in 2006. In the Proceedings had been published 121 articles from 80 authors. In 2006 the Faculty of Electrical Engineering has changed the name in Faculty of Electrical Engineering and Information Technologies. The new Journal of Electrical Engineering and Information Technologies in fact is continuation of the old Proceedings. In this survey the articles are numbered according the year of publishing, and this numeration is continuing in the new Journal, with new ISSN number 2545–4250 and 2545–4269 for print and on line version respectively.

**ПРЕГЛЕД
НА ОБЈАВЕНИТЕ ТРУДОВИ ВО 22 ГОДИШНОТО ИЗЛЕГУВАЊЕ
НА ЗБОРНИКОТ НА ТРУДОВИ НА ЕЛЕКТРОТЕХНИЧКИОТ ФАКУЛТЕТ ВО СКОПЈЕ
од, год. 1. број 1 (1977) до, год. 22, број 1–2 (2006)**

А п с т р а к т: Даден е преглед на трудовите објавени во Зборникот на трудови на Електротехничкиот факултет при Универзитетот „Кирил и Методиј“ во Скопје, кој излегуваше повремено во периодот од 1977 до 2006 година. Првиот број е објавен во 1977 година кога Електротехничкиот факултет ја започна својата работа како самостојна наставна и научно-истражувачка институција и излегуваше до 2006 година. Во него се објавени 121 статија од 80 автори. Во 2006 година Електротехничкиот факултет е преименуван во Факултет за електротехника и информациона технологии а Списанието за електротехника и информациски технологии всушност се надврзува на Зборникот. Во прегледот трудовите се нумерирани според редоследот на нивното објавување, а нумерацијата продолжува во сегашново Списание, заедно со новите ISSN броеви 2545–4250 за печатената верзија и 2545–4269 за електронската верзија.

1. Драгослав Рајичиќ: Еден доказ на алгоритмот за формирање на матрицата, *Зборник на трудови*, год. 1, бр. 1, стр. 7–14, 1977. (Резиме на руски јазик: Драгослав Раичич: Одно доказателство алгоритма для образования матрицы, *Proceedings*, Vol. 1, No. 1, pp. 7–15, 1977).
2. Татјана Улчар-Ставрова: Една постапка за намалување на веројатноста на грешка во системите за распознавање, *Зборник на трудови*, год. 1, бр. 1, стр. 15–24, 1977 (Резиме на англиски јазик: Tatjana Ulčar-Stavrova: A procedure for decreasing the probability of error in pattern recognition

- systems, *Proceedings*, Vol. 1, No. 1, pp. 15–24, 1977).
3. Методија Камилевски: Непосредно мерење на модул и аргумент на импедација при високи фреквенции. *Зборник на иџрудови*, год. 1, бр. 1, стр. 25–30, 1977 (Резиме на англиски јазик: Metodija Kamilovski: Direct impedance modul and argument measurement method at high frequency, *Proceedings*, Vol. 1, No. 1, pp. 25–30, 1977).
 4. Бојан Соколов: Развој на програми за апроксимација на функции, *Зборник на иџрудови*, год. 1, бр. 1, стр. 31–46, 1977 (Резиме на англиски јазик: Bojan Sokolov: Function approximation program development, *Proceedings*, Vol. 1, No. 1, pp. 31–46, 1977).
 5. Љубен Јанев: Еден метод за пресметување на полето во зоната на напојувањето на монопол антена прекриена со диелектрик, *Зборник на иџрудови*, год. 3, бр. 2, стр. 5–14, 1979 (Резиме на англиски јазик: Ljuben Jauev: A method for calculating the excitation zone field of dielectric coated monopole antenna, *Proceedings*, Vol. 3, No. 2, pp. 5–14, 1979).
 6. Панчо Врангалов: Тиристорски претворувач за средни и високи фреквенции *Зборник на иџрудови*, год. 3, бр. 2, стр. 15–30, 1979 (Резиме на руски јазик: Панчо Врангалов: Тиристорный преобразователь средних и высоких частотах *Proceedings*, Vol. 3, No. 2, pp. 15–30, 1979).
 7. Властимир Гламочанин: Една постапка за избор на оптимална конфигурација на електроенергетска мрежа, *Зборник на иџрудови*, год. 3, бр. 2, стр. 31–42, 1979 (Резиме на англиски јазик: Vlastimir Glamocann: A procedure for the selection of an optimal configuration of electrical power networks, *Proceedings*, Vol. 3, No. 2, pp. 31–42, 1979).
 8. Љубомир Николовски: Примена на методот на симулација со електрични товари, за пресметување на електростатичкото поле во околината на површинска нерамнина на рамна електрода, *Зборник на иџрудови*, год. 3, бр. 2, стр. 43–66, 1979 (Резиме на англиски јазик: Ljubomir Nikolovski: A charge simulation method for calculation of electric fields in the vicinity of protrusions from a plate electrode, *Proceedings*, Vol. 3, No. 2, pp. 43–66, 1979).
 9. Благој Ханџиски: Проширена примена на методот на најмали квадрати со употреба на сметачките машини, *Зборник на иџрудови*, год. 3, бр. 2, стр. 67–76, 1979 (Резиме на англиски јазик: Blagoj Handžiski: Enlarged application of the method of least squares with the application of the computing systems, *Proceedings*, Vol. 3, No. 2, pp. 67–76, 1979).
 10. Јованка Кепеска: Научно-техничката револуција и промените на производните сили и општествените односи на капитализмот *Зборник на иџрудови*, год. 3, бр. 2, стр. 77–96, 1979 (Резиме на англиски јазик: Jovanka Kepeska: The scientific-technical revolution and transformation of forces and relationships of production of the capitalism *Proceedings*, Vol. 3, No. 2, pp. 77–96 (1979).
 11. Драгослав Рајичиќ, Ристо Ачковски: Метод на енергетски еквиваленти, *Зборник на иџрудови*, год. 6, бр. 3, стр. 5–12, 1982 (Резиме на руски јазик: Драгослав Раичич, Ристо Ачковски: Метод энергетических эквивалентов, *Proceedings*, Vol. 6, No. 3, pp. 5–12, 1982).
 12. Драгослав Рајичиќ, Ристо Ачковски: Приближна неитеративна пресметка на распределбата на моќностите и напонските прилики во ЕЕС, *Зборник на иџрудови*, год. 6, бр. 3, стр. 13–20, 1982. (Резиме на руски јазик: Драгослав Раичич, Ристо Ачковски: Приблизительный неитеративный расчет потокораспределения при планировании электроэнергетических систем, *Proceedings*, Vol. 6, No. 3, pp. 13–20, 1982).
 13. Арсен Арсенов: Електродинамички сили на пакетни собирници во трифазни системи, *Зборник на иџрудови*, год. 6, бр. 3, стр. 21–40, 1982 (Резиме на руски јазик: Арсен Арсенов: Электродинамические силы в трехфазных системах пакетных шин, *Proceedings*, Vol. 6, No. 3, pp. 21–40, 1982).
 14. Драгослав Рајичиќ, Мито Златаноски: Постапка за пресметување на редуцирана матрица Z , *Зборник на иџрудови*, год. 6, бр. 3, стр. 41–46, 1982. (Резиме на руски јазик: Драгослав Раичич, Мито Златаноски: Метод получения сокращенной матрицы узловых сопротивлений, *Proceedings*, Vol. 6, No. 3, pp. 41–46, 1982).
 15. Милан Чундев: Примена на Клосовата равенка на асинхронен мотор со двоен кафеџ, *Зборник на иџрудови*, год. 6, бр. 3, стр.

- 47–56, 1982 (Резиме на англиски јазик: Milan Čundev: Application of the Kloss'es equation to the double squirrel cage induction motor, *Proceedings*, Vol. 6, No. 3, pp. 47–56, 1982).
16. Лидија Петковска: Линеарни трансформации врз матрицата на индуктивности на синхрони машини со испакнати магнетни полови, *Зборник на иџрудови*, год. 6, бр. 3, стр. 57–68, 1982 (Резиме на англиски јазик: Lidija Petkovska: Linear transformations on the matrix of inductances in synchronous salient pole machines, *Proceedings*, Vol. 6, No. 3, pp. 57–68, 1982).
 17. Милан Чундев: Една метода на конструкција на кружен дијаграм на асинхронен мотор со двоструки кафез, *Зборник на иџрудови*, год. 6, бр. 3, стр. 69–80, 1982 (Резиме на англиски јазик: Milan Čundev: One method of construction the circle diagram for double squirrel cage induction motor, *Proceedings*, Vol. 6, No. 3, pp. 59–80 (1982).
 18. Елизибета Лазарееска: Откривање и одделување на кратните полови кај динамичките системи, *Зборник на иџрудови*, год. 6, бр. 3, стр. 81–88, 1982 (Резиме на англиски јазик: Elizabeta Lazarevska: Dynamic systems multiple poles detection and separation, *Proceedings*, Vol. 6, No. 3, pp. 81–88 (1982).
 19. Гоце Арсов: Пример на управување на циклоконвертор применет за напојување на асинхрон мотор во електромоторен погон ео константен момент на оптоварување, *Зборник на иџрудови*, год. 6, бр. 3, стр. 89–100, 1982 (Резиме на англиски јазик: Gose Arsov: Control of cycloconverter for feeding induction motors in constant torque drive, *Proceedings*, Vol. 6, No. 3, pp. 89–100, 1982).
 20. Панчо Врангалов: Распоредувач на импулси наменет за каскадно вклучување на поголем број тиристорни кај повеќекелијските инвертори, *Зборник на иџрудови*, год. 6, бр. 3, стр. 101–106, 1982 (Резиме на руски јазик: Панчо Врангалов: Распределительное устройство для поорчередного отпирания тиристоров в многоячейковых инверторах, *Proceedings*, Vol. 6, No. 3, pp. 101–106, 1982).
 21. Михаил Толев: Експериментални прилози околу локацијата на γ -фазата на системот Cu-Sb, *Зборник на иџрудови*, год. 9, бр. 4, стр. 5–12, 1986. (Резиме на англиски јазик: Mihail Tolev: Experimental Contribution to the γ -phase Location in the Cu-Sb Alloy, *Proceedings*, Vol. 9, No. 4, pp. 5–12, 1986).
 22. Боро Пиперевски: За линеарните диференцијални равенки од втор ред, чие општо решение е полином, *Зборник на иџрудови*, год. 9, бр. 4, стр. 13–18, 1986. (Резиме на француски јазик: Boro Piperevski: Sur des egnations differentielles lineaires du duxieme ordre qui solution generale est polynom, *Proceedings*, Vol. 9, No. 4, pp. 13–18, 1986).
 23. Никола Попов: Критериуми за одредување на режимите на двофазно струење на разладувачот во симнувачкиот вод на PWR реакторски сад во акбидентален случај, *Зборник на иџрудови*, год. 9, бр. 4, стр. 19–44, 1986 (Резиме на англиски јазик: Nikola Popov: Coolant Two-Phase Flow Regime Criteria in the PWR Reactor Vessel Downcomer in Accidental Situations. *Proceedings*, Vol. 9, No. 4, pp. 19–44, 1986).
 24. Елизабета Лазаревска: Аналитичка синтеза на класата линеарни дискретни регулациони системи од втор ред со константни концентрирани параметри, *Зборник на иџрудови*, год. 9, бр. 4, стр. 45–56, 1986. (Резиме на англиски јазик: Elizabeta Lazarevska: Analytic Synthesis of Second Order Linear Discrete Control Systems with Constant Parameters, *Proceedings*, Vol. 9, No. 4, pp. 45–56, 1986).
 25. Кирил Коцев, Благој Димитров: Средни и константни саатни вредности на интензитетот на сончевото зрачење и нивната употребна вредност, *Зборник на иџрудови*, год. 9, бр. 4, стр. 57–68, 1986 (Резиме на француски јазик: Kiril Koccev, Blagoj Dimitrov: Valeurs moyennes et constantes de l'intensite du rayonnement solaire et leur application, *Proceedings*, Vol. 9, No. 4, pp. 57–68, 1986).
 26. Ристо К. Ачковски: Еден брз и ефикасен алгоритам за решавање на равенката на состојбата, *Зборник на иџрудови*, год. 10, бр. 5, стр. 5–18, 1987 (Резиме на англиски јазик: Risto Ačkovski: Fast and effcient method for solving the state equation, *Proceedings*, Vol. 10, No. 5, pp. 5–18, 1987).
 27. Никола К. Попов: Нестационарен двомензионален двофазен модел на бајпас струењето на разладувачот во реакторскиот симнувачки вод при ЛОСА, *Зборник на*

- џрудови*, год. **10**, бр. 5, стр. 19–40, 1987 (Резиме на англиски јазик: Nikola K. Popov: A transient two-dimensional two-phase model of ECC bypass flow in the reactor vessel downcomer in case of loca, *Proceedings*, Vol. **10**, No. 5, pp. 19–40, 1987).
28. Димитар Хаџи-Мишев, Никола Попов: Модел на повторно потопување на активната зона на PWR реактор по максимална проектна хаварија, *Зборник на џрудови*, год. **10**, бр. 5, стр. 41–54, 1987 (Резиме на англиски јазик: Dimitar Hadžt-Mišeв, Nikola Popov: A model of PWR reactor core reflooding following a large break loca, *Proceedings*, Vol. **10**, No. 5, pp. 41–54, 1987).
 29. Љубен Јанев: За енергијата на електрично-то и магнетно поле, *Зборник на џрудови*, год. **10**, бр. 5, стр. 55–62, 1987 (Резиме на англиски јазик: Ljuben Janev: On the energy of electro and magnetic field, *Proceedings*, Vol. **10**, No. 5, pp. 55–62, 1987).
 30. Љубен Јанев: За постоењето на една класа решенија на Максвеловите равенки, *Зборник на џрудови*, год. **10**, бр. 5, стр. 63–70, 1987 (Резиме на англиски јазик: Ljuben Janev: On existence of one class of solutions of Maxwell's equations, *Proceedings*, Vol. **10**, No. 5, pp. 63–70, 1987).
 31. Кирил Коцев: Функционирање на фотоволтаичен систем со акумулаторска батерија за пумпање на вода, *Зборник на џрудови*, год. **10**, бр. 5, стр. 71–82, 1987 (Резиме на француски јазик: Kiril Kocев: Fonctionnement d'un system photovoltaique de pompage aо fil de batterie, *Proceedings*, Vol. **10**, No. 5, pp. 71–82, 1987).
 32. Ристо К. Ачковски, Драгослав А. Рајичиќ: Нов метод за пресметка на потенцијалите на столбовите при еднофазна куса врска, *Зборник на џрудови*, год. **10**, бр. 5, стр. 83–90, 1987 (Резиме на англиски јазик: Risto K. Ačkovski, Dragoslav A. Rajičič: A new method for transmission tower potentials calculation under ground faults, *Proceedings*, Vol. **10**, No. 5, pp. 83–92, 1987).
 33. Боро М. Пиперевски: За една генерализација на формулата на Родригес, *Зборник на џрудови*, год. **10**, бр. 5, стр. 93–98, 1987 (Резиме на англиски јазик: Boro M. Piperevski: One generalization for ones of Rodrigues' formula, *Proceedings*, Vol. **10**, No. 5, pp. 93–98, 1987).
 34. Марија Кујумџиева-Николовска: Ефективни услови за конвергенција на итеративниот метод на Њутн со брзина три за решавање на реални равенки, *Зборник на џрудови*, год. **10**, бр. 5, стр. 99–104, 1987 (Резиме на англиски јазик: Marija Kujumdžieva-Nikolovska: The effective conditions for convergence of Newton's iterative method of order three for solving real equations, *Proceedings*, Vol. **10**, No. 5, pp. 99–104, 1987).
 35. Илија А. Шапкарев: Една формула за полиномно решение на една класа линеарни диференцијални равенки од втор ред, *Зборник на џрудови*, год. **10**, бр. 5, стр. 105–112, 1987 (Резиме на германски јазик: Ilija Šapkarev: Eine Formel der Polynomnngung einer Klasse der linearen Differentialgleichung der zweiten Ordnung, *Proceedings*, Vol. **10**, No. 5, pp. 105–112, 1987).
 36. Петар Р. Лазов, Љупчо М. Коцарев: Неповратност на случајно скитање по права опишано со ланец од втор ред, *Зборник на џрудови*, год. **11–13**, бр. 6–7, стр. 7–18, 1990 (Резиме на англиски јазик: Petar R. Lazov, Ljupčo M. Kocarev: Nonrecurrency of a random walk along a straight line described with second order chain, *Proceedings*, Vol. **11–13**, No. 6–7, pp. 7–18, 1987).
 37. Љубен Јанев, Лидија Ололоска: Еквивалентен полупречник на проводници со правоаголен и L напречен пресек, *Зборник на џрудови*, год. **11–13**, бр. 6–7, стр. 19–26, 1990 (Резиме на англиски јазик: Ljuben Janev, Lidija Ololoska: Equivalent radius of conductors with rectangular and L cross section, *Proceedings*, Vol. **11–13**, No. 6–7, pp. 19–26, 1990).
 38. Боро М. Пиперевски: За една трансформација на класа линеарни диференцијални равенки од втор ред, *Зборник на џрудови*, год. **11–13**, бр. 6–7, стр. 27–34, 1990. (Резиме на англиски јазик: Boro M. Piperevski: One transformation of a class of linear differential equations, of the second order, *Proceedings*, Vol. **11–13**, No. 6–7, pp. 27–34, 1990).
 39. Боро М. Пиперевски: За еден резултат во врска со општи полиномни решенија на класа линеарни диференцијални равенки, *Зборник на џрудови*, год. **11–13**, бр. 6–7,

- стр. 35–38, 1990 (Резиме на англиски јазик: Boro M. Piperevski: On a result concerning general polynomial solutions of a class of differential equations, *Proceedings*, Vol. 11–13, No. 6–7, pp. 35–38, 1990).
40. Боро М. Пиперевски: За една специјална детерминанта, *Зборник на трудови*, год. 11–13, бр. 6–7, стр. 39–46, 1990 (Резиме на англиски јазик: Boro M. Piperevski: On one special determinant, *Proceedings*, Vol. 11–13, No. 6–7, pp. 39–46, 1990).
41. Илија А. Шапкарев: За еден контурен проблем од трети ред, *Зборник на трудови*, год. 11–13, бр. 6–7, стр. 47–54, 1990 (Резиме на англиски јазик: Пија А. Šapkarev: On a third-order contour problem, *Proceedings*, Vol. 11–13, No. 6–7, pp. 47–54, 1990).
42. Илија А. Шапкарев: Конструкција на линеарни диференцијални равенки од четврти ред чии интегралите се производи од интегралите и нивните изводи на линеарни диференцијални равенки од втор ред, *Зборник на трудови*, год. 11–13, бр. 6–7, стр. 55–62, 1990 (Резиме на англиски јазик: Пија А. Šapkarev: Construction of fourth-order linear differential equations, the integrals of which are products of the integrals and their derivatives of second-order linear differential equations, *Proceedings*, Vol. 11–13, No. 6–7, pp. 55–62, 1990).
43. Софија Богданов: Оптимални дигитални филтри со конечна должина на коефициентите, *Зборник на трудови*, год. 11–13, бр. 6–7, стр. 63–72, 1990 (Резиме на англиски јазик: Sofija Boqdanov: Optimal digital filters with finite word length coefficients, *Proceedings*, Vol. 11–13, No. 6–7, pp. 63–72, 1990).
44. Марија Кацарска: Еден начин за забрзување на процесот на анализа на дигитални филтри со симетрична структура, *Зборник на трудови*, год. 11–13, бр. 6–7, стр. 73–82, 1990 (Резиме на англиски јазик: Marija Kacarska: One way to make faster analysing digital filters with symmetric structure, *Proceedings*, Vol. 11–13, No. 6–7, pp. 73–82, 1990).
45. Драгослав Рајчиќ, Ристо Ачковски: Практична недетерминистичка постапка за определување на оптималната инсталирана моќност на уредите за компензација на реактивна моќност, *Зборник на трудови*, год. 11–13, бр. 6–7, стр. 83–90, 1990 (Резиме на англиски јазик: Dragoslav Rajičić: Practical nondeterministic method for optimal compensation in radical networks, *Proceedings*, Vol. 11–13, No. 6–7, pp. 83–90, 1990).
46. Дамјан Д. Христовски: Мерење на коефициентот на загубите на моќност при различни температури на генераторите во смисол на процена на состојбата на изолацијата, *Зборник на трудови*, год. 11–13, бр. 6–7, стр. 91–100, 1990 (Резиме на англиски јазик: Damjan D. Hristovski: Measurement of the coefficient of losses at various temperatures of generators in the sense of estimation of the state of isolation, *Proceedings*, Vol. 11–13, No. 6–7, pp. 91–100, 1990).
47. Кирил Коцев: Струјно напонска карактеристика на панел во реални услови, *Зборник на трудови*, год. 11–13, бр. 6–7, стр. 101–112, 1990 (Резиме на англиски јазик: Kiril Kocsev: Current-voltage panel characteristic in real conditions, *Proceedings*, Vol. 11–13, No. 6–7, pp. 101–112, 1990).
48. Емил Рушков: Оптички резонатор, *Зборник на трудови*, год. 11–13, бр. 6–7, стр. 113–130, 1990 (Резиме на англиски јазик: Emil Ruškov: Optical resonators, *Proceedings*, Vol. 11–13, No. 6–7, pp. 113–130, 1990).
49. Влатко Чингоски: Еден начин за определување на стабилноста на кафезен асинхронен мотор напојуван од извор на променлива фреквенција, *Зборник на трудови*, год. 11–13, бр. 6–7, стр. 131–140, 1990 (Резиме на англиски јазик: Vlatko Čingoski: A method for determination the stability of squirrel-cage induction motor with changeable frequency supply, *Proceedings*, Vol. 11–13, No. 6–7, pp. 131–140, 1990).
50. Елизабета Лазаревска: Моделирање на хоризонталното движење и правецот на движење на брод, *Зборник на трудови*, год. 11–13, бр. 6–7, стр. 141–170, 1990 (Резиме на англиски јазик: Elizabeta Lazarevska: Modelling of the horizontal movement and the direction of a ship, *Proceedings*, Vol. 11–13, No. 6–7, pp. 141–170, 1990).
51. Љубен Јанев: Еден подобрен алгоритам за решавање на дводимензионата Лапласова диференцијална равенка, *Зборник на трудови*

- дови, год. **11–13**, бр. 6–7, стр. 171–176, 1990 (Резиме на англиски јазик: Ljuben Janev: One improved algorithm for colving the the twodimensional Laplace's differential equation, *Proceedings*, Vol. **11–13**, No. 6–7, pp. 171–176, 1990).
52. Ристо Миновски: 20 години од лабораторијата за висок напон на Електротехничкиот факултет во Скопје, *Зборник на трудови*, год. **11–13**, бр. 6–7, стр. 177–194, 1990. (Резиме на англиски јазик: Risto Minovski: Twenty years of the high voltage laboratory at the Faculty of Electrical Engineering in Skopje, *Proceedings*, Vol. **11–13**, No. 6–7, pp. 177–194, 1990).
53. Стојан Чундев, Никола Чекреци, Велимир Филиповски, Стојан Николовски: Дваесет години јубилеј на лабораторијата за електротермија при Електротехничкиот факултет во Скопје, *Зборник на трудови*, год. **11–13**, бр. 6–7, стр. 195–208, 1990 (Резиме на англиски јазик: Stojan Čundev, Nikola Čekredži, Velimir Filipovski, Stojan Nikolovski: Twenty years of the electroheat laboratory at the Faculty of Electrical Engineering in Skopje, *Proceedings*, Vol. **11–13**, No. 6–7, pp. 195–208, 1990).
54. Методија Камилоски: Развој на електрониката како индустриска гранка во среднорочниот период 1986–1990 година во СРМ, *Зборник на трудови*, год. **11–13**, бр. 6–7, стр. 209–224, 1990 (Резиме на англиски јазик: Metodija Kamilovski: The development of the electronics industry during the middle-term period 1986–1990 in SR Macedonia, *Proceedings*, Vol. **11–13**, No. 6–7, pp. 209–224, 1990).
55. Љубомир Стрезов: Веројатност на грешка во М-QAM сигналите, *Зборник на трудови*, год. **11–13**, бр. 6–7, стр. 225–239, 1990 (Резиме на англиски јазик: Ljubomir Strezov: Probability of error by M-QAM signals, *Proceedings*, Vol. **11–13**, No. 6–7, pp. 225–239, 1990).
56. Илија Шапкарев: Конструкција на линеарни диференцијални равенки од трет ред чии интегралите се произведени од интегралите и нивните изводи на линеарни диференцијални равенки од втор ред, *Зборник на трудови*, год. **11–13**, бр. 6–7, стр. 240–249, 1990 (Резиме на англиски јазик: Ilija Šapkarev: Construction of third-order linear differential equations, the integrals of which are products of the integrals and their derivatives of second-order linear differential equations, *Proceedings*, Vol. **11–13**, No. 6–7, pp. 240–249, 1990).
57. Благој Ханџиски: Дали сегашната постапка за одредување на потенцијалот на заземјувачите е оптоварена со една систематска грешка. *Зб. ипр. Електроинџ. фак. – Скопје*, год. **14**, бр. 8, стр. 1–6, 1991 (Резиме на англиски јазик: Blagoj Handžiski: Is the Present Procedure of the Determining the Values of Electrical Power Station Ground Potential Rise an Error, *Proceedings*, Vol. **14**, No. 8, pp. 1–6, 1990).
58. Драгослав Рајичиќ, Весна Борозан, Ристо Ачковски: Алгоритам за формирање на матрицата на импеданциите на независните контури и за нејзината модификација, *Зб. ипр. Електроинџ. фак. – Скопје*, год. **14**, бр. 8, стр. 7–14, 1991 (Резиме на англиски: Dragoslav Rajičić, Vesna Borozan, Risto Ačkovski: An Algorithm for Loop Impedance Matrix Construction and It's Modifications, *Proceedings*, Vol. **14**, No. 8, pp. 7–14, 1990).
59. Владимир Димчев, Благој Ханџиски: Нумеричка метода за интерпретација на резултатите од геоелектричното сондирање добиени со Вернеровата метода, *Зб. ипр. Електроинџ. фак. – Скопје*, год. **14**, бр. 8, стр. 15–22 (1991 (Резиме на англиски: Vladimir Dimčev, Blagoj Handžiski: Numerical Method for Interpretation of Soil Resistivity Measurements Obtained by the Wernner Method, *Proceedings*, Vol. **14**, No. 8, pp. 15–22, 1990).
60. Горан Рафајловски, Никола Пашалиќ: Примена инкременталните енкодери во микропроцесорско управуваните електромоторни погони, *Зб. ипр. Електроинџ. фак. – Скопје*, год. **14**, бр. 8, стр. 23–26, 1991 (Резиме на англиски: Goran Rafajlovski, Nikola Pašalić: Application of digital speed encoder in microprocessor-controlled motor drives, *Proceedings*, Vol. **14**, No. 8, pp. 23–26, 1990).
61. Кирил Коцев, Владимир Димчев, Благој Димитров: Математичко моделирање на напонските и енергетските процеси во оловните акумулатори, *Зб. ипр. Електроинџ. фак. – Скопје*, год. **14**, бр. 8, стр. 27–32, 1991 (Резиме на англиски јазик: Kiril

- Kocev, Vladimir Dimčev, Blagoj Dimitrov: Mathematical Modeling of Voltage and Energy Processes in a Lead-acid Battery, *Proceedings*, Vol. **14**, No. 8, pp. 27–32, 1990).
62. Петар Лазов: Реални полиноми, кои се линеарна комбинација од степени на некој полином, *Зб. љр. Елекџроџех. фак. – Скопје*, год. **14**, бр. 8, стр. 39–40, 1991 (Резиме на англиски јазик: Petar Lazov: Real Polynomials Expressed by Linear Combinations of Powers of Certain Polynomials, *Proceedings*, Vol. **14**, No. 8, pp. 33–40, 1990).
63. Горан Рафајловски, Никола Пашалиќ: Синтеза на регулациониот круг на брзината на микропроцесорски управуван електромоторен погон во старт-стоп режим на работа, *Зб. љр. Елекџроџех. фак. – Скопје*, год. **14**, бр. 8, стр. 42–47, 1991 (Резиме на англиски јазик: Goran Rafajlovski, Nikola Pašalić: Synthesis of Speed Control Loop of Mikroprocesor-Controlled Motor Drive in a start-stop working Mode, *Proceedings*, Vol. **14**, No. 8, pp. 41–47, 1990).
64. Никола Речкоски: Некои аналитички функции дефинирани со дистрибуции, *Зб. љр. Елекџроџех. фак. – Скопје*, год. **14**, бр. 8, стр. 46–51, 1991 (Резиме на руски јазик: Никола Речкоски: Некоторые аналитические функции определенных распределениями, *Proceedings*, Vol. **14**, No. 8, pp. 46–51, 1990).
65. Љупчо Коцарев, Љупчо Карацинов, Жарко Тасев: Синхронизација на двојна спирала хаотичниот атрактор, *Зб. љр. Елекџроџех. фак. – Скопје*, год. **14**, бр. 8, стр. 53–61, 1991 (Резиме на англиски јазик: Ljupčo. Kocarev, Ljupčo. Karadžinov, Žarko Tasev: Synchronization of Double Scroll Chaotic Attractor, *Proceedings*, Vol. **14**, No. 8, pp. 53–58, 1990).
66. Лидија Петковска, Милан Чундев: Современ пристап кон анализата на карактеристиките на електронички управуван синхрон мотор, *Зб. љр. Елекџроџех. фак. – Скопје*, год. **15**, бр. 9–10, стр. 1–8, 1991 (Резиме на англиски јазик: Lidija Petkovska, Milan Čundev: A modern access to the analysis of an electronically operated synchronous motor's characteristics, *Proc. Dep. Electr. Eng. – Skopje*, Vol. **15**, No. 9–10, pp. 1–8, 1992).
67. Dragoslav Rajičić, Risto Ačkovski: Weakly meshed power flow using oriented ordering and voltage corrections, *Proc. Dep. Electr. Eng. – Skopje*, Vol. **15**, No. 9–10, pp. 9–14, 1992 (Резиме на македонски јазик: Драгослав Рајичиќ, Ристо Ачковски: Пресметка на напони во мрежите со релативно мал број на контури со помош на ориентирано посредување и корекции на напоните, *Зб. љр. Елекџроџех. фак. – Скопје*, год. **15**, бр. 9–10, стр. 9–14, 1991).
68. Владимир Димчев, Благој Ханџски: Примена на метод на оптичка аналогија за добивање на теоретските криви на привидниот специфичен отпор во повеќеслојна геоелектрична средина, *Зб. љр. Елекџроџех. фак. – Скопје*, год. **15**, бр. 9–10, стр. 15–21, 1991 (Резиме на англиски јазик: Vladimir Dimčev, Blagoj Handžiski: Determination of apparent resistivity theoretical curves in multi-layer earth structure with the method of optical analogy, *Proc. Dep. Electr. Eng. – Skopje*, Vol. **15**, No. 9–10, pp. 15–21, 1992).
69. Љубен Јанев, Лидија Ололоска: Анализа на преодните режими кај цилиндричните антени во временски домен, *Зб. љр. Елекџроџех. фак. – Скопје*, год. **15**, бр. 9–10, стр. 23–26, 1991 (Резиме на англиски јазик: Ljuben) Janev, Lidija Ololoska: Time domain analysis of transient responses of cylindrical antennas, *Proc. Dep. Electr. Eng. – Skopje*, Vol. **15**, No. 9–10, pp. 23–26, 1992).
70. Софија Богданова: Пресликување на индексите при индиректно пресметување на ДСТ со декомпозиција на прости фактор, *Зб. љр. Елекџроџех. фак. – Скопје*, год. **15**, бр. 9–10, стр. 27–29, 1991 (Резиме на англиски јазик: Sofija Bogdanova: Index mapping for a prime-factor-decomposed indirect computation of DCT, *Proc. Dep. Electr. Eng. – Skopje*, Vol. **15**, No. 9–10, pp. 27–29, 1992).
71. Драган Ничота: Анализа на грешките на квантизација кај алгоритмите за DFT во аритметика со фиксна точка, *Зб. љр. Елекџроџех. фак. – Скопје*, год. **15**, бр. 9–10, стр. 31–36, 1991 (Резиме на англиски јазик: Dragan Ničota: Fixed-point error analysis of algorithms for discrete Fourier transform, *Proc. Dep. Electr. Eng. – Skopje*, Vol. **15**, No. 9–10, pp. 31–36, 1992).
72. Mihail. Tolev, Kornelija Stojanova, Zafir Stojanov, Stanoja Stojmenov, Aleksandar Niko-

- lovski: Debay's Temperature of the Sintered Cu-Ni Alloys estimated by ultrasonic measurements, *Proc. Dep. Electr. Eng. – Skopje*, Vol. **15**, No. 9–10, pp. 37–41, 1992 (Резиме на македонски јазик: Михаил Толев, Корнелија Стојанова, Зафир Стојанов, Станоја Стоименов, Александар Николовски: Дебаева температура на синтерувани Cu-Ni легури определени со помош на ултразвучни мерења, *Зб. ѓр. Елекѓроѓех. фак. – Скопје*, год. **15**, бр. 9–10, стр. 37–41, 1991).
73. Илија. А. Шапкарев: Квадрати од решенија на диференци равенки од втор ред како решенија на диференци равенки од трет ред, *Зб. ѓр. Елекѓроѓех. фак. – Скопје*, год. **15**, бр. 9–10, стр. 43–44, 1991 (Резиме на германски јазик: Илија А. Шапкарев: Quadrate der Integrale der Differenzgleichungen der zweiten Ordnung als Losungen der Differenzgleichungen der dritten Ordnung, *Proc. Dep. Electr. Eng. – Skopje*, Vol. **15**, No. 9–10, pp. 43–44, 1992).
74. Боро Пиперевски, Митруш Петрушев: За еден резултат на Fényes Tamás, *Зб. ѓр. Елекѓроѓех. фак. – Скопје*, год. **15**, бр. 9–10, стр. 45–48, 1991 (Резиме на англиски јазик: Boro Piperevski, Mitruš Petrušev: On a result of Fényes Tamás, *Proc. Dep. Electr. Eng. – Skopje*, Vol. **15**, No. 9–10, pp. 45–46, 1992).
75. Tomislav. Džekov: What is refractive optica bistability?, *Proc. Dep. Electr. Eng. – Skopje*, Vol. **16–17**, No. 1–2, pp. 3–19, 1993/94 (Резиме на македонски јазик: Томислав Џеков: Што е тоа рефрактивна оптичка бистабилност?, *Зб. ѓр. Елекѓроѓех. фак. – Скопје*, год. **16–17**, бр. 1–2, стр. 3–16, 1993/94).
76. Стојан Чундев: Едноставни експерименти за докажување на постоењето на моќноста на дисторзија, *Зб. ѓр. Елекѓроѓех. фак. – Скопје*, год. **16–17**, бр. 1–2, стр. 17–30, 1993/94 (Резиме на англиски јазик: Stojan Čundev: Experiments simples demonstrant que la puissance de distorsion existe vraiment, *Proc. Dep. Electr. Eng. – Skopje*, Vol. **16–17**, No. 1–2, pp. 17–30, 1993/94).
77. Драгослав Рајичиќ, Рубин Талески: Метод за анализа на заземјувачки системи, *Зб. ѓр. Елекѓроѓех. фак. – Скопје*, год. **16–17**, бр. 1–2, стр. 31–37, 1993/94 (Резиме на англиски јазик: Dragoslav Rajičić, Rubin Taleski: A method for grounding system analysis *Proc. Dep. Electr. Eng. – Skopje*, Vol. **16–17**, No. 1–2, pp. 31–37, 1993/94).
78. Горан Рафајловски: Синтеза на колото за регулација на положбата кај микропроцесорски управуван еднонасочен мотор, *Зб. ѓр. Елекѓроѓех. фак. – Скопје*, год. **16–17**, бр. 1–2, стр. 39–45, 1993/94 (Резиме на англиски јазик: Goran Rafajlovski: Synthesis of position control system with microcomputer and motor, *Proc. Dep. Electr. Eng. – Skopje*, Vol. **16–17**, No. 1–2, pp. 39–45, 1993/94).
79. Nikola Čekredži: Determination of the approximative mathematical model of the transient temperature field at inductive heat treatment of longitudinally welded tubes, *Proc. Dep. Electr. Eng. – Skopje*, Vol. **16–17**, No. 1–2, pp. 47–55, 1993/94 (Резиме на македонски јазик: Никола Чекеѓи: Определување на приближен математички модел на транзиентно температурно поле при индукционен третман на надолжно заварени цевки, *Зб. ѓр. Елекѓроѓех. фак. – Скопје*, год. **16–17**, бр. 1–2, стр. 47–55, 1993/94).
80. Марјан Попов: Пренапони на прекинувач при исклучување на струја на куса врска, *Зб. ѓр. Елекѓроѓех. фак. – Скопје*, год. **16–17**, бр. 1–2, стр. 57–62, 1993/94 (Резиме на англиски јазик: Marjan Popov: Oweroltages due to disconnection on the fault current at the circuit breaker, *Proc. Dep. Electr. Eng. – Skopje*, Vol. **16–17**, No. 1–2, pp. 57–62, 1993/94).
81. Ljupčo V. Karadžinov, Goce L'. Arsov. David J. Jefferies: Alpha-parameters charge control piecewise-linear BJT model!, *Proc. Dep. Electr. Eng. – Skopje*, Vol. **18**, No. 1–2, pp. 3–11, 1995 (Резиме на македонски јазик: Љупчо. В. Караѓинов, Гоце Љ. Арсов, David J. Jefferies: Алфа-параметарски сегментно-линеарен модел на биполарен транзистор со контрола на полнежи, *Зб. ѓр. Елекѓроѓех. фак. – Скопје*, год. **18**, бр. 1–2, стр. 3–11, 1995).
82. Жарко Тасев, Љупчо Коцарев, Дончо Димовски: За хаотичните атрактори во дел по дел линеарните електрични кола и нивната класификација со помош на цели броеви, *Зб. ѓр. Елекѓроѓех. фак. – Скопје*, год. **18**, бр. 1–2, стр. 13–20, 1995 (Резиме на англиски јазик: Žarko Tasev, Ljupčo Kocarev, Dončo Dimovski: On chaotic attractors in piece-wise linear electric circuits and their

- classification with integers, *Proc. Dep. Electr. Eng. – Skopje*, Vol. **18**, No. 1–2, pp. 13–20, 1995).
83. Ристо Ачковски: Една итеративна постапка за пресметување на граничниот распон, *Зб. ѓпр. Елекѓроѓех. фак. – Скопје*, год. **18**, бр. 1–2, стр. 21–26, 1995 (Резиме на англиски јазик: Risto Aĉkovski: An iterative procedure for boundary span calculation, *Proc. Dep. Electr. Eng. – Skopje*, Vol. **18**, No. 1–2, pp. 21–26, 1995).
84. Никола Чекреци: Нумеричка анализа на загревање на единичен контакт во тврда фаза, *Зб. ѓпр. Елекѓроѓех. фак. – Скопје*, год. **18**, бр. 1–2, стр. 27–40, 1995 (Резиме на англиски јазик: Nikola ĆekredŹi: Numerical analysis of single contact heating in solid state, *Proc. Dep. Electr. Eng. – Skopje*, Vol. **18**, No. 1–2, pp. 27–40, 1995).
85. Верка Георгиева: Определување на диоден фактор на тенкослојни фотоволтаични ќелии со основа од Cu_2O , *Зб. ѓпр. Елекѓроѓех. фак. – Скопје*, год. **18**, бр. 1–2, стр. 41–45, 1995, (Резиме на англиски јазик: Verka Georgieva: Diode quality factor determination for thin solar cells with Cu_2O , *Proc. Dep. Electr. Eng. – Skopje*, Vol. **18**, No. 1–2, pp. 41–45, 1995).
86. Илија А. Шапкарев: Über einige Bedingungen der existenz und der Konstruktion der Lösungen einer linearen Differentialgleichung der zweiten Ordnung, *Proc. Dep. Electr. Eng. – Skopje*, Vol. **18**, No. 1–2, pp. 47–52, 1995 (Резиме на македонски јазик: Илија А. Шапкарев: За некои услови за егзистенција и конструкција на решението на една линеарна диференцијална равенка од втори ред, *Зб. ѓпр. Елекѓроѓех. фак. – Скопје*, год. **18**, бр. 1–2, стр. 47–52, 1995).
87. Кирил И. Коцев: Моделирање енергетски процеси во оловен акумулатор, *Зб. ѓпр. Елекѓроѓех. фак. – Скопје*, год. **18**, бр. 1–2, стр. 53–57, 1995 (Резиме на англиски јазик: Kiril I. Kocев: Mathematical model of energetic process in the lead-acid battery, *Proc. Dep. Electr. Eng. – Skopje*, Vol. **18**, No. 1–2, pp. 53–57, 1995).
88. Методија Камиловски: Одредување на вкупната средна вредност и стандардна девијација од поединечните средни вредности и стандардни девијации од повеќе мерени серии, *Зб. ѓпр. Елекѓроѓех. фак. – Скопје*, год. **18**, бр. 1–2, стр. 59–61, 1995 (Резиме на англиски јазик: Metodija Kamiiovski: Calculated total mean vaiiue and total standard deviation from mean values and standard deviations of more measurent series, *Proc. Dep. Electr. Eng. – Skopje*, Vol. **18**, No. 1–2, pp. 59–61, 1995).
89. Јосиф Ќосев, Гоце Арсов: За проблемот со управување на MOS-прекинувачите кај прекинувачките преобразувачи на напон, *Зб. ѓпр. Елекѓроѓех. фак. – Скопје*, год. **19**, бр. 1–2, стр. 3–10, 1996 (Резиме на англиски јазик: Josif Ćosev, Goce Arsov: The MOSFET driving problem in the switching voltage convertors, *Proc. Dep. Electr. Eng. – Skopje*, Vol. **19**, No. 1–2, pp. 3–10, 1996).
90. Dragostav Rajiĉiĉ, Rubin Taleski: Radial distribution systems short circuit analysis using admittance summation method, *Proc. Dep. Electr. Eng. – Skopje*, Vol. **19**, No. 1–2, pp. 11–14, 1996 (Резиме на македонски јазик: Драгослав Рајичиќ, Рубин Талески: Пресметка на напоните и струите во случај на куси врски во радијалните дистрибутивни мрежи, *Зб. ѓпр. Елекѓроѓех. фак. – Скопје*, год. **19**, бр. 1–2, стр. 11–14, 1996).
91. Marjan Popov, Mito Zlatanovski: A circuit breaker model for digital simutation using Mayr's and Cassie's differential equations, *Proc. Dep. Electr. Eng. – Skopje*, Vol. **19**, No. 1–2, pp. 15–21, 1996 (Резиме на македонски јазик: Марјан Попов, Мито Златаноски: Модел на прекинувач на струјно коло за дигитална симулација со примена на диференцијалните равенки на Mayr's и Cassie, *Зб. ѓпр. Елекѓроѓех. фак. – Скопје*, год. **19**, бр. 1–2, стр. 15–21, 1996).
92. Снежана Чундева: Дали трансформаторскиот модел PSPICE може да се прифати како генерален трансформаторски модел, *Зб. ѓпр. Елекѓроѓех. фак. – Скопје*, год. **19**, бр. 1–2, стр. 23–30, 1996 (Резиме на англиски јазик: SneŹana Ćundeва: Coult the PSPICE transformer model be seen as a general transformer model, *Proc. Dep. Electr. Eng. – Skopje*, Vol. **19**, No. 1–2, pp. 23–30, 1996).
93. Никола Љ. Чекреци: Почетно интермитирано загревање кај челното заварување со искрење, *Зб. ѓпр. Елекѓроѓех. фак. – Скопје*, год. **19**, бр. 1–2, стр. 31–39, 1996

- (Резиме на англиски јазик: Nikola Lj. Čekredži: Initial intermittent heading in flush butt welding, *Proc. Dep. Electr. Eng. – Skopje*, Vol. **19**, No. 1–2, pp. 31–39, 1996).
94. Goran Rafajlovski: Modelling and analysis of different modulation techniques for inverter fed induction motor, *Proc. Dep. Electr. Eng. – Skopje*, Vol. **19**, No. 1–2, pp. 41–45, 1996 (Резиме на македонски јазик: Горан Рафајловски: Моделирање и анализа на различни модулатиони техники на инвертор совти-нат напон, *Зб. ипр. Електироинџ. фак. – Скопје*, год. **19**, бр. 1–2, стр. 41–45 (1996).
 95. Боро М. Пиперевски: Егзистенција и кон-струкција на полиномно решение на една класа диференцијални равенки од трет ред, *Зб. ипр. Електироинџ. фак. – Скопје*, год. **19**, бр. 1–2, стр. 47–48, 1996 (Резиме на англиски јазик: Boro M. Piperevski: On existence and construction of a polynomial solutions of a class of linear differential equation of the third order, *Proc. Dep. Electr. Eng. – Skopje*, Vol. **19**, No. 1–2, pp. 47–48, 1996).
 96. Горан Трајковски, Марјан Богатиновски: Невронски мрежи на Марков, *Зб. ипр. Електироинџ. фак. – Скопје*, год. **19**, бр. 1–2, стр. 49–52, 1996 (Резиме на англиски јазик: Goran Trajkovski, Marjan Bogatinoski: Markovian neural networks, *Proc. Dep. Electr. Eng. – Skopje*, Vol. **19**, No. 1–2, pp. 49–52, 1996).
 97. Зоран А. Ивановски: Прилог кон обработката на слика со примена на фази-множества и оператори, *Зб. ипр. Електироинџ. фак. – Скопје*, год. **19**, бр. 1–2, стр. 53–60, 1996 (Резиме на англиски јазик: Zoran A. Ivanovski: A contribution to image processing using fuzzy sets and operators, *Proc. Dep. Electr. Eng. – Skopje*, Vol. **19**, No. 1–2, pp. 53–60, 1996).
 98. Горан Рафајловски: Состојби, развој и идни трендови во регулацијата на асинхроните мотори, *Зб. ипр. Електироинџ. фак. – Скопје*, год. **20**, бр. 1–2, стр. 3–20, 1997 (Резиме на англиски јазик: Goran Rafajlovski: Present state, development and future trends in control of induction motors, *Proc. Dep. Electr. Eng. – Skopje*, Vol. **20**, No. 1–2, pp. 3–20, 1997).
 99. Ристо Ачковски, Валентин Кирчев: Загуби на моќност во заштитните јажиња кај надземните водови со висок и највисок напон, *Зб. ипр. Електироинџ. фак. – Скопје*, год. **20**, бр. 1–2, стр. 21–26, 1997 (Резиме на англиски јазик: Risto Ačkovski, Valentin Kirtchev: Power losses in ground wires systems of HV and EHV transmission lines, *Proc. Dep. Electr. Eng. – Skopje*, Vol. **20**, No. 1–2, pp. 21–26, 1997).
 100. Ристо Ачковски, Мирко Тодоровски: Нов метод за пресметување на загубите на моќност во заштитните јажиња кај високонапонските надземни водови, *Зб. ипр. Електироинџ. фак. – Скопје*, год. **20**, бр. 1–2, стр. 27–37, 1997 (Резиме на англиски јазик: Risto Ačkovski, Mirko Todorovski: A new method for calculation the power losses in ground wires of HV and EHV transmission lines, *Proc. Dep. Electr. Eng. – Skopje*, Vol. **20**, No. 1–2, pp. 27–37, 1997).
 101. Владимир Димчев, Благој Ханџиски, Леонид Грчев: Мерење и пресметка на електричното и магнетното поле под надземни електроенергетски водови, *Зб. ипр. Електироинџ. фак. – Скопје*, год. **20**, бр. 1–2, стр. 39–45, 1997 (Резиме на англиски јазик: Vladimir Dimčev, Blagoj Handžiski, Leonid Grčev: Measurements and calculations of electric and magnetic fields under power transmission lines, *Proc. Dep. Electr. Eng. – Skopje*, Vol. **20**, No. 1–2, pp. 39–45, 1997).
 102. Марјан Попов: Модел на вакуумски прекинувач за дигитална симулација на преодните појави, *Зб. ипр. Електироинџ. фак. – Скопје*, год. **20**, бр. 1–2, стр. 47–53, 1997 (Резиме на англиски јазик: Marjan Popov: A vacuum circuit breaker model for digital simulation of transient phenomena, *Proc. Dep. Electr. Eng. – Skopje*, Vol. **20**, No. 1–2, pp. 47–53, 1997).
 103. Lupčo V. Karadžinov, Katerina J. Raleva, Goce L. Arsov, Metodija A. Kamilovski: An algorithm for parameter determination for piecewise-linear BJT model for transient behaviour, *Proc. Dep. Electr. Eng. – Skopje*, Vol. **20**, No. 1–2, pp. 55–63, 1997 (Резиме на македонски јазик: Љупчо В. Караџинов, Катерина Ј. Ралева, Гоце Љ. Арсов, Методија А. Камиловски: Алгоритам за одредување на параметрите на сегментно-линеарниот модел на транзистор за преодни одзиви, *Зб. ипр. Електироинџ. фак. – Скопје*, год. **20**, бр. 1–2, стр. 55–63 (1997).

104. Марјан Богатиновски, Горан Трајковски, Билјана Стојчевска: Моделирање на статистички мултиплексер на видео извори за АТМ мрежи, *Зб. њр. Елекџроџех. фак. – Скопје*, год. **20**, бр. 1–2, стр. 65–67, 1997 (Резиме на англиски јазик: Marjan Bogatinovski, Goran Trajkovski, Biljana Stojčevska: Modelling a statistical multiplexer of video sources for ATM networks, *Proc. Dep. Electr. Eng. – Skopje*, Vol. **20**, No. 1–2, pp. 65–67, 1997).
105. Тони Белчовски, Тодор Јакимов: Споредба меѓу моделите на асинхрон мотор со и без занемарување на загубите во железо, *Зб. њр. Елекџроџех. фак. – Скопје*, год. **20**, бр. 1–2, стр. 69–76, 1997 (Резиме на англиски јазик: Tony Belčovski, Todor Jakimov: Comparison between the models of induction motor with and without neglecting the iron loss, *Proc. Dep. Electr. Eng. – Skopje*, Vol. **20**, No. 1–2, pp. 69–76, 1997).
106. Марија Кацарска, Леонид Грчев: Влијание на магнетното и електричното поле врз здравјето на луѓето, *Зб. њр. Елекџроџех. фак. – Скопје*, год. **21**, бр. 1–2, стр. 1–10, 2001 (Резиме на англиски јазик: Marija Kacarska, Leonid Grčev: The influence of electric and magnetic field on people's health, *Proc. Dep. Electr. Eng. – Skopje*, Vol. **21**, No. 1–2, pp. 1–10, 2001).
107. Кирил И. Коцев: Фотоволтаични системи – можности и перспектива, *Зб. њр. Елекџроџех. фак. – Скопје*, год. **21**, бр. 1–2, стр. 11–16, 2001 (Резиме на англиски јазик: Kiril I. Kocsev: Photovoltaic systems – ability and perspective, *Proc. Dep. Electr. Eng. – Skopje*, Vol. **21**, No. 1–2, pp. 11–16, 2001).
108. Ристо Ачковски, Мирко Тодоровски: Упростен метод за пресметка на загубите на моќност во заземјувачкиот систем на надземните водови со две заштитни јажиња, *Зб. њр. Елекџроџех. фак. – Скопје*, год. **21**, бр. 1–2, стр. 17–23, 2001 (Резиме на англиски јазик: Risto Ačkovski, Mirko Todorovski: A simplified method for power losses calculation in a grounding system of 400 kV transmission lines, *Proc. Dep. Electr. Eng. – Skopje*, Vol. **21**, No. 1–2, pp. 17–23, 2001).
109. Мирко Тодоровски, Ристо Ачковски: Оптимална компензација на реактивната моќност во дистрибутивните мрежи со примена на детерминистички иницијализиран генетски алгоритам, *Зб. њр. Елекџроџех. фак. – Скопје*, год. **21**, бр. 1–2, стр. 25–36, 2001 (Резиме на англиски јазик: Mirko Todorovski, Risto Ačkovski: Optimal capacitor placement in distribution networks by means of a determinatively initiated genetic algorithm, *Proc. Dep. Electr. Eng. – Skopje*, Vol. **21**, No. 1–2, pp. 25–36, 2001).
110. Nikolay D. Bankov, Stefan E. Tabakov, Cvetan V. Gavrovski: Analysis of a transistor series-resonant inverter operating at frequencies higher than the resonance, *Proc. Dep. Electr. Eng. – Skopje*, Vol. **21**, No. 1–2, pp. 37–43, 2001 (Резиме на македонски јазик: Николај Д. Банков, Стефан Е. Табаков, Цветан В. Гавровски: Испитување на работата на транзисторски сериски резонантен инвертор кој работи на фреквенции повиооки од резонантната, *Зб. њр. Елекџроџех. фак. – Скопје*, год. **21**, бр. 1–2, стр. 37–43, 2001).
111. Ljubomir Nikolovski, Goran Rafajlovski: Voltage quality in residential areas, *Proc. Dep. Electr. Eng. – Skopje*, Vol. **21**, No. 1–2, pp. 45–50, 2001 (резиме на македонски јазик: Љубомир Николовски, Горан Рафајловски: Квалитет на напонот во станбени квартаови, *Зб. њр. Елекџроџех. фак. – Скопје*, год. **21**, бр. 1–2, стр. 45–50, 2001).
112. Благој Ханџиски, Владо Ханџиски, Панчо Врангалов, Владимир Димчев: Компјутеризирани методи за дизајнирање и мерење на параметрите на заземјувачите, *Зб. њр. Елекџроџех. фак. – Скопје*, год. **21**, бр. 1–2, стр. 51–64, 2001 (Резиме на англиски јазик: Blagoj Handžiski, Vlado Handžiski, Pančo Vrangalov, Vladimir Dimčev: Computer design measurement of grounding systems parameters, *Proc. Dep. Electr. Eng. – Skopje*, Vol. **21**, No. 1–2, pp. 51–64, 2001).
113. Сашо Георгиески, Слободан Мирчевски: Идентификација на параметрите на асинхрон мотор со втиснат еднонасочен напон, *Зб. њр. Елекџроџех. фак. – Скопје*, год. **21**, бр. 1–2, стр. 65–72, 2001 (Резиме на англиски јазик: Sašo Georgieski, Slobodan Mirčevski: Parameter identification of induction motor with impressed DC voltage, *Proc. Dep. Electr. Eng. – Skopje*, Vol. **21**, No. 1–2, pp. 65–72, 2001).

114. Dragoslav Rajičić, Risto Ačkovski: Under-ground power cable model for grounding system analysis, *Proc. Dep. Electr. Eng. – Skopje*, Vol. **22**, No. 1–2, pp. 1–7, 2006 (Резиме на македонски јазик: Драгослав Рајичиќ, Ристо Ачковски: Модел на анализа на заземјувачкиот систем на енергетските кабли, *Зб. ѓпр. Елекѓроѓех. фак. – Скопје*, год. **22**, бр. 1–2, стр. 1–7, 2006).
115. Ристо Ачковски, Николче Ацевски: Нов метод за анализа на приликите при земјоспој во заземјувачкиот систем на надземните водови, *Зб. ѓпр. Елекѓроѓех. фак. – Скопје*, год. **22**, бр. 1–2, стр. 9–16, 2006 (Резиме на англиски јазик: Risto Ačkovski, Nikolče Acevski: New method for overhead line grounding system under fault conditions analysis, *Proc. Dep. Electr. Eng. – Skopje*, Vol. **22**, No. 1–2, pp. 9–16, 2006).
116. Goga Svetkovski: An original approach to optimal design of electromagnetic devices by using genetic algorithm, *Proc. Dep. Electr. Eng. – Skopje*, Vol. **22**, No. 1–2, pp. 17–26, 2006 (Резиме на македонски јазик: Гога Цветковски: Оригинален пристап кон оптималното проектирање на електромагнетни уреди со примена на генетски алгоритам, *Зб. ѓпр. Елекѓроѓех. фак. – Скопје*, год. **22**, бр. 1–2, стр. 17–26, 2006).
117. Христина Спасевска: Електрично двојно прекршување на светлината во разредени раствори од сегментно неконјугиран полимер, *Зб. ѓпр. Елекѓроѓех. фак. – Скопје*, год. **22**, бр. 1–2, стр. 27–34, 2006 (Резиме на англиски јазик: Hristina Spasevska: Electric birefringence in diluted solutions of segmented non-conjugated polymer, *Proc. Dep. Electr. Eng. – Skopje*, Vol. **22**, No. 1–2, pp. 27–34, 2006).
118. Marija Kujumdžieva Nikoloska, Jordanka Mitevska: Conditions for existence of quasi-periodic solutions for some nonlinear differential equations of second order, *Proc. Dep. Electr. Eng. – Skopje*, Vol. **22**, No. 1–2, pp. 35–40, 2006 (Резиме на македонски јазик: Марија Кујумѓиева Николоска, Јорданка Митевска: Услови за постоење квазипериодични решенија за некои нелинеарни диферендијални равенки од втор ред, *Зб. ѓпр. Елекѓроѓех. фак. – Скопје*, год. **22**, бр. 1–2, стр. 35–40, 2006).
119. Боро М. Пиперевски: За некои специјални типови двојни интеграли, *Зб. ѓпр. Елекѓроѓех. фак. – Скопје*, год. **22**, бр. 1–2, стр. 41–42, 2006 (Резиме на англиски јазик: Boro M. Piperevski: On some special double integrals, *Proc. Dep. Electr. Eng. – Skopje*, Vol. **22**, No. 1–2, pp. 41–42, 2006).
120. Боро М. Пиперевски: Инваријантност на една бројчена карактеристика за една класа линеарни диференцијални равенки од втор ред, *Зб. ѓпр. Елекѓроѓех. фак. – Скопје*, год. **22**, бр. 1–2, стр. 43–45, 2006 (Резиме на англиски јазик: Boro M. Piperevski: An invariation for a class of differential equations of the second order numerical characteristic, *Proc. Dep. Electr. Eng. – Skopje*, Vol. **22**, No. 1–2, pp. 43–45, 2006).
121. Љупчо В. Караѓинов: Студиите по електроника во самоевалуацијата на Електротехничкиот факултет во Скопје, *Зб. ѓпр. Елекѓроѓех. фак. – Скопје*, год. **22**, бр. 1–2, стр. 47–56, 2006 (Резиме на англиски јазик: Ljupčo V. Karadžinov: Studies on electronics in the quality assesment report of the Faculty of Electrical Engineering – Skopje, *Proc. Dep. Electr. Eng. – Skopje*, Vol. **22**, No. 1–2, pp. 47–56, 1997).

INDEX

of the authors published in the Proceedings of the Faculty of Electrical Engineering in Skopje Issues from Vol. 1. No. 1 (1977) to Vol. 22, No. 1–2 (2006)

(ИНДЕКС на авторите на трудовите објавени во на Зборникот на трудови на Електротехничкиот факултет во Скопје од Год. 1, број 1 (1977) до, год. 22, број 1–2 (2006))

- Arsov, Goce L.: 103
Arsov, Goce L': 81,
Ačkovski, Risto: 67, 114,
Bankov, Nikolay D.: **110***,
Čekredži, Nikola: **79**,
Cvetkovski, Goga: **116**,
Džekov, Tomislav: **75**,
Gavrovski Cvetan V.: 110,
Jefferies, David J.: 81,
Kamilovski, Metodija A.: 103,
Karadžinov, Ljupčo V.: **81, 103**,
Kujumdžieva Nikoloska, Marija: **118**,
Mitevka, Jordanka: 118,
Nikolovski, Alekssndar: 72,
Nikolovski, Ljubomir: **111**,
Popov, Marjan: **91**,
Rafajiovski, Goran: 94, 111,
Rajičić, Dragoslav: **67, 90, 114**,
Raleva, Katerina J.: 103,
Šapkarev, Ilija A.: **86**,
Stojanov, Zafir: 72,
Stojanova, Kornelija: 72,
Stojmenov, Stanoja: 72,
Tabakov, Stefan E.: 110,
Taleski, Rubin: 90,
Tolev, Mihail: **72**,
Zlatanovski, Mito: 91,
- Арсенов, Арсен: **13**,
Арсов, Гоце: **19, 89**,
Ацевски, Николче: 115,
Ачковски, Ристо К.: **26, 32**,
Ачковски, Ристо: 11, **12, 45, 58, 83, 99, 100, 108**,
109, 115,
Белчовски, Тони: **105**,
Богатиновски, Марјан: 96, **104**,
Богданов, Софија: **43**,
Богданова, Софија: **70**,
Борозан, Весна: 58,
Врангалов, Панчо: **6, 20, 112**,
Георгиева, Верка: **85**,
Георгиевски, Сашо: **113**,
Гламочанин, Властимир: **7**,
Грчев, Леонид: 101, 106,
Димитров, Благој: 25, 61,
Димовски, Дончо: 82,
Димчев, Владимир: **59, 61, 68, 101, 112**,
Златаноски, Мито: 14,
Ивановски, Зоран А.: **97**,
Јакимов, Тодор: 105,
Јанев, Љубен: **5, 29, 30, 37, 51, 69**,
Камиловски, Методија: **3, 54, 88**,
Караџинов, Љупчо: 65,
Караџинов, Љупчо В.: **121**,
Кацарска, Марија: 44, **106**,
Кепеска, Јованка: **10**,
Кирчев, Валентин: 99,
Коцарев, Љупчо М.: 36, **65, 82**,
Коцев, Кирил И.: **87, 107**,
Коцев, Кирил: **25, 31, 47, 61**,
Кујумџиева-Николовска, Марија: **34**,
Лазарееска, Елизлбета: **18, 24, 50**,
Лазов, Петар: **62**,
Лазов, Петар Р.: **36**,

* In bold is signified first author (*Со болд е означен првиот автор)

- Миновски, Ристо: **52**,
 Мирчевски, Слободан: 113,
 Николовски, Љубомир: **8**,
 Николовски, Стојан: 53,
 Ничота, Драган: **71**,
 Ололоска, Лидија: 37, 69,
 Пашалиќ, Никола: 60, 63,
 Петковска, Лидија: **16, 66**,
 Петрушев, Митруш: 74,
 Пиперевски, Боро: **22, 74**,
 Пиперевски, Боро М.: **33, 38, 39, 40, 95, 119, 120**,
 Попов, Марјан: **80, 102**,
 Попов, Никола К.: **27**,
 Попов, Никола: **23, 28**,
 Рајичиќ, Драгослав А.: 32,
 Рајпчиќ, Драгослав: **1, 11, 12, 14, 45, 58, 77**,
 Рафајловски, Горан: **60, 63, 78, 98**,
 Речкоски, Никола: **64**,
 Рушков, Емил: **48**,
 Соколов, Бојан: **4**,
 Спасевска, Христина: **117**,
 Стојчевска, Билјана: 104,
 Стрезов, Љубомир: **55**,
 Талески, Рубин: 77,
 Тасев, Жарко: 65, **82**,
 Тодоровски, Мирко: 100, 108, **109**,
 Толев Михаил: **21**,
 Трајковски, Горан: **96, 104**,
 Ќосев, Јосиф: **89**,
 Улчар-Ставрова, Татјана: **2**,
 Филиповски, Велимир: 53,
 Ханџиски, Благој: **9, 57, 59, 68, 101, 112**,
 Ханџиски, Владо: 112,
 Хаџи-Мишев, Димитар: **28**,
 Христовски, Дамјан Д.: **46**,
 Чекреци, Никола: 53, **84**,
 Чекреци, Никола Љ.: **93**,
 Чингоски, Влатко: **49**,
 Чундев, Милан: **15, 17, 66**,
 Чундев, Стојан: **53, 76**,
 Чундева, Снежана: **92**,
 Шапкарев, Илија: **56**,
 Шапкарев, Илија А.: **35, 41, 42, 73**,

INSBEARD OF CONCLUSION

The Proceedings was reference journal for the scientific work of the Faculty. The Proceedings was published twice per year for 22 years with short interruptions. It has been exchange with around 40 universities and scientific institutions in Europe. The Proceeding was registered as international journal with ISSN 0351-6075 number and is

searchable through University Library "Kliment Ohridski" from Skopje.

The Proceedings will continue to be published under new name Journal of Electrical Engineering and Information Technologies in printed version and on-line.

НАМЕСТО ЗАКЛУЧОК

Зборникот претставуваше референтно гласило во кое се објавуваа резултати од научната работа на Факултетот. Зборникот со кратки прилики излегуваше два пати годишно 22 години. Според принципот на размена се разменуваше со околу 40 високошколски установи во Европа. Зборникот беше регистриран како меѓународно списание со број ISSN

0351-6075 и може да се пребарува преку Универзитетската библиотека "Климент Охридски" од Скопје.

Зборникот ќе продолжи да излегува со ново име Списание за електротехника и информациски технологии во печатена и електронска форма.